AFFDL-TR-71-177

ANALYSIS OF DATA RATE REQUIREMENTS FOR LOW VISIBILITY APPROACH WITH A SCANNING BEAM LANDING GUIDANCE SYSTEM

JAMES D. DILLOW, MAJOR, USAF
PAUL R. STOLZ, CAPTAIN, USAF
MEYER D. ZUCKERMAN, 1ST LT, USAF

FOREWORD

This report describes the results of an inhouse investigation into the guidance and control requirements associated with low visibility landing with a scanning beam landing guidance system. The work was performed under Project 8219, Task 821911, Work Unit 003. Task 821911 involves the application of modern control techniques to the synthesis and analysis of control systems. This investigation was specifically performed in support of Project 404L which is an Air Force project to develop a new advanced landing system for the Air Force and to support the New National All-Weather Landing Program.

Two students from the Air Force Institute of Technology, WPAFB, Ohio, participated in this investigation as a part of their research project for a Master's degree. Lt Meyer Zuckerman developed a portion of the digital computer program used in the analysis and developed some of the results for the DC-8. This is reported in his Masters Thesis which is Reference 3 of this report. Capt Paul Stolz modified the computer program and developed all the results for the CH-53A. This effort is reported in Reference 13.

Dunston Graham, Warren Clement, and Lee Gregor Hoffman of Systems Technology, Inc., contributed technical support to the investigation, particularly in the areas of the aircraft model, the model for the scanning beam transmitter, and the measures of approach performance. Certain subroutines of the computer program used in the analysis were provided by Ferit Konor, Gunter Stein, and Michael Ward of Honeywell, Inc.

Ronald Anderson of the Air Force Flight Dynamics Laboratory conceived and suggested the general analysis approach used in this investigation. In particular, he suggested the use of an optimal model for the automatic flight control system in order to investigate those measurements which were critical to successful landing approach.

This investigation was performed during the period from August 1969 to February 1972. The manuscript was submitted by the author on 1 July 1972.

This technical report has been reviewed and is approved.

C. B. WESTBROOK
Chief, Control Criteria Branch
Flight Control Division
Air Force Flight Dynamics Laboratory

ABSTRACT

Data rate requirements for low visibility approach with a sample data measurement of glideslope deviation is investigated analytically.

A "window" is defined by specifying certain allowable deviations in the aircraft motion variables which are acceptable for continuation of the landing at a 100-ft-decision altitude. The approach performance is defined as the probability of missing the window, which corresponds to the probability of a missed approach.

The landing approach process is modeled by a system of stochastic differential equations, which account for the aircraft dynamics, atmospheric disturbances, guidance errors, and data rate. The flight control system is modeled by a state estimator and a state feedback matrix which is optimized so as to minimize the probability of a missed approach subject to rms constraints on control activity.

Performance as a function data rate was computed using DC-8 and CH-53A dynamics. Variations considered in the model include gust environment, guidance errors, window definition, control authority, control points, and onboard sensors. For each case considered, the performance degradation due to data rate was computed and plotted. Based on the allowable degradation in performance from that obtainable with continuously measured glideslope deviation, the data rate requirements can be determined.

The study reveals that the flight control system is the limiting factor in achieving an all-weather Category II low visibility landing capability with a state-of-the-art scanning beam guidance system and data rates above 5 samples/sec. This is due to the requirements to suppress gust upset. The tradeoffs between the flight control system and scanning beam guidance system data rate requirements are illustrated by comparing the results for various flight control schemes. For example, data rate requirements are significantly reduced via onboard

inertial measurements. However, the results indicate that a data rate between 10 and 20 samples/sec is extremely desirable in order to fully realize the flight control system's potential for suppressing glideslope tracking errors due to gust upset if onboard inertial sensors are not used.

TABLE OF CONTENTS

TABLE OF CONTENTS (CONTD)

TABLE OF CONTENTS (CONTD)

LIST OF ILLUSTRATIONS

LIST OF ILLUSTRATIONS (CONTD)

LIST OF TABLES

LIST OF TABLES (CONTD)

TABLE OF NOTATION

A	A matrix of coefficients used in the first order representation of the system differential equations
AFCS	Automatic Flight Control System
A_n	A matrix of coefficients used in the first order representation of the system difference equations
A_T	A matrix of coefficients used in the first order representation of the system and estimation error difference equations
a	A constant used in the equation for the longitudinal gust gradient effect
B	A matrix of coefficients used in the first order representation of the system differential equations
B_n	A matrix of coefficients used in the first order representation of the system difference equations
B_T	A matrix of coefficients used in the first order representation of the system and estimation error difference equations
B_l	Cyclic pitch deflection, rad
B_{lc}	Commanded cyclic pitch deflection, rad
C_n	A matrix used to transform the continuous inputs due to headwind and wind shear to a discrete input at each sample instant
d	Glideslope deviation, ft
E{ }	Expected value operator
e	Estimation error, $x - \hat{x}$
F	Feedback matrix used in control law
g	Constant of gravity, 32.2 ft/sec^2
H	Observation or measurement matrix
h	Altitude, ft
I	The identity matrix

TABLE OF NOTATION (CONTD)

I_1	A diagonal matrix with zero or one entries used to partition those state variables which are continuously and perfectly measured, i.e., the non zero entries of $I_1 x$ are continuously and perfectly measured.
I_2	$I - I_1$
J	Quadratic cost functional
J_1	A quadratic cost functional with weighting on σ_d and rms control activity
J_2	A quadratic cost functional with weighting on σ_d, $\sigma_{u_{as}}$, and rms control activity
K	Gain matrix used in discrete Kalman filter
k_1, k_2, k_3	Weighting coefficients used in quadratic cost functionals J_1 and J_2
M	Pitching moment divided by pitching moment of inertia
M_{B1}	$\partial M/\partial B_1$, $1/sec^2$
$M_{\dot{B}1}$	$\partial M/\partial \dot{B}_1$, $1/sec$
M_q	$\partial M/\partial_q$, $1/sec$
M_u	$\partial M/\partial_u$, $1/ft\text{-}sec$
M_w	$\partial M/\partial_w$, $1/ft\text{-}sec$
M_w	$\partial M/\partial_w$, $1/ft$
M_α	$\partial M/\partial\alpha$, $1/sec^2$
M_α	$\partial M/\partial\alpha$, $1/sec$
$M_{\delta c}$	$\partial M/\partial\delta_c$, $1/sec^2$
$M_{\delta d}$	$\partial M/\partial\delta_d$, $1/sec^2$
$M_{\delta e}$	$\partial M/\partial\delta_e$, ft/sec^2
$M_{\delta th}$	$\partial M/\partial\delta_{th}$, $1/\%\ RPM\text{-}sec^2$
n	Denotes the nth sample data measurement and is used interchangeably with nT_o
n_z	Normal acceleration, ft/sec^2

TABLE OF NOTATION (CONTD)

P	The solution to the nonlinear matrix equations used to solve for the optimal feedback matrix, F, and estimator gains, K
PA1	Probability of Accident if the window is made and landing is continued
PA2	Probability of Accident if the window is missed and landing is continued
PD	Probability of discontinuing the approach if the window is missed
PMA	Probability of a missed approach
PMA/ARR	Probable missed approaches per arrival
$\overline{\text{PMA/ARR}}$	PMA/ARR for a given data rate divided by the PMA/ARR for continuously measured glideslope deviation
PMW	Probability of missing the window
Q	Matrix used to weight the state in the quadratic cost functional J
q	pitch rate, rad/sec
q_g	longitudinal gust gradient, 1/sec
R	Matrix used to weight the control in the quadratic cost functional J
rms	Root mean squared
S	Covariance of the "plant noise" for the system difference equations
S*	Covariance of the "plant noise" for the system differential equations
SAS	Stability Augmentation System
S_h	Wind shear velocity gradient, ft/sec/ft
T_e	Lag time constant for elevator response to a commanded input, sec
T_d	Lag time constant for direct lift control response to a commanded input, sec

TABLE OF NOTATION (CONTD)

T_o	Time interval between sample data measurements, sec
T_{th}	Lag time constant for thrust response to commanded input, sec
t	time, sec
U_o	Nominal longitudinal velocity, ft/sec
u	Perturbed longitudinal velocity, ft/sec; or control input vector
u_{as}	Perturbed longitudinal airspeed, ft/sec
u_g	Longitudinal gust intensity, ft/sec
u_w	Longitudinal component of wind intensity due to steady wind and wind shear, ft/sec
V	Convariance of "measurement" noise, $E\{\eta(n)\eta(m)'\xi = V\delta_{nm}$
v	Input to system difference equations due to steady wind and wind shear
v*	Input to system differential equations due to steady wind and wind shear
w	Perturbed normal velocity, ft/sec; or a vector for which the non zero entries are the states which are not continuously and perfectly measured
$\bar{w}(n+1)$	Estimate of w(n+1) given n observations
$\hat{w}$	Estimate of w
w_d	Wind intensity due to steady wind and wind shear, ft/sec
w_g	Normal gust intensity, ft/sec
w_{sh}	Wind intensity due to wind shear, ft/sec
w_{st}	Wind intensity due to steady wind (positive value represents steady headwind), ft/sec
w_T	Input due to steady wind and wind shear for augmented difference equation, i.e. $w_T(n) = \begin{bmatrix} v(n) \\ 0 \end{bmatrix}$

TABLE OF NOTATION (CONTD)

X	Longitudinal force divided by aircraft mass
X_{B1}	$\partial X/\partial B_1$, ft/sec^2
$X_{\dot{B}1}$	$\partial X/\partial \dot{B}_1$, ft/sec
X_q	$\partial X/\partial q$, ft/sec
X_u	$\partial X/\partial u$, 1/sec
X_w	$\partial X/\partial w$, 1/sec
X_α	$\partial X/\partial \alpha$, ft/sec^2
$X_{\delta c}$	$\partial X/\partial \delta_c$, ft/sec^2
$X_{\delta d}$	$\partial X/\partial \delta_d$, ft/sec^2
$X\delta_e$	$\partial X/\partial \delta_e$, ft/sec^2
$X_{\delta th}$	$\partial X/\partial \delta_{th}$, ft/% RPM-sec^2
x	State vector for the system differential equation
$\hat{x}$	Estimate of x
x^*	Optimal estimate of x
y	Sample data measurement
y_1	State representing measurement errors due to beam bends, ft
y_2	State representing measurement errors due to fluxuation noise, ft
y_3	State representing integral of glideslope deviation, d, ft-sec
Z	Normal force divided by aircraft mass for defining stability derivatives, or steady state covariance matrix for z
Z_{B1}	$\partial Z/\partial B_1$, ft/sec^2
$Z_{\dot{B}1}$	$\partial Z/\partial \dot{B}_1$, ft/sec
Z_q	$\partial Z/\partial q$, ft/sec
Z_u	$\partial Z/\partial u$, 1/sec
Z_w	$\partial Z/\partial_w$, 1/sec

TABLE OF NOTATION (CONTD)

Z_{α}	$\partial Z/\partial\alpha$, ft/sec^2
$Z_{\delta c}$	$\partial Z/\partial\delta_c$, ft/sec^2
$Z_{\delta d}$	$\partial Z/\partial\delta_d$, ft/sec^2
$Z_{\delta e}$	$\partial Z/\partial\delta_e$, ft/sec^2
$Z_{\delta th}$	$\partial Z/\partial\delta_{th}$, ft/sec^2
z	Augmented state vector $z = \begin{bmatrix} x \\ e \end{bmatrix}$
α	Angle of attack, rad
γ_o	Steady-state flight path angle
Δd	Glideslope deviation tolerance used to define the 100 ft decision altitude window, ft
Δu_{as}	Airspeed deviation tolerance used to define the 100 ft decision altitude, ft/sec
Δy	Lateral centerline deviation tolerance used to define the 100 ft decision altitude window, ft
Γ_o	Reference glidepath angle, deg
δ_c	Collective pitch deflection, rad
δ_{cc}	Commanded collective pitch deflection, rad
δ_d	Direct lift control deflection, rad
δ_{dc}	Commanded direct lift control deflection, rad
δ_e	Elevator deflection, rad
δ_{ec}	Commanded elevator deflection, rad
δ_{th}	Perturbed thrust, % RPM
δ_{thc}	Commanded perturbed thrust, % RPM
$\delta(t-s)$	Impulse function
δ_{nm}	Kronecker delta $\delta_{nm} = \begin{cases} 1, & n = m \\ 0, & n \neq m \end{cases}$

TABLE OF NOTATION (CONTD)

ζ	Input due to white noise for augmented difference equation for z, $\zeta(n) = \begin{bmatrix} \xi(n) \\ \eta(n+1) \end{bmatrix}$
η	Gaussian amplitude white measurement noise, ft
θ	Perturbed pitch attitude, rad
ξ	Gaussian amplitude discrete white noise process used as an input to the system difference equation due to finite bandwidth measurement noise and gust disturbances
ξ^*	Gaussian amplitude white noise process used as an input to the system differential equations due to finite bandwidth measurement noise and gust disturbances
ξ_{bb}	Gaussian amplitude white noise process used in the model for beam bend errors, y_1
ξ_{fn}	Gaussian amplitude white noise process used in the model for the fluctuation noise errors, y_2
ξ_{ug}	Gaussian amplitude white noise process used in the model for the longitudinal gust disturbances, u_g
ξ_{wg}	Gaussian amplitude white noise process used in the model for the normal gust disturbances, w_g
σ_{B1}	The standard deviation of B_1
$\sigma_{\dot{B}1}$	The standard deviation of $\dot{B}_1$
σ_{bb}	The standard deviation of the beam bend errors, y_1
σ_d	The standard deviation of d
σ_{fn}	The standard deviation of the fluctuation noise, y_2
σ_{nZ}	The standard deviation of n_Z
σu_{as}	The standard deviation of u_{as}
σ_{ug}	The standard deviation of u_g
σ_w	The standard deviation of w
σ_{wg}	The standard deviation of w_g
σ_{y3}	The standard deviation of y_3

TABLE OF NOTATION (CONTD)

$\sigma_{\delta c}$	The standard deviation of δ_c
$\sigma_{\dot{\delta} c}$	The standard deviation of $\dot{\delta}_c$
$\sigma_{\delta ci}$	The standard deviation of the ith control activity
$\sigma_{\delta e}$	The standard deviation of δ_e
$\sigma_{\dot{\delta} e}$	The standard deviation of $\dot{\delta}_e$
$\sigma_{\delta th}$	The standard deviation of δ_{th}
σ_{η}	The standard deviation of η
σ_{θ}	The standard deviation of θ
τ_{B1}	Lag time constant for cyclic pitch response to a commanded input, sec^{-1}
$\tau_{\delta c}$	Lag time constant for collective pitch response to a commanded input, sec^{-1}
Φ	Primary matrix solution for $\dot{x} = Ax$
Φ_F	Primary matrix solution for $\dot{x} = (A + BF)x$
Φ_1	Primary matrix solution for $\dot{x} = (A + BF1_1)x$
Ψ	Covariance matrix for ζ
ω_{bb}	Break frequency of the beam bend errors, y_1
ω_{fn}	Break frequency of the fluctuation noise, y_2
ω_{ug}	Break frequency of the longitudinal gust intensity
ω_{wg}	Break frequency of the normal gust intensity

Superscripts

.	Derivative with respect to time, d/dt
'	Matrix transpose
—	Overbar denotes mean value, except for $\overline{PMA/ARR}$

SECTION I

INTRODUCTION

1.1 BACKGROUND

One of the goals of the United States is to develop a new National Landing System (NLS) which will make it possible to perform routine approach and landing under Category III-C weather conditions (zero ceiling and zero runway visibility range). To achieve this goal, the Radio Technical Commission for Aeronautics (RTCA) has established Special Committee 117 (SC 117) and given it the responsibility of determining guidance system requirements and developing the landing guidance system specification which best satisfies these requirements. At this point in time, RTCA SC-117 has decided that the new system will use either microwave scanning beam transmitters or a doppler system for lateral and vertical guidance information for the landing aircraft. However, the scan rate requirements for the microwave scanning beam system have not been determined. Also, other parameters in the landing guidance system specification are still undefined, such as transmitter geometry, signal quality, etc.

In conjunction with the national microwave landing system development program, the Air Force is conducting supporting studies and development efforts to ensure that the requirements of the USAF will be met. Although the prime objective for both civil and military efforts is to develop a capability to perform routine all-weather landings, there are landing guidance system requirements that are peculiar to military operations. These requirements include considerations for mobility, security (anti-jamming), and versatility of operation. However, despite these additional considerations, the basic ground rule for the military system is that it be compatible with the new national system. Thus, the new Air Force All-Weather Landing System will also be a microwave scanning beam system or a doppler system. It follows then that the proper resolution of scan rate requirements and other guidance system parameters is a necessary prerequisite to the successful development of a military all-weather landing capability.

The problem of selecting the appropriate scan rate is extremely complex and involves a large number of interrelating factors.

The current state of the art seems to be most advanced in mechanically scanned systems, i.e., the transmitting antenna is mechanically swept through an appropriate arc, depending on the desired angular coverage. The mechanically scanned system, however, is limited by the physical and mechanical problem of rapidly changing angular rates with the moving transmitting antenna. Larger angular coverages can be achieved with a corresponding compromise in scan rate. A large angular coverage is desirable for smoother glideslope and centerline capture, steep angle approach, and variable approach geometry. The transmitting antenna's size is also affected by the transmission frequency used. For certain desirable microwave transmission frequencies, the transmitting antenna size must be scaled up with a corresponding decrease in the scan rate that can be realized.

Another hardware approach is to use an electronically scanned system. In this case, the antenna is fixed and the narrow beam of transmitted energy is electronically swept through the appropriate angular coverage. For the electronically scanned system, there is very little problem in achieving high scan rates. However, the beam transmitted by an electronically scanned system is conical rather than the more desirable planar beam. This means that a false indication of glideslope deviation would be indicated off the centerline. Furthermore, the errors in the glideslope deviation due to a centerline offset would be different for different glideslope angles. An analogous situation would exist with lateral deviation information. Additional electronic complexity is required to "flatten" the beam so that it is planar or to derive the appropriate guidance information from the conical beam.

An additional factor, which is basically independent of the type of scanning beam used, is the method of encoding the guidance information in the beam and subsequently decoding the information so as to provide an updated angular position measurement to the aircraft. The time that

the airborne receiver is illuminated by the beam is a function of the beam width and scan rate. A narrower beam provides the capability for improved accuracy, for a fixed scan rate. However, increasing the scan rate or decreasing the beam width reduces the dwell time of the beam at the airborne receiver, and hence the time for information transmission. An added complexity is introduced by the fact that certain demodulation techniques require more than one scan to provide a guidance information update in order to reduce the guidance errors to a desirable level.

Thus the question of "what is the right scan rate for a scanning beam system" involves a complex tradeoff of economics, reliability, modulation-demodulation techniques, feasibility, and landing performance. The specification of exceedingly high scan rates may result in a new landing system that is so expensive that its use is very limited. On the other hand, if the new system is to be effective, the scan rate must not be so low as to degrade approach and landing performance to the point that missed approaches create conjestion in the terminal area or compromise landing safety. In addition, the new system should have a sufficient scan rate to accommodate future innovations in aircraft control systems such as direct lift control. Otherwise, the new system could soon become obsolete! Thus landing performance and safety are dominant factors in the determination of scan rate requirements.

Landing performance is not solely dependent upon the accuracy of the landing guidance system. In fact, it was demonstrated in a landing approach analysis by Dunstan Graham, Warren Clement, and Lee Gregor Hofmann, et al. (References 1 and 2) that the aircraft flight control system is a limiting factor in achieving a Category II low visibility landing capability with a state-of-the-art microwave scanning beam landing guidance system. Thus, a realistic evaluation of landing performance involves the aircraft dynamics and the related ability to control the aircraft motions.

In References 1 and 2, the information data rate requirements for a microwave scanning beam landing guidance system were studied. However the explicit dependence of landing performance on information data rate

was not determined. The fact is that the method of analysis used in References 1 and 2 does not lend itself to an easy evaluation of the landing performance tradeoff with information data rate; and, that up to now, there are no published results which can be used to evaluate the tradeoff between landing performance and landing guidance data rate. (Landing guidance data relates to scan rate depending upon the number of scans required to provide an information update from the landing guidance system.)

1.2 PURPOSE AND SCOPE

The purpose of this report is

(1) to describe an analysis technique for examining landing approach performance as a function of landing guidance data rates.

(2) to validate the mathematical model used in the analysis technique by comparison of results obtained using a more conventional analysis technique (References 1 and 2).

(3) to determine and analyze the landing approach performance tradeoffs with landing guidance data rates.

The analysis described in this report is only developed for landing approach. Only the portion of the landing involving glideslope and "localizer" or centerline tracking are considered. It is assumed that glideslope and centerline capture have been achieved, and the analysis doesn't include consideration of flare and decrab maneuvers or touch down. This is roughly equivalent to consideration of a landing under Category II visibility conditions, i.e., a 100-ft ceiling and 1/4-mile-runway visibility range.

For a Category II landing, the approach is made to a 100-ft-decision altitude. If the aircraft is within certain tolerances with respect to vertical and lateral deviations at the 100-ft-decision altitude, the landing continues. Otherwise, a go around is executed. It is also

assumed that flare is not initiated prior to the 100-ft altitude. The current FAA Category II landing accuracy criteria is ± 72 ft lateral deviation from centerline and ± 12 ft vertical deviation from glideslope (Figure 1). The accuracy criteria is called the landing approach "window."

The analysis technique used in this report is only used to investigate the landing approach longitudinal tracking errors as a function of landing guidance data rate. This restriction is based on the results of Reference 1, which indicate that even under worst-case conditions, the lateral accuracy criteria of ± 72 ft is easily achieved. Thus with the ± 72-ft lateral window, lateral tracking errors about the runway centerline can be easily reduced to the point that the lateral errors do not significantly affect landing approach performance. This by no means implies that the ± 72-ft lateral window is indeed a valid accuracy requirement for safe continuation of the approach or that lateral tracking errors are not consequential to landing approach success.

The analysis technique developed in this report is only claimed to apply to the consideration of an automatic approach and does not explicitly consider the effects of data rate on a piloted or pilot coupled with low visibility approach. This restriction is based upon the fact that a pilot model doesn't appear explicitly in the mathematical model of the landing approach process. The consequence of this limitation is discussed in the Summary and Conclusions section of this report.

1.3 OVERVIEW

First, a measure of landing approach performance is quantified. The performance measure is based on the assumption that if certain prespecified aircraft variables are within a given tolerance at a 100-ft-decision altitude (corresponding to a Category II approach), then the landing proceeds to touch down. Otherwise a missed approach has occurred and a "go around" is executed. With this assumed definition of a missed approach, the probability of a missed approach (PMA) is a quantitative and computable measure of landing approach performance.

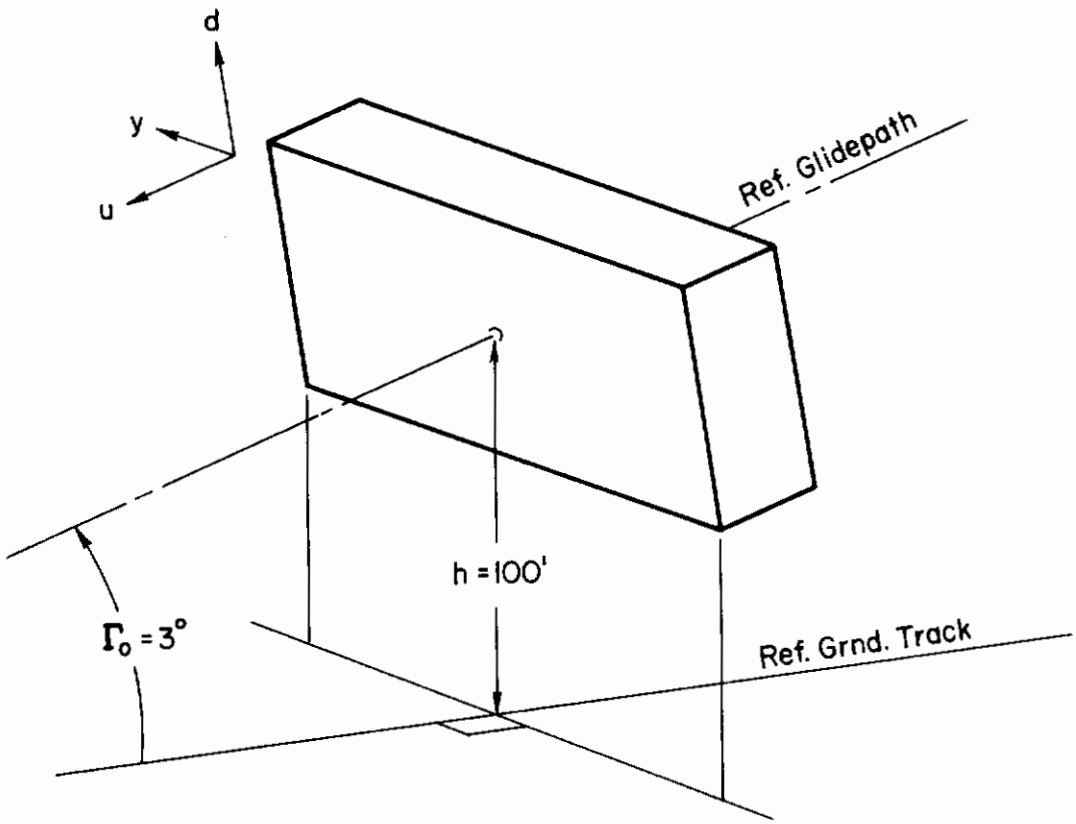

$\Delta d = \pm 12$ ft

$\Delta y = \pm 72$ ft

$\Delta AS = \pm 5$ kts $= \pm 8.45$ ft/sec

Figure 1. The Recommended Category II Window

Given the probability of a missed approach, the probable number of missed approaches per arrival at the terminal area (PMA/ARR) can be computed from the relation

$$PMA/ARR = \frac{PMA}{1 - PMA}$$

This performance measure is related to the likely number of go arounds that will have to be executed and the congestion in the terminal area due to missed approaches. In this report, the probable number of missed approaches per arrival is taken as the measure of landing approach performance, and is evaluated as a function of data rate.

A mathematical model of the landing approach process is developed. The model includes the following elements:

(1) the linearized longitudinal equations of motion for an aircraft in landing approach

(2) a stochastic model of the normal and longitudinal gust disturbances

(3) a "deterministic" model for the steady head or tail winds and wind shear

(4) a measurement model which includes

(a) the continuous measurement of certain specified system states. This accounts for measurements sensed aboard the aircraft and usually associated with the flight control system related sensors.

(b) a noisy sampled data measurement of glideslope deviation where the noise which is superimposed on the true glideslope deviation

accounts for the effects of beam bends*, fluctuation noise**, and white noise. This accounts for scanning beam landing guidance, and guidance system, and is usually considered a guidance (or outer loop) measurement.

(5) a flight control system or controller which is defined by a state estimator and a feedback matrix.

(a) The state estimate is developed from a combination of the continuous measurements and the sample data measurements.

(b) The feedback matrix is selected to be optimal for a quadratic cost functional. The weightings in the quadratic cost functional, which defines the feedback matrix, are selected to minimize the probability of a missed approach subject to root mean square (rms) constraints on the control activity.

The math model described above is definitized for two aircraft configurations: a DC-8 is conventional approach and a CH-53A helicopter in a steep low speed approach. The DC-8 represents a large class of conventional aircraft and the CH-53A provides an example of an aircraft with a high lift curve slope and direct lift control through collective pitch.

A digital computer program was developed to implement the landing approach model and to automatically compute the probability of a missed

---

* Beam bends appear as a spacial distortion of the zero reference line in the glideslope measurement and are created by local obstacles and any other deviation from an ideal medium for wave propagation. To an aircraft moving along the reference glideslope, they appear as an extremely low bandwidth noise.

** Fluctuation noise is a noise component associated with a sample data measurement. The bandwidth is relatively high and increases with data rate, although the total power is assumed to be independent of data rate.

approach as a function of the data rate of the glideslope deviation measurements. The computer program takes as inputs the data rate; the aircraft stability derivatives; nominal longitudinal airspeed; glide path angle; gust, headwind, wind-shear, and guidance noise parameters; constraints on the control activity; and the tolerances on the aircraft variables that define a missed approach (i.e., the "window dimensions"). The program is structured so that changes in the system equations can be easily implemented in the program. Changes in the system equation result from

(1) changes in the aircraft equations of motion (for example, inclusion of flexure modes and effect of sensor location)

(2) addition or deletion of control points (i.e., auto-throttle, direct lift control, etc.)

(3) changes in the measurement model or sensor complement (for example, consideration of sensed normal acceleration, sensed glideslope deviation rate, and noise in the continuous measurements).

A "baseline" configuration was established for each aircraft type. Landing performance was computed as a function of data rate. The "baseline" configuration was based on

(1) using only glideslope deviation to define the 100-ft-decision altitude "window"

(2) a severe turbulence environment

(3) glideslope deviation measurements using a state-of-the-art microwave scanning beam system. This results in the consideration of relatively small beam bends and fluctuation noise.

(4) comparatively restrictive control rate authorities for the automatic control system (elevator actuator rate for the DC-8; collective pitch and cyclic pitch actuator rates for the CH-53A)

(5) using continuously measured pitch attitude, pitch rate, and airspeed.

Using the control law developed from the "baseline" configuration for each data rate, the following variations were considered:

(1) low gust intensities

(2) low gust intensities and moderate beam bends (DC-8 only)

(3) low gust intensities and severe beam bends (DC-8 only)

(4) moderate beam bends (CH-53A only)

(5) severe beam bends (CH-53A only)

In each case the landing performance was evaluated as a function of data rate.

The model was also exercised for the following variations from the "baseline" configuration:

(1) low gust intensities (DC-8 only)

(2) severe beam bends (CH-53A only)

(3) using an airspeed and glideslope deviation at the 100-ft-decision altitude (DC-8 only)

(4) using an elevator position constraint instead of an elevator control rate constraint (DC-8 only)

(5) relaxed control rate constraints

(6) addition of an "ideal" direct lift control (DC-8 only)

(7) continuously sensed glideslope deviation rate

(8) integral feedback of glideslope deviation (DC-8 only)

For each of these variations from the "baseline" configuration, approach performance was computed as a function of data rate.

In addition, for each of the cases described above, the effect of a steady headwind and wind shear on approach performance was computed as a function of data rate.

The detailed computational results are tabulated in Appendix A.

In Section V the results from this investigation are compared with similar results given in References 1 and 2, where a detailed flight control system design was considered and continuously measured glideslope deviation was assumed. These comparisons tend to verify the validity of the optimal model for the flight control system.

In order to compare the effects of data rate where the actual performance varies widely over the different cases, a measure of performance sensitivity to data rate is defined. This is done by normalizing the PMA/ARR for each data rate by the PMA/ARR for continuously sensed glideslope deviation for that corresponding case. The continuous case was approximated by a data rate of 100 samples/sec. Notationally, this is represented by

$$\overline{\text{PMA/ARR}}(1/T_o) = \frac{\text{PMA/ARR}(1/T_o)}{\text{PMA/ARR}(100)}$$

and the value of $\overline{\text{PMA/ARR}}(1/T_o)$ represents the approach performance degradation at a given sample rate, $(1/T_o)$, relative to the approach performance for continuously sensed glideslope deviation.

The performance sensitivity to data rate is analyzed by examining $\overline{PMA/ARR}$ as a function of data rate for the various cases considered.

The results indicate that in a moderate to severe turbulence environment, the flight control system is critical in achieving a Category II low visibility landing capability with a state-of-the-art scanning beam guidance system and data rates above 5 samples/sec. This is due to the requirement to suppress gust upset.

The tradeoffs between the flight control system and the guidance system are illustrated by comparing the results for various flight control schemes, which include (1) increased control authority, (2) direct lift control, and (3) the complementary use of sensed glideslope deviation rate. In the first two cases, the approach performance is improved over the baseline case; however the approach performance is more sensitive to data rate. In the third case approach performance is improved over the baseline case and the approach performance is less sensitive to data rate.

In general it appears that a data rate between 10 and 20 samples/sec is extremely desirable to fully realize the flight control systems potential for suppressing glideslope tracking errors due to gust upset if onboard inertial sensors are not used. If glideslope deviation rate is sensed continuously onboard the aircraft, then a data rate of 5 samples/sec is adequate.

SECTION II

MEASURES OF LANDING APPROACH PERFORMANCE

The measures of landing approach performance used in this report are adopted from the landing approach analysis described in References 1 and 2. They are the probability of a missed approach (PMA) and probable missed approaches per arrival at the terminal area (PMA/ARR). They are well suited to the analysis technique described in this report since the landing approach process is modeled by a system of stochastic differential equations. With the assumptions described below and the assumptions made in defining the mathematical model, these measures of approach performance are easily computed.

Consider the probability tree shown in Figure 2, which describes the possible outcomes, given an aircraft arrival at the terminal area (Reference 1). The first event, given an approach, corresponds to making or missing the window. The window is defined as a set of specified accuracy tolerances on the aircraft. Making the window corresponds to having all of the aircraft variables within the specified tolerances at the decision altitude. In the event the window is made, it is assumed that the landing continues to touchdown and that either a safe landing is accomplished or an accident occurs. If the window is missed, then a decision is made whether or not to continue the landing. If the landing is continued, it can result in a safe landing or an accident. A decision to discontinue the approach results in a missed approach. Thus the three pertinent outcomes are

(1) an accident

(2) a safe landing

(3) a missed approach.

Clearly, the most consequential outcome (at least to those aboard the aircraft) is an accident and the probability of an accident is a key performance measure in the evaluation of a low visibility landing system.

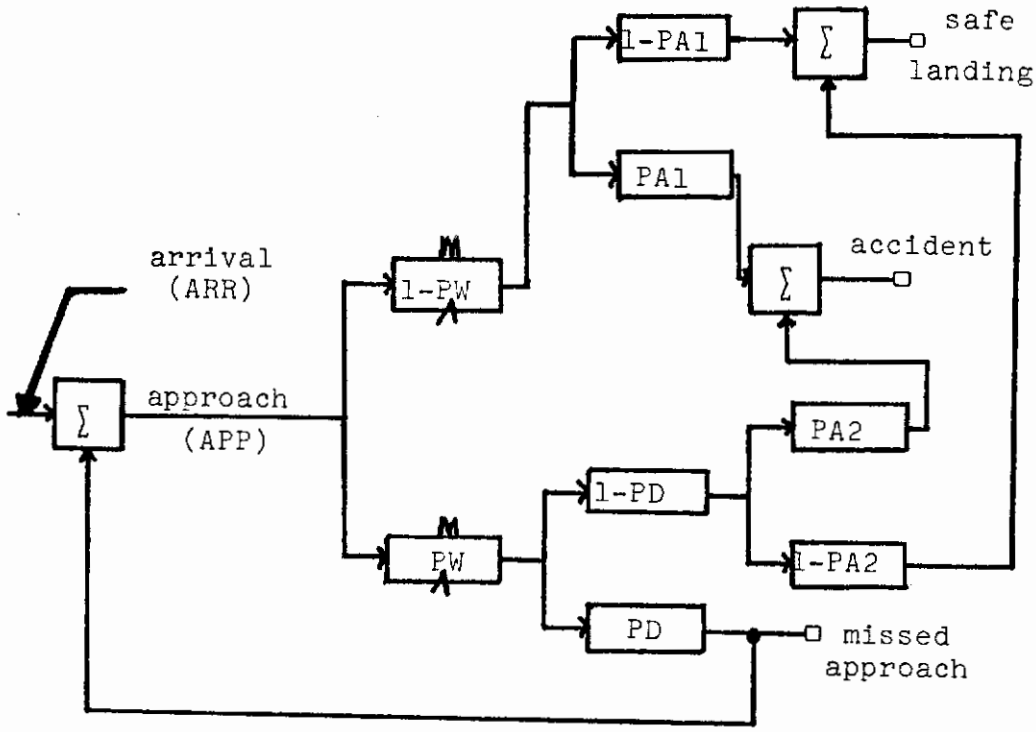

PMW - Probability of Missing the Window

PD - Probability of Discontinuing Approach if the window is missed (Assumed to be 1.0-no pilot error considered)

PMA - Probability of Missed Approach

PA1 - Probability of Accident if the Window is made and landing is continued.

PA2 - Probability of Accident if the Window is missed and landing is continued.

Figure 2. Aircraft Landing Probability Tree

However, the probabilities of an accident (PA1 and PA2) are extremely difficult to evaluate as a function of the aircraft's state at the decision altitude and are not generally available statistically. Furthermore, it is beyond the scope of this investigation to consider the landing process through flare, touchdown, and rollout. Thus, the evaluation of the probability of an accident as a function of approach performance is very difficult, if not impossible.

The probability of missed approach (PMA) is given by

$$PMA = PMW \cdot PD$$

That is, the probability of missed approach (PMA) is the product of the probability of missing the window (PMW) and the probability that the pilot discontinues the landing given that he missed the window (PD). Assuming that PD is very close to one (which is valid if the pilot's measure of an acceptable approach agrees closely with the window definition), then

$$PMA \doteq PMW$$

With this assumption, the probability of missed approach is a computationally tractible measure of landing approach performance.

In addition, an expression for the probable missed approaches per arrival at the terminal area is

$$PMA/ARR = \frac{PMA}{1 - PMA}$$

(For derivation see Reference 3.) This landing approach performance measure is more sensitive to missed approaches, and relates directly to the number of go arounds that are executed and aircraft congestion in the terminal area. It is also more intuitively meaningful.

Two different window definitions were used in this investigation. The primary window definition is based upon the current FAA Category II

approach accuracy criteria of ± 12 ft normal deviation from the reference glideslope and ± 72 ft lateral deviation from the runway centerline (Reference 4).

The landing approach analysis described in Reference 1 revealed that with continuous landing guidance information, the probability of missing the lateral window was extremely small compared to the probability of missing the glideslope window. For an A7-D, with a manual approach, the probabilities of missing the lateral window and missing the glideslope window were 0.0274 and 0.486, respectively. For a DC-8, with an automatic approach, those probabilities were 2×10^{-11} and 0.037. Similar results were obtained in Reference 2, where a CH-53A automatic approach was considered. Thus, for the current FAA Category II approach criteria, the errors associated with the longitudinal aircraft variables completely dominate the probability of a missed approach. So that, in this investigation, only the longitudinal motion variables were considered in the computation of a missed approach. The implications of this assumption are discussed in Section VI, Summary and Conclusions.

Thus, the landing approach window used in this investigation is defined as a ± 12-ft normal deviation from glideslope at the decision altitude.

In one case evaluated, an additional dimension of airspeed was added to the window. The airspeed accuracy requirement in this case was taken to be ± 5 kts or ± 8.45 ft/sec. This was taken from Reference 1 and is based upon a "guesstimate" by several airline pilots as an acceptable tolerance for Category II operations (Reference 5). This turns out to be a rather severe tolerance in severe turbulence and, in fact, it may be more reasonable that higher frequency fluctuations in airspeed may be ignored by the pilot in making a decision about the adequacy of his airspeed at the 100-ft-decision altitude.

The longitudinal window used in this investigation is shown schematically in Figure 3.

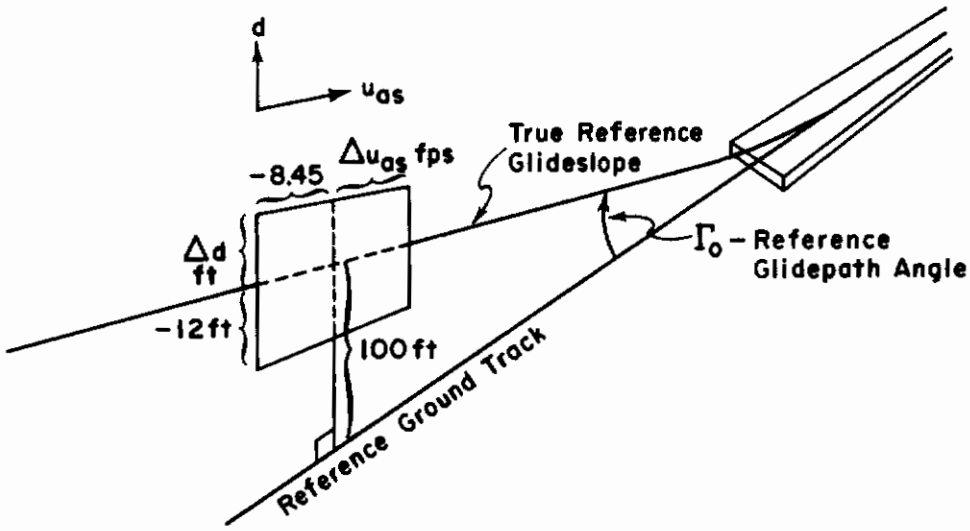

Δd = ± 12 ft

Δu_{as} = ± 5.48 ft/sec (Case D6 Only)

Figure 3. Longitudinal Category II Window

Obviously, other longitudinal motion variables could be added to the window definition. Possible candidates are given in Table I and are taken from Reference 6. These values are based upon pilot opinions of acceptable automatic approach tolerances for the indicated motion variables. These variables were not considered in the window definition; however, the effects of data rate on steady-state rms pitch attitude and normal acceleration is examined in the Section V of the report.

TABLE I

SOME MEASURES OF PILOT ACCEPTANCE
FOR AUTOMATIC APPROACH

Motion Variables	Maximum Acceptable Deviation in Steady-State Approach Tracking
Pitch Angle, θ	± 6.0 deg
Normal acceleration, $\frac{n_z}{g}$	± 0.5 g

SECTION III

MATHEMATICAL MODEL OF LANDING APPROACH

In this section a mathematical model of the landing approach process is described for a scanning beam landing guidance system. The assumptions used in developing the model are described and the equations used in the analysis are developed. The resulting system equations are stochastic difference equations and account for the aircraft dynamics, the atmospheric environment, the landing guidance system data rate and errors, the aircraft onboard sensors, and the flight control system capabilities.

3.1 THE AIRCRAFT EQUATIONS OF MOTION

It is assumed that the aircraft can be adequately represented by a set of perturbed, linear differential equations of motion. This is because the landing approach task basically involves tracking a fixed rectilinear path in space where disturbances are induced by the atmospheric environment (gusts, steady winds, and wind shears), and measurement errors are induced by sensor noise and noisy or erroneous guidance measurements. It is further assumed that the longitudinal and lateral equations of motion are uncoupled. For trimmed rectilinear flight with small perturbations, this is a reasonable assumption. Since it is assumed that the longitudinal motion variables dominate the probability of a missed approach, only the longitudinal equations of motion are considered. These include as variables pitch attitude, θ; pitch rate, q; longitudinal perturbed velocity, u; normal perturbed velocity, w; and glideslope deviation, d. The specific equations used are given in Section IV, where the system model is definitized for the two aircraft considered (i.e., the DC-8 and the CH-53A).

Additional states may be introduced to account for lags between a commanded control input and the resulting force or moment generated.

3.2 ATMOSPHERIC DISTURBANCES

Three types of atmospheric disturbances were considered in this investigation. They are stochastic turbulence or gusts, steady wind, and wind shear.

The gust disturbance is assumed to have two independent components. They are represented by a longitudinal gust velocity, u_g, and a normal gust velocity w_g, which are described by the following first-order stochastic differential equations.

$$\dot{u}_g = -\omega_{ug}\, u_g + \xi_u$$

$$\dot{w}_g = -\omega_{wg}\, w_g + \xi_w$$

where ω_{ug} and ω_{wg} are the half power or break frequencies for the longitudinal and normal gusts, respectively. ξ_u and ξ_w are zero-mean Gaussian-amplitude white-noise processes. The statistics of ξ_u and ξ_w are given by

$$E\left\{\xi_u(t)\,\xi_u(s)\right\} = 2\,\omega_{ug}\,\sigma_{ug}^2\,\delta(t-s)$$

$$E\left\{\xi_w(t)\,\xi_w(s)\right\} = 2\,\omega_{wg}\,\sigma_{wg}^2\,\delta(t-s)$$

$$E\left\{\xi_u(t)\,\xi_w(s)\right\} = 0$$

where σ_{ug} is the rms longitudinal gust intensity and σ_{wg} is the rms normal gust intensity. The expression $\delta(t-s)$ is an impulse function.

The steady wind is a time-invariant wind assumed to be blowing horizontally with the ground and may be either a head wind or tail wind. With respect to the aircraft, it has a steady longitudinal and normal component, depending upon the aircrafts attitude with respect to the horizon.

The wind shears account for a gradient in the wind intensity as a function of altitude. The wind shear, ω_{sh}, is represented by the equation

$$\omega_{sh} = \begin{cases} 0, & h \geq 200 \text{ ft} \\ s_h(200-h), & 100 \text{ ft} \leq h \leq 200 \text{ ft} \end{cases}$$

where s_h denotes the linear rate at which the wind velocity changes as a function of altitude. s_h may be positive or negative. With respect to the aircraft, the wind shear has a longitudinal and normal component, depending upon the aircraft's altitude with respect to the horizon.

The steady wind and the wind shears are treated as deterministic or nonstochastic disturbances and are used to determine the mean value of the system states at the decision altitude. Thus, they are combined into a single expression for the "deterministic" wind velocity, w_d.

$$w_d = w_{st} + \omega_{sh}$$

where w_{st} is the steady wind velocity. w_d is resolved into a longitudinal component, u_w, and a normal component w_w by the following relationships

$$u_w = w_d \cos(\gamma_o + \theta)$$

$$w_w = w_d \sin(\gamma_o + \theta)$$

where γ_o is the steady-state flight path angle and θ is the pitch attitude. For small θ, u_w and w_w are approximated by

$$u_w = w_d \left[\cos \gamma_o - \theta \sin \gamma_o \right]$$

$$w_w = w_d \left[\sin \gamma_o + \theta \cos \gamma_o \right]$$

These are the expressions used to represent the "deterministic" wind inputs to the aircraft equations of motion.

A summary of "severe" atmospheric disturbances for landing approach is given in Table II and is basically extracted from Reference 1.

TABLE II

SUMMARY OF "SEVERE" ATMOSPHERIC DISTURBANCES FOR LANDING APPROACH

Type of Disturbance	Component	Disturbance Velocity		Comment
		kt	ft/sec	
Steady wind	Head Tail	25 10	42.2 16.9	
Wind Shear (S_h)		$\pm \frac{4 \text{ kts}}{100 \text{ ft}}$	$\pm$ 0.0675 ft/sec/ft	100 ft $\leq$ h $\leq$ 200
Stochastic Turbulence	u_g w_g	5.92 3.85	10.0 6.5	rms values

3.3 MEASUREMENT MODEL

A measurement model is developed which accounts for the two different types of measurements associated with a low visibility landing approach with a scanning beam guidance system. The first part of the model accounts for the glideslope deviation measurements derived from the scanning beam system, and as such are considered sample data measurements. These measurements are usually associated with guidance measurements or guidance inputs to the flight control system. The other measurements considered are those usually associated directly as a part of the flight control system and are continuously sensed. These may include sensed pitch attitude, pitch rate, airspeed, normal acceleration, etc.

The model for the glideslope deviation measurement as derived from the scanning beam guidance system is based on data depicted in Table III. This table is based on information contained in Reference 7 and the table is extracted directly from Reference 1. Table III depicts the type and magnitude of errors in the measurement of elevation angle from a state-of-the-art microwave scanning beam system. The model for measured glideslope deviation used in this investigation accounts for four error components in the difference between the measured value of glideslope and the true reference landing glideslope. These components include a fixed bias, a low bandwidth noise component representing the spacial beam bends or multipath reflection anomalies, fluctuation noise associated with the sample data feature of the measurement, and white noise representing the very broadband thermal noise in the circuits and random electromagnetic noise.

The fixed bias is taken as a zero mean Gaussian random variable. It is not directly included as a part of the measurement since it is assumed that this error cannot be detected without some other external reference. Thus, the true glideslope plus the fixed bias is taken as the reference glideslope track for the aircraft. Its effect is accounted for by computing a root sum squared glideslope deviation using the fixed bias and the rms glideslope deviation due to all other disturbances and measurement errors.

TABLE III

ESTIMATED CONTRIBUTIONS TO ROOT-SUM-SQUARED ERRORS IN THE 2.5° ELEVATION ANGLE OF A MICROWAVE SCANNING BEAM RECEIVED AT 100 FT ALTITUDE (Reference 7)

The effective number of hits/beamwidth (H) reduces resultant effects of six fluctuation errors as noted below. In this table H = 16 hits/beamwidth. The root-mean-squared value of the source of fluctuation error is given in parentheses; after the source error has been divided by H, the effective root-mean-squared value is listed without parentheses.

Type of Error	Effective Half-Power Bandwidth of Power Spectral Density (rad/sec)	Source of Contribution		Probability Distribution	Source Error (deg)	RMS Source Error (deg)	ITEM	Effective RMS Error (deg)	Sub-total Root-Sum-Squared Error (deg)	Grand Total Root-Sum Squared Error (deg)
Bias	≐ 0 (Effectively static errors during an approach)	Ground Crystal Drift		Gaussian	(Not Applicable)	0.0005	(1)	(Not reduced by averaging over hits/ beamwidth)	0.0283	0.0341
		Air Crystal Drift				0.001	(2)			
		Angle Pickoff Bias				0.02	(3)			
		Boresight Bias				0.02	(4)			
Reflection Bias	Usually much less than the glide slope displacement loop crossover	Multipath Reflection Anomalies				0	(5)		0	
Fluctuation	$\frac{2.8}{T_o}$ $\frac{\text{rad}}{\text{sec}}$ where T_o is updating interval (sec)	Perturbation	Receiver Noise	Gaussian	(Not Applicable)	(0.05)	(6)	0.0031	0.019	
			Ground Circuit Jitter			(0.015)	(7)	0.0009		
			Air Circuit Jitter			(0.015)	(8)	0.0009		
		Pulse Increment Errors	Angle Pickoff Increment	Uniform	(0.125)	(0.0361)*	(9)	0.0023		
			Encoder Clock Increment		(0.125)	(0.0361)*	(10)	0.0023		
			Decoder Clock Increment		(0.25)	(0.0722)*	(11)	0.0045		
		Beam-Data Increment Error	(Beam packing error) Scan Degrees per Hit	Uniform	(0.062 deg/ transmission)	0.0179†	(12)	(Not reduced by averaging)		

* RMS Value is (Increment) ÷ $\sqrt{12}$

† RMS Value is (Deg/Transmission) ÷ $\sqrt{12}$

The spacial beam bends were modeled by a narrow-band, first-order, Gaussian-shaped noise which represents the beam bend deviation from the true glideslope as they appear to the aircraft flying down the reference glideslope path. The beam bend deviation, y_1, is represented by the stochastic differential equation

$$\dot{y}_1 = -\omega_{bb}\, y_1 + \xi_{bb}$$

where ω_{bb} is the half power or break frequency of the beam bend deviations and ξ_{bb} is a zero mean Gaussian amplitude white noise process. Furthermore

$$E\left\{\xi_{bb}(t)\,\xi_{bb}(s)\right\} = 2\omega_{bb}\,\sigma_{bb}^2\,\delta(t-s)$$

where σ_{bb} is the rms-beam-bend deviation. In this study, ω_{bb} = 0.0775 rad/sec was used.

The fluctuation noise was also modeled by a first-order Gaussian-shaped noise of the form

$$\dot{y}_2 = -\omega_{fn}\, y_2 + \xi_{fn}$$

where y_2 is the fluctuation noise, ω_{fn} is the half power frequency of the fluctuation noise, and ξ_{fn} is a zero-mean Gaussian-amplitude white-noise process. Furthermore

$$E\left\{\xi_{fn}(t)\,\xi_{fn}(s)\right\} = 2\omega_{fn}\,\sigma_{fn}^2\,\delta(t-s)$$

$$E\left\{\xi_{fn}(t)\,\xi_{bb}(s)\right\} = 0$$

where σ_{fn} is the rms fluctuation noise. The break frequency is taken to be

$$\omega_{fn} = \frac{2.8}{T_0} \text{ rad / sec}$$

where T_0 is the information update interval.

Finally, thermal noise and random electromagnetic noise is modeled by zero-mean Gaussian-amplitude white noise, η. It is assumed that η is statistically independent of y_1 and y_2.

The combined measured glideslope deviation from the true reference glideslope is represented pictorially in Figure 4. The measured deviation from the reference glideslope track, y,

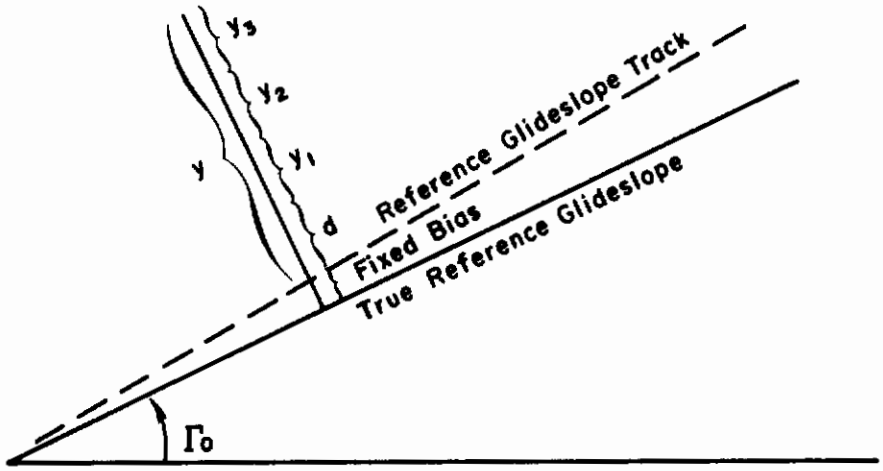

Figure 4. Glideslope Deviation Measurement Model

is given by

$$y = d + y_1 + y_2 + \eta$$

The measured glideslope deviation, y, is sampled at the information update intervals and $y(nT_o)$ is the sample data glideslope deviation on the time interval $nT_o \leq t < (n+1)T_o$, where T_0 is the sampling interval and $1/T_0$ is the sample data rate.

In addition to the sample data measurements of glideslope deviation, it is assumed that certain aircraft variables are continuously measured. The model is developed so as to include consideration for continuously sensed motion variables; however, the following restriction is imposed on the continuous measurements:

> Only those variables appearing explicitly as states in a first-order state variable representation of the system equations,
>
> $$\dot{x} = Ax + Bu + \xi^* + v^*$$
>
> can be measured continuously. Furthermore, those measurements are perfect, i.e., not noisy.

The reason for imposing this restriction is discussed in Section 3.6. At first this restriction may seem to severely limit the type of continuous measurements that can be considered. This is, in fact, not the case. It does turn out that some experimenting with the state equations may be required to get them in a suitable form. For example, all of the results in this report are based on the assumption that longitudinal airspeed is continuously measured. The perturbed longitudinal airspeed is

$$u_{as} = u - u_g - u_w$$

and the differential equation for u_{as} is derived from

$$\dot{u}_{as} = \dot{u} - \dot{u}_g - \dot{u}_w$$

where the u equation is defined by the longitudinal aircraft equations of motion and u_g and u_w can be derived from the expressions in Section 3.2. The u equation is then replaced by the u_{as} equation and the state variable u is replaced by $u_{as} + u_g + w_d$.

In a similar manner, noisy measurements of aircraft motion variables can be considered. This can be done by introducing the appropriate linear stochatic differential equations describing the measurement noise and introducing a new state equation representing the sum of the sensed motion variable and the measurement noise.

3.4 SYSTEM EQUATIONS

The linearized equations of motion for the aircraft, the wind disturbance model, and the equations used in the measurement model make up a set of first-order-system equations of the form

$$\dot{x}(t) = Ax(t) + Bu(t) + \xi^*(t) + v^*(x(t), t) \qquad (1)$$

where x is the state vector, u is the control input, ξ^* is zero-mean Gaussian-amplitude-vector white-noise process, and v* is an input made up of the terms introduced by the steady wind and wind shear. The state vector includes states representing the aircraft motion variables, the

control lags, the gust velocities, and the measurement noise. For an example, see Section IV, Definitized Models for the DC-8 and the CH-53A.

At this point two assumptions are made which enhance the computational tractibility of the problem without degrading the suitability of the model at the decision altitude (where the landing approach measure of performance is indeed defined).

The first assumption is that the model parameters are not time varying. Mathematically, this means that the A and B matrix of Equation 1 and the statistics of ξ^* are constants. Physically, this is not true. It is recognized that, in fact, the aircraft trim conditions vary throughout the landing approach, that bandwidth of the turbulence is usually considered to be a function of altitude, and that certain components of the glideslope deviation errors are range-dependent due to the fact that glideslope deviation involves an angular measurement. Thus, in physical terms, it is assumed that parameters of the process vary at a sufficiently slow rate to allow the process to be modeled by a time-invariant process. The parameters used, then, correspond to the values of those parameters at the time of window passage, i.e., the 100-ft-decision altitude.

This same assumption is used in the landing approach analysis of Reference 1, and, in which a more detailed justification for the assumption can be found.

The second assumption is that in the absence of wind shear and for a well-designed flight control and approach guidance system, the system statistics achieve a steady-state value during the glideslope tracking process phase of the landing approach. This assumption implies that the glideslope tracking phase of the landing approach lasts long enough compared to the tracking dynamics of the aircraft so that the initial transients, due to beam capture, effectively die out by the time the decision altitude is reached. It also implies that sufficient time expires during the glideslope tracking so that the system statistics

"steady out" by the time that the decision altitude is reached. The validity of this assumption can be demonstrated by considering a first-order approximation to the aircraft glideslope tracking dynamics. This is done in Reference 1 for the DC-8 with a well-designed flight control system, and the adequacy of the assumption was demonstrated.

Mathematically, this assumption means that in the absence of wind shears, the system steady-state statistics can be used to define the system statistics at the window (or decision altitude). Thus, the process can be treated as an infinite-time problem.

3.5 CONTROL LAW

In developing the model for the flight control system, the steady winds and the wind shear are not considered. The control law representing the flight control system is developed for the linear Gaussian system of equations

$$\dot{x}(t) = Ax(t) + Bu(t) + \xi^{*}(t) \tag{2}$$

where u(t) represents the control input generated by the control law. The effects of a deterministic steady wind and wind shear on the system are then evaluated in the absence of the stochastic disturbances and measurement noise to determine the mean value of the process at the window.

Assuming that the glideslope (and of course localizer) has been captured, the landing approach (not considering flare, touch down and rollout) becomes a tracking problem with respect to the deviation from the reference glideslope track and with respect to the nominal or trim values of the other aircraft motion variables. For a fixed reference glideslope track angle, this is a regulator problem from a control point of view. Thus, the model for the flight control system is developed from the control theory relating to the optimal regulator problem.

As an aside, consider the linear system

$$\dot{x}(t) = Ax(t) + Bu(t) + \xi^*(t) \tag{2}$$

where the observations of the form

$$y(t) = Hx(t) + \eta(t) \tag{3}$$

where η is a zero-mean Gaussian-amplitude white-noise process. Let J be a quadratic functional in state and control defined by

$$J(u) = \lim_{T\to\infty} E\left\{x(T)' Qx(T) + u(T)' Ru(T)\right\} \tag{4}$$

where Q and R are symmetric, Q is non-negative definite, and R is positive definite. The symbol "'" is used to denote matrix or vector transpose. It is well known that the control law defined on the observations, y, which minimize the functional (4), subject to the differential constraint (2), is of the form (Reference 8)

$$u(t) = Fx^*(t) \tag{5}$$

where F is the optimal feedback for the deterministic problem (i.e., $\xi^* = 0$) and is given by the equation

$$F = -R^{-1}B'P \tag{6}$$

and P is the solution to the nonlinear matrix Ricatti equation

$$AP + PA' + Q - PBR^{-1}B'P = 0 \tag{7}$$

In Equation 5, x* is the "best estimate" of x and is the output of a system of differential equations (called a Kalman filter) which have as their input the observations, y.

Based upon this familiar optimal control result for the so-called linear, quadratic, Gaussian problem, the flight control system is modeled by the control law

$$u(t) = F\hat{x}(t) \tag{8}$$

where F is the optimal feedback matrix for a quadratic cost functional of the form given by Equation 4 and $\hat{x}(t)$ is a "sub-optimal" estimate of the state, x.

The quadratic cost functional used to define F is of the form

$$J_1(u) = \sigma_d^2 + k_1 \sigma_{\delta_{c1}}^2 + k_2 \sigma_{\delta_{c_2}}^2 \qquad (9)$$

where σ_d is the rms glideslope deviation from the reference glideslope track, $\sigma_{\delta_{ci}}$, i = 1, 2 are the rms control inputs. For the DC-8 these control inputs are commanded elevator position and commanded engine RPM; for the CH-53A these control inputs are commanded collective pitch and cyclic pitch of the rotor blade. The weighting coefficients, k_1 and k_2, were selected so as to minimize the probability of a missed approach (PMA), subject to prespecified limits on the rms control activity. In this manner, the structure of the solution to the linear, quadratic, Gaussian optimal control problem was used to define the feedback gains, and the cost functional (9) was determined so as to optimize the landing approach performance while accounting for the control authorities that are imposed on the flight control system. The value of the structure of the solution to the linear, quadratic, Gaussian problem is that Equations 6 and 7 for the optimal feedback matrix, F, can be easily and rapidly solved via modern digital computer techniques. Thus, the problem is reduced to solving for k_1 and k_2 of Equation 4 which minimizes PMA, subject to rms constraints on the control activity. This was done numerically by a direct search minimization technique called "pattern search." The details of this minimization technique and the digital computer implementation are given in Reference 3. It should be noted that the constrained minimization of the probability of a missed approach (PMA) is equivalent to the constrained minimization of the probable missed approaches per arrival at the terminal area (PMA/ARR), which is the key measure of landing approach performance as described in Section II. This is because PMA/ARR is a monotone increasing function of PMA.

In one case considered, an exception was taken to the cost functional given by Equation 9. In the case where the deviation in airspeed was

also considered as one of the window dimensions, the following cost functional was used:

$$J_2(u) = \sigma^2_{u_{as}} + k_1 \sigma^2_{\dot{d}} + k_2 \sigma^2_{\delta_{c1}} + k_3 \sigma^2_{\delta_{c2}} \qquad (10)$$

where $\sigma_{u_{as}}$ is the rms deviation in airspeed from the nominal approach airspeed. The feedback matrix was again defined as the optimal for the cost functional of Equation 10 and the weightings, k_1, k_2, and k_3, were selected to minimize the probability of a missed approach (PMA), subject to rms constraints on the control activity. This treatment of the solution for the feedback matrix, F, is identical to the case where only glideslope deviation is used to define the window, except that it is more general and the relationships between the variables in the cost function and the probability of a missed approach are more complex. This case also serves as a demonstration of the fact that the analysis technique described in this report can be easily extended to a variety of window definitions.

As previously mentioned, a "sub-optimal" state estimate, $\hat{x}$, is used in the control law formulation given by Equation 8. The form of the "sub-optimal" state estimator and the reasons for not using an optimal estimate of the state in the control law definition are given in the next section, Section 3.6.

Since the control law given by Equation 8 was developed for the case where disturbances and measurement noise are zero mean and Gaussian, it does not directly deal with the cases where steady winds and wind shear are considered. This approach was taken to avoid the intractibility of dealing with a probabilistic description of these types of disturbances. It would also be unrealistic to prescribe a flight control law which would take into account a given deterministic wind directly because they are, in fact, random from day to day and from one geographic location to another. It is possible, however, to develop a control law which suppresses the effect of steady winds and wind shear on the deviation from glideslope. This can be done by including a state in the system

equations, Equation 1, which is the integral of glideslope deviation. In this way, the control law given by Equation 8 incorporates an integral control which suppresses steady errors in the glideslope deviation due to steady winds and compensates for the wind shears. This approach was taken for one of the cases considered for the DC-8 in order to demonstrate the versatility of the approach used in this report and to evaluate the effects of data rate on a flight control system using integral feedback in glideslope tracking.

3.6 THE STATE ESTIMATOR

In this section, the equations are developed for $\hat{x}$, the sub-optimal estimate of the state, x, that is used in the model for the flight control system, Equation 8. As a preliminary to this development, two other alternatives to the state estimator used in this analysis are discussed and the reasons for not using them are given.

For the linear Guassian dynamic system given by Equation 2 where both noisy continuous and noisy sample data measurements are made, it is quite easy to develop the equations which describe the optimal estimate of the state. The optimal estimator consists of a continuous Kalman filter and a discrete Kalman filter, where the discrete Kalman filter is used to update the optimal estimate of the state and the covariance of the estimation error for the continuous filter at each sample data instant. This results in a filter structure that is time varying; and even in a steady-state condition, the structure of the continuous filter is periodic time varying with a periodicity of the sample data measurement. This poses no theoretical problem; however, computationally it is quite a different matter. For an nth order system equation, this involves integrating an n by n nonlinear error covariance differential equation over the sample interval, one iteration of an n by n difference equation to account for the sample data measurement, and repeating this process until a steady-state periodic solution is achieved. This computation is numerically difficult and is relatively slow. An additional problem is introduced by the complexity of computing the state covariance where the continuous filter has a periodic time-varying structure. Because of the

problem of computation time and large storage requirements associated with a digital computer implementation of this approach, this "pure" approach was not attempted.

An alternate approach is to consider that all of the measurements are processed as sample data information and extrapolate the estimate at the sample instant to any time in the interval between the samples without the benefit of the continuous measurements. The theory behind this type of approach is simple: the state estimator consists of a discrete Kalman filter which is developed from the discretized representation of the system Equations 2 and an optimal intersample extrapolator, the equations of which are derived as follows.

It is shown in Reference 9 that for a zero mean, Gaussian distributed random variable $x(t)$, the best estimate of $x(t)$, $x^*(t)$, given the observation $y(t_0), \ldots, y(t_n)$, $t_n \leq t$, is

$$x^*(t) = E\left\{ x(t) \setminus y(t_0), \ldots, y(t_n) \right\} \tag{11}$$

For an optimal feedback law, the system differential equation is of the form

$$\dot{x}(t) = Ax(t) + BFx^*(t) + \xi^*(t)$$

and the solution can be formally written as

$$x(t) = \Phi(t, t_n)\, x(t_n) + \int_{t_n}^{t} \Phi(t, s)\, BF x^*(s)\, ds + \int_{t_n}^{t} \Phi(t, s)\, \xi^*(s)\, ds \tag{12}$$

where Φ is the primary matrix solution for the differential equation

$$\dot{x}(t) = Ax(t)$$

Substitute Equation 12 into Equation 11 and use the fact that ξ^* is a zero mean process and the $\xi^*(t)$ is independent of $y(t_0), \ldots, y(t_n)$ for $t \geq t_n$ to obtain

$$x^*(t) = E\left\{\Phi(t,t_n)\, x(t_n) \,\middle|\, y(t_0), \ldots, y(t_n)\right\}$$
$$+ E\left\{\int_{t_n}^{t} \Phi(t,s)\, BF x^*(s)\, ds \,\middle|\, y(t_0), \ldots, y(t_n)\right\}$$
$$= \Phi(t,t_n)\, x^*(t_n) + \int_{t_n}^{t} \Phi(t,s)\, BF\, x^*(s)\, ds$$

The last step follows from the fact that

$$E\left\{x^*(s) \,\middle|\, y(t_0), \ldots, y(t_n)\right\} = x^*(s),\ s \geq t_n$$

Differentiating with respect to t,

$$\frac{dx^*(t)}{dt} = A\left[\Phi(t,t_n)\, x^*(t_n) + \int_{t_n}^{t} \Phi(t,s) BF x^*(s) ds\right]$$
$$+ \Phi(t,t)\, BF x^*(t)$$

$$= Ax^*(t) + BFx^*(t)$$

$$= (A+BF)\, x^*(t)$$

Let Φ_F denote the primary matrix solution for

$$\dot{x}(t) = (A+BF)\, x(t)$$

Then

$$x^*(t) = \Phi_F(t,t_n)\, x^*(t_n),\ t \geq t_n \qquad (13)$$

is the expression for the optimal intersample extrapolator.

This approach to the model for the state estimate, $\hat{x}(t)$, used in the control law of Equation 8 is extremely simple to implement on the digital computer. Furthermore, the steady-state covariance at the instant after a sample data measurement is taken can be solved algebraically. This represents an ideal approach with respect to computer time for implementation of the analysis. However, continuous measurements during the time between samples are not used and the results become extremely sensitive to the data rate. Since the primary objective of the investigation is to evaluate landing approach performance as a function of the guidance system data rate, it is feared that this approach would show an unrealistic degradation of performance with decreasing data rates.

The approach used to model the state estimate, $\hat{x}$, is based on the assumption that the state, x, can be partitioned into a set of perfectly measured states and a disjoint set of states that are to be reconstructed by the state estimator. This is mathematically expressed by letting I_1 and I_2 be two diagonal matrices, such that

$$I_1 + I_2 = I$$

$$I_1 I_2 = 0$$

where I is the identity matrix. Denote

$$w(t) = I_2 x(t)$$

Pick I_1 such that the nonzero entries of $I_1 x$ are the states that are continuously and perfectly measured, and then the nonzero entries of w are the states to be reconstructed by the state estimator.

Assuming that an estimate of w, $\hat{w}$ is available at the sample time, nT_0, then the state estimate at time nT_0 is taken to be

$$\hat{x}(nT_0) = I_1 x(nT_0) + \hat{w}(nT_0)$$

Using a more compact notation where "n" denotes the sample instant "nT_0"

$$\hat{x}(n) = I_1 x(n) + \hat{w}(n) \qquad (14)$$

Based on the form of the optimal intersample extrapolator given by Equation 13, the estimate for x(n) can be updated during the sample interval by the expression

$$\Phi_F(t, nT_0)\,\hat{x}(nT_0),\ nT_0 \le t < (n+1)T_0$$

where, as before, Φ_F is the primary matrix solution for

$$\dot{x}(t) = (A + BF)x(t)$$

The information available from the continuous measurements is included, and the state estimate is expressed as

$$\hat{x}(t) = I_1 x(t) + I_2 \Phi_F(t, nT_0)\hat{x}(nT_0),\ nT_0 \le t < (n+1)T_0 \qquad (15)$$

Note that for $t = nT_0$,

$$\begin{aligned}\hat{x}(nT_0) &= I_1 x(nT_0) + I_2 \Phi_F(nT_0, nT_0)\hat{x}(nT_0)\\ &= I_1 x(nT_0) + I_2\left[I_1 x(n, T_0) + \hat{w}(nT_0)\right]\\ &= I_1 x(nT_0) + \hat{w}(nT_0)\end{aligned}$$

since

$$I_2 \hat{w}(nT_0) = \hat{w}(nT_0)$$

Thus Equation 15 is consistent with Equation 14.

It is assumed that the sample data measurements are of the form

$$y(nT_0) = Hx(nT_0) + \eta(nT_0)$$

which is consistent with the measurement model described in Section 3.3 where

$$y = d + y_1 + y_2 + \eta$$

It is further assumed that $HI_1 = 0$, which is equivalent to assuming that none of the continuously measured states are involved with the sample data measurement. Then, using n for nT_0,

$$\begin{aligned} y(n) &= Hx(n) + \eta(n) \\ &= H(I_1 + I_2)x(n) + \eta(n) \\ &= HI_2 x(n) + \eta(n) \end{aligned}$$

and

$$y(n) = Hw(n) + \eta(n) \tag{16}$$

and the problem is structured so that the discrete Kalman filter equations can be used to obtain the expression for $\hat{w}(n)$. The development of the filter equations is deferred to the next section where the system equations are discretized and a difference equation is developed for the system state and the estimation error.

3.7 DEVELOPMENT OF THE SYSTEM AND ESTIMATION DIFFERENCE EQUATIONS, ZERO MEAN

At this point, the structure of the landing approach model has been definitized to the point that a block diagram of the process can be developed. Such a diagram is given in Figure 5. As previously mentioned, the control law is developed for the case where the steady winds and wind shear are not considered. The effects of these disturbances on the system are then evaluated in the absence of the stochastic disturbances and measurement noise to determine the mean value of the process at the window or decision altitude. In this section the discretized equations for the state and the estimation error are developed for the case where the steady winds and wind shear disturbances are not considered. Since the gust disturbances and measurement noise are zero mean processes, the resulting difference equations are a zero mean process.

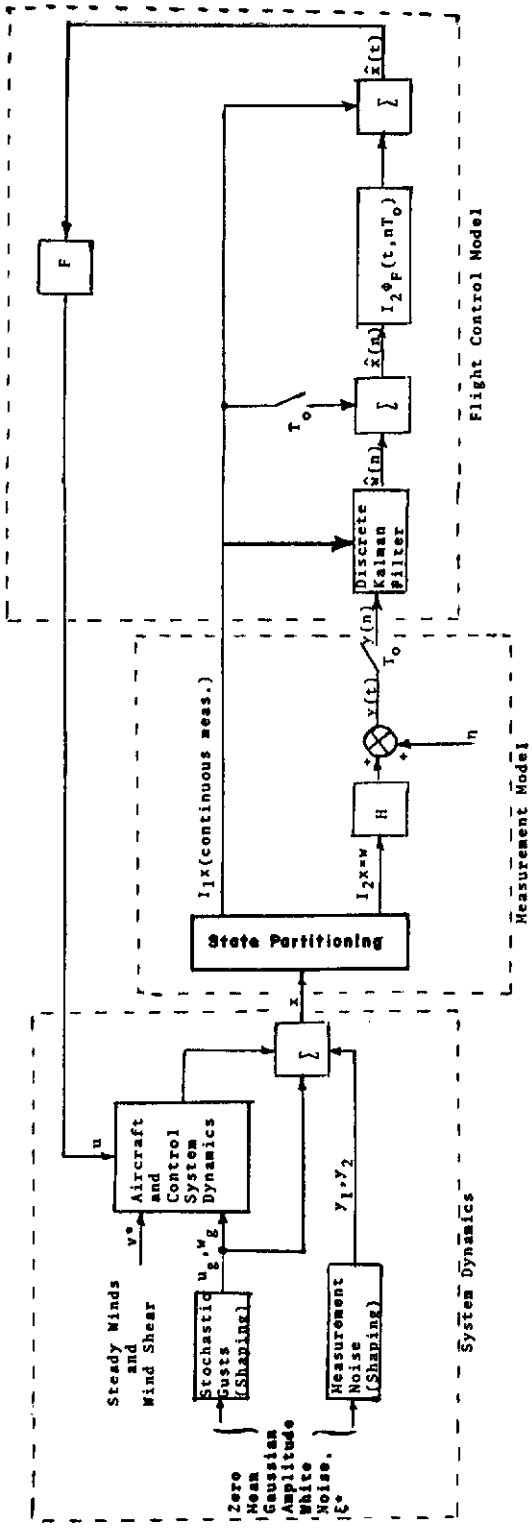

Figure 5. Block Diagram of the Landing Approach Model

First of all the form of the state estimate, Equation 15, and the feedback law, Equation 8, are substituted into the system differential equation given by Equation 2 (where the steady wind and wind shear disturbances are not included). Then on $nT_0 \leq t < (n+1)T_0$

$$\dot{x}(t) = (A + BFI_1)x(t) + BFI_2 \Phi_F(t, nT_0)\hat{x}(nT_0) + \xi^*(t)$$

The solution to this stochastic differential equation can be expressed formally as

$$x(t) = \Phi_I(t, nT_0)x(nT_0) + \int_{nT_0}^{t} \Phi_I(t,s)\, BFI_2\, \Phi_F(t, nT_0)\hat{x}(nT_0)\, ds + \int_{nT_0}^{t} \Phi_I(t,s)\, \xi^*(s)\, ds$$

where Φ_I is the primary matrix solution for

$$\dot{x}(t) = (A + BFI_1)x(t)$$

For $t = (n+1)T_0$ and using the notation n for nT_0 and n + 1 for $(n+1)T_0$, then

$$x(n+1) = \Phi_I(n+1, n)x(n) + \int_{n}^{n+1} \Phi_I(n+1, s)\, BFI_2\, \Phi_F(s, n)\, ds\, \hat{x}(n) + \int_{n}^{n+1} \Phi_I(n+1, s)\, \xi^*(s)\, ds$$

Then the discretized state equations are of the form

$$x(n+1) = A_n x(n) + B_n \hat{x}(n) + \xi(n) \tag{17}$$

where

$$A_n = \Phi_I(n+1, n) \tag{18}$$

$$B_n = \int_n^{n+1} \Phi_I(n+1, s) BFI_2 \Phi_F(s, n) ds \tag{19}$$

$$\xi_{(n)} = \int_n^{n+1} \Phi_I(n+1, s) \xi^*(s) ds \tag{20}$$

In Equation 17, $\xi(n)$ is a sequence of zero mean, Gaussian amplitude random variables. Also

$$E\left\{\xi(n)\,\xi(m)'\right\} = S\,\delta_{nm} \tag{21}$$

where δ_{nm} is the Kronecker delta and

$$S = \int_n^{n+1} \Phi_I(n+1, s) S^* \Phi_I(n+1, s)' ds$$

and S* is defined by the relationship

$$E\left\{\xi^*(t)\,\xi^*(s)\right\} = S^*\,\delta(t-s)$$

Substitute the expression for $\hat{x}(n)$ into Equation 17 and

$$x(n+1) = (A_n + B_n I_1) x(n) + B_n \hat{w}(n) + \xi(n) \tag{22}$$

Equation 22 is a difference equation in the state, x, and the output of the discrete Kalman filter $\hat{w}$.

The difference equation for w is obtained by multiplying Equation 22 by I_2. Then

$$\begin{aligned} w(n+1) &= I_2(A_n + B_n)(I_1 + I_2) x(n) \\ &\quad + I_2 B_n \hat{w}(n) + I_2 \xi(n) \\ &= I_2 A_n w(n) + I_2(A_n + B_n) I_1 x(n) \\ &\quad + I_2 B_n \hat{w}(n) + I_2 \xi(n) \end{aligned} \tag{23}$$

The simplifications result from the fact that $I_1 I_1 = I_1$ and $I_1 I_2 = 0$. From the observation equation

$$y(n) = Hw(n) + \eta(n) \tag{16}$$

and the difference equation for w, the discrete Kalman filter equations for $\hat{w}$ can be developed.

The Kalman filter equations are developed based upon the formulation given in Reference 10. Assuming that the error covariance matrix has reached a steady-state condition, the estimate of w(n+1) is

$$\hat{w}(n+1) = \bar{w}(n+1) + K\left[y(n+1) - H\bar{w}(n+1) \right]$$

where K is the optimal filter gains and

$$\bar{w}(n+1) = E\left\{ w(n+1) \setminus y(0), \ldots, y(n) \right\}$$

Use the expression for w(n+1) given by Equation 23 to obtain

$$\begin{aligned} \bar{w}(n+1) &= E\left\{ I_2 A_n w(n) + I_2 (A_n + B_n) I_1 x(n) \right. \\ &\qquad \left. + I_2 B_n \hat{w}(n) + I_2 \xi(n) \setminus y(0), \ldots, y(n) \right\} \\ &= I_2 A_n \hat{w}(n) + I_2 (A_n + B_n) I_1 x(n) \\ &\qquad + I_2 B_n \hat{w}(n) \end{aligned}$$

since $I_1 x(n)$ are known and

$$\hat{w}(n) = E\left\{ w(n) \setminus y(0), \ldots, y(n) \right\}$$

Thus,

$$\bar{w}(n+1) = I_2 (A_n + B_n)\left[\hat{w}(n) + I_1 x(n) \right]$$

Use the difference equation for x (Equation 22), to express y(n+1) in terms of x(n) and $\hat{w}(n)$. Then

$$y(n+1) = HI_2\left[A_n w(n)+(A_n+B_n)I_1 x(n) + B_n \hat{w}(n)+\xi(n)\right]+\eta(n+1) \tag{24}$$

Now the equation for $\hat{w}(n+1)$ can be written as

$$\begin{aligned}\hat{w}(n+1) = &\left[I_2(A_n+B_n)-KHI_2A_n\right]\hat{w}(n)\\ &+\left[I_2(A_n+B_n)I_1+KHI_2A_nI_2\right]x(n)\\ &+KHI_2\xi(n)+K\eta(n+1)\end{aligned} \tag{25}$$

Equations 22 and 25 make up a system of difference equations for the state, x, and the estimate of w, $\hat{w}$.

Denote the estimation error at time n as e(n), then

$$e(n) = w(n)-\hat{w}(n)$$

Equations 23 and 25 are used to derive the difference equation for e,

$$\begin{aligned}e(n+1) = &\left[(I-KH)I_2A_n\right]e(n)\\ &+(I-KH)I_2\xi(n)-K\eta(n+1)\end{aligned} \tag{26}$$

Use the relationship

$$e(n) = I_2x(n)-\hat{w}(n)$$

or

$$\hat{w}(n) = I_2x(n)-e(n)$$

with Equation 22 to obtain

$$x(n+1) = (A_n+B_n)x(n)-B_ne(n)+\xi(n) \tag{27}$$

Equations 26 and 27 make up a system of difference equations in the state, x, and the estimation error, e.

Let

$$z(n) = \begin{bmatrix} x(n) \\ e(n) \end{bmatrix}$$

and

$$\zeta(n) = \begin{bmatrix} \xi(n) \\ \eta(n+1) \end{bmatrix}$$

Then the difference equation for state and estimation error can be written as

$$z(n+1) = A_T z(n) + B_T \zeta(n) \tag{28}$$

where

$$A_T = \begin{bmatrix} A_n + B_n & -B_n \\ 0 & (I - KH) I_2 A_n \end{bmatrix}$$

$$B_T = \begin{bmatrix} I & 0 \\ (I - KH) I_2 & -K \end{bmatrix}$$

Recall that A_n and B_n are given by Equations 18 and 19, respectively. Also

$$E\left\{ \zeta(n)\, \zeta(m)' \right\} = \begin{bmatrix} S & 0 \\ 0 & V \end{bmatrix} \delta_{nm}$$

where S is defined by Equation 21 and V is defined by

$$E\left\{ \eta(n)\, \eta(m)' \right\} = V \delta_{nm}$$

The steady-state discrete filter gains matrix, K, is the solution to the simultaneous matrix equations

$$K = PH'V^{-1}$$

$$P = (I-KH)I_2 A_n P A_n' I_2'(I-KH)' + (I-KH)I_2 S I_2'(I-KH)' + KVK'$$

Note that P is the steady-state estimation error covariance matrix.

A_n and B_n given by Equations 18 and 19, respectively, depend upon the feedback matrix F. Thus, the separation property (i.e., the separation of the feedback and estimator problems) of the linear, quadratic, Gaussian problem is sacrificed by using the sub-optimal estimator derived in this section.

Equation 28 defines the system model structure. Once the weighting coefficients in the quadratic cost functional [Equation 9 or 10] are determined so that the probability of a missed approach is minimized subject to rms constraints on the control activity, then the feedback matrix, F, and subsequently the filter gains, K, are determined, and the system dynamics are defined in terms of the difference equation of Equation 28.

3.8 DEVELOPMENT OF THE SYSTEM AND ESTIMATION DIFFERENCE EQUATION, DETERMINISTIC DISTURBANCES INCLUDED

The next step of the procedure is to account for effect of the deterministic inputs as represented by the steady wind and wind shear. In this section the equations are developed which provide for the determination of these effects within the framework of the discrete system Equation 28.

Recall from Section 3.2 that the velocity of the deterministic winds, w_d, is given by the expression

$$w_d = w_{st} + w_{sh}$$

where w_{st} is the steady-wind velocity and w_{sh} is the wind-shear velocity given by

$$w_{s_h} = \begin{cases} 0, & h > 200 \text{ ft} \\ s_h(200 - h), & 100 \text{ ft} \le h \le 200 \text{ ft} \end{cases}$$

where s_h is the velocity gradient and h is altitude. Also w_d is resolved into longitudinal and normal components, u_w and w_w respectively, and they are

$$u_w = w_d \left[\cos \gamma_o - \theta \sin \gamma_o \right]$$

$$w_w = w_d \left[\sin \gamma_o + \theta \cos \gamma_o \right]$$

It was mentioned in Section 3.3. that, in order to consider airspeed as a continually sensed variable, the deviation from the nominal airspeed, u_{as}, is introduced as a state variable using

$$u_{as} = u - u_g - u_w$$

and the differential equation for u_{as} is developed from the relationship

$$\dot{u}_{as} = \dot{u} - \dot{u}_g - \dot{u}_w$$

The state variable u (longitudinal velocity) is then replaced in the system equations by $u_{as} + u_g + u_w$. In writing the system differential equations,

$$\dot{x}(t) = Ax(t) + Bu(t) + \xi^*(t) + v^*(x(t), t), \tag{1}$$

v* is made up of all the terms in the system equation introduced by the deterministic wind model for steady wind and wind shear. (v* = 0 was assumed in the developments of the three preceding sections.)

Including the expression for the control, u, the system equation becomes

$$\begin{aligned} \dot{x}(t) = {} & (A + BFI_1)\, x(t) + BFI_2\, \Phi(t, nT_o)\, I_1\, x(nT_o) \\ & + BFI_2\, \Phi(t, nT_o)\, \hat{w}(nT_o) \\ & + \xi^*(t) + v^*(x(t), t) \end{aligned} \tag{29}$$

The mean value of the states at the window can now be determined by making $\xi^* = 0$ and $\eta = 0$ and integrating Equation 29 in conjunction with the discrete Kalman filter equations,

$$\hat{\bar{w}}(n+1) = \bar{w}(n+1) + K\left[y(n+1) - H\bar{w}(n+1)\right]$$

$$\bar{w}(nH) = I_2(A_n + B_n)\left[\hat{\bar{w}}(n) + I_1 x(n)\right]$$

down to the 100-ft-decision altitude.

An approximation to this approach was taken in the actual computation. The simplification made is based on the assumption that

$$v^*(x(t),t) \doteq v^*(x(n),n),\ nT_0 \le t < (n+1)T_0$$

where, as before, nT_0 and n are used interchangeably. For the range of sample rates considered this is a reasonable approximation, since the state variables involved in the definition of v* will be changing relatively slowly, compared to the sample frequency, for a steady-wind plus shear-wind disturbance.

With this assumption, the discrete representation of Equation 29 can be written

$$x(n+1) = (A_n + B_n I_1)x(n) + B_n \hat{\bar{w}}(n) + \xi(n) + v(n) \tag{30}$$

where

$$\begin{aligned} v(n) &= \left[\int_n^{n+1} \Phi_I(n+1,s)\,ds\right] v^*(x(n),n) \\ &= c_n\, v^*(x(n),n) \end{aligned} \tag{31}$$

Furthermore, the difference equation for the states processed by the discrete Kalman filter becomes

$$\begin{aligned} w(n+1) = {} & I_2 A_n w(n) + I_2(A_n + B_n) I_1 x(n) \\ & + I_2 B_n \hat{\bar{w}}(n) + I_2 \xi(n) + I_2 v(n) \end{aligned} \tag{32}$$

The input to the discrete Kalman Filter is

$$y(n) = H w(n) + \eta(n) \tag{16}$$

From Equation 32, the input to the discrete Kalman filter can be written as

$$\begin{aligned} y(n+1) = H I_2 \Big[& A_n w(n) + (A_n + B_n) I_1 x(n) \\ & + B_n w(n) + \xi(n) + v(n) \Big] + \eta(n+1) \end{aligned} \tag{33}$$

The input to the filter given by Equation 33 can be expressed by replacing $\xi(n)$ by $\xi(n) + v(n)$ in Equation 24, which is the input to the discrete Kalman filter for the case where $v^* = 0$. Since the filter is linear, the output of the filter, $\hat{w}$, can be obtained from Equation 25, the filter output for the case where $v^* = 0$, by replacing $\xi(n)$ by $\xi(n) + v(n)$. Doing this,

$$\begin{aligned} \hat{w}(n+1) = & \Big[I_2 (A_n + B_n) - K H I_2 A_n \Big] \hat{w}(n) \\ & + \Big[I_2 (A_n + B_n) I_1 + K H I_2 A_n I_2 \Big] x(n) \\ & + K H I_2 \xi(n) + K H I_2 v(n) + K \eta(n+1) \end{aligned} \tag{34}$$

Denote

$$e(n) = w(n) - \hat{w}(n)$$

From Equations 30 and 34

$$\begin{aligned} x(n+1) = & (A_n + B_n) x(n) - B_n e(n) \\ & + \xi(n) + v(n) \end{aligned} \tag{35}$$

$$\begin{aligned} e(n+1) = & \Big[(I - K H) I_2 A_n \Big] e(n) + (I - K H) I_2 \xi(n) \\ & + (I - K H) I_2 v(n) \\ & + K \eta(n+1) \end{aligned} \tag{36}$$

So for

$$z(n) = \begin{bmatrix} x(n) \\ e(n) \end{bmatrix}$$

$$\xi(n) = \begin{bmatrix} \xi(n) \\ \eta(n+1) \end{bmatrix}$$

and

$$w_T(n) = \begin{bmatrix} v(n) \\ 0 \end{bmatrix}$$

Equations 35 and 36 can be combined in terms of z as follows:

$$z(n+1) = A_T z(n) + B_T \xi(n) + B_T w_T(n) \tag{36}$$

where, as before,

$$A_T = \begin{bmatrix} A_n + B_n & -B_n \\ 0 & (I - KH) I_2 A_n \end{bmatrix}$$

$$B_T = \begin{bmatrix} I & 0 \\ (I - KH) I_2 & -K \end{bmatrix}$$

The stochastic difference Equation 36 is taken as the dynamic model for the low visibility approach process.

3.9 COMPUTATION OF THE PROBABILITY OF A MISSED APPROACH

With the assumptions made in this section, the process described by Equation 36 is Gaussian. Under these conditions, the mean and covariance of the state at the window (i.e., the 100-ft-decision altitude) completely define the probability distribution at the window, which is used to compute the probability of a missed approach.

First of all, with no steady wind and wind shear, $v^* = 0$, and consequently $v = 0$. Under this condition, the process described by the difference Equation 36 is zero mean and Gaussian, since $\xi(n)$ is a zero-mean Gaussian-amplitude sequence. The difference equation is

$$z(n+1) = A_T z(n) + B_T \zeta(n) \tag{28}$$

and the steady-state covariance matrix,

$$Z = \lim_{n \to \infty} E\left\{ z(n)\, z(n)' \right\} \tag{37}$$

is the solution to

$$Z = A_T Z A_T' + B_T \psi B_T'$$

where

$$\psi = \begin{bmatrix} S & 0 \\ 0 & V \end{bmatrix}$$

Thus, the probability distribution at the window is completely defined by Z and the probability of a missed approach (PMA) can be computed.

In the case where $v \neq 0$, the problem is more complicated since

$$v(n) = C_n v^*(x(n), n) \tag{31}$$

and this input is state dependent. Furthermore, with nonzero wind shear, v^* includes terms in "θh." To be precise, the longitudinal and normal components of the steady wind and wind shear are

$$\begin{aligned} u_w &= w_d \left[\cos \gamma_0 - \theta \sin \gamma_0 \right] \\ &= (w_{st} + w_{sh})(\cos \gamma_0 - \theta \sin \gamma_0) \\ &= \begin{cases} w_{st}(\cos \gamma_0 - \theta \sin \gamma_0), & h > 200\,\text{ft} \\ \left[w_{st} + s_h(200 - h) \right](\cos \gamma_0 - \theta \sin \gamma_0), & 100\,\text{ft} \le h \le 200\,\text{ft} \end{cases} \end{aligned} \tag{39}$$

and

$$w_w = \begin{cases} w_{st}(\sin\gamma_o + \theta\cos\gamma_o), & h > 200\,ft \\ \left[w_{st} + s_n(200 - h)\right](\sin\gamma_o + \theta\cos\gamma_o), & 100\,ft \le h \le 200\,ft \end{cases} \quad (40)$$

Thus v(n) may even be nonlinear in the states (i.e., if $s_h \neq 0$), and the Gaussian distribution for z is no longer guaranteed. In order to deal with this problem, the relative magnitudes of the variables under consideration must be examined.

First of all, altitude, h, as a function of time is dominated by the nominal longitudinal speed, U_o, and the nominal glide path angle, γ_o. Although the aircraft state variables enter into the altitude rate, they only define perturbations about the nominal altitude rate defined by U_o and γ_o. For h in the order of 100 ft, these perturbations are second order and it may be assumed that in fact h is approximately deterministic.

The expression for u_w, given by Equation 32, involves ($\cos\gamma_o + \theta \sin\gamma_o$) and for a nominal glide path angle of between -3° and -6° and for small values of perturbed pitch attitude,

$$\cos\gamma_o + \theta\sin\gamma_o \doteq \cos\gamma_o$$

Thus the expression for u_w is weakly dependent on pitch attitude, θ.

The dependence of w_w on θ is more profound, however. The term ($\sin\gamma_o + \theta\cos\gamma_o$) can be approximated by $\gamma_o + \theta$ for small values of γ_o and θ. Assume a worst case rms value for θ of 0.05 rad. Values of this magnitude were encountered with the CH-53A. For the DC-8 a worst case rms value for θ of 0.02 rad could be assumed (see data given in Appendix A). This corresponds to the θ response with a rms normal gust, σ_{wg}, of 6.5 ft/sec. From Table II, the extreme ranges for w_d are -32.2 to 49.0 ft/sec. Thus for the worst absolute value of w_d, the rms value

of w_w is 2.5 ft/sec. The root sum squared value of w_g and w_w is 6.9 ft/sec compared to the rms value of w_g of 6.5 ft/sec. Thus the gust dominates the stochastic contribution of the normal winds.

With nonzero wind and wind shear, the following assumptions are made.

(1) The z in the difference Equation 36 is Gaussian, (i.e., altitude is essentially deterministic and consequently v* is linear in the states).

(2) $\overline{v^*(x(t),t)} \doteq v^*(\overline{x(t)},t)$, where the over bar is used to denote mean value. This follows from h being approximately deterministic and consequently v* is linear in the states.

(3) $v^*(\overline{x(t)},t) \doteq v^*(x(t),t)$. This is based on the assumption that the stochastic contribution of the steady-wind and wind-shear effects can be neglected in comparison to the gust effects.

With these assumptions, the difference equation for the mean value of z, $\bar{z}$, is

$$\bar{z}(n+1) = A_T \bar{z}(n) + B_T \begin{bmatrix} C_n v^*(\bar{x}(n), n) \\ 0 \end{bmatrix} \qquad (41)$$

$$= A_T \bar{z}(n) + B_T \bar{w}_T(n)$$

First s_h is taken to be zero and the steady-state value of $\bar{z}$ is computed from Equation 41. This corresponds to the mean value of z at 200 ft altitude. Then with the specified value of s_h, the difference Equation 41 is iterated, starting with the steady-state value, through -100 ft altitude to give a mean value of z corresponding to the 100-ft-decision altitude.

With assumption (3) above

$$z(n-1) - \bar{z}(n-1) = A_T \left[z(n) - \bar{z}(n) \right] + B_T \xi(n)$$

and the steady-state covariance matrix can be determined from Equation 38 as in the case where v = 0. In this case

$$Z = \lim_{n \to \infty} E\left\{\left[z(n) - \bar{z}(n)\right]\left[z(n) - \bar{z}(n)\right]'\right\}$$

With the Gaussian distribution for z, the mean value of z at the window and the steady-state covariance matrix define the probability distribution at the window. The probability of making the approach is computed by integrating across the tolerances in the motion variables that define the window. PMA is one minus this value. For example, using the glideslope window of $\pm$ 12 ft,

$$PMA = 1 - \frac{1}{\sqrt{2\pi}\,\sigma_d} \int_{-12-\bar{d}}^{12-\bar{d}} e^{-\frac{1}{2\sigma_d^2} x^2} \, dx$$

This result is easily generalized to a normal distribution function of more than one variable (for example, see Reference 3).

In the case where the fixed bias error between the reference glideslope track and the true reference glideslope is not zero, the rms glideslope deviation, σ_d, is taken to be the root-sum-square of the rms fixed bias error and the rms glideslope deviation due to atmospheric disturbance inputs and measurement noise.

SECTION IV

DEFINITIZED MODELS FOR THE DC-8 AND THE CH-53A

In this section, the system equations are definitized for the DC-8 and the CH-53A helicopter. This is done by definitizing Equations 1 and 16 for each aircraft. The aircraft stability derivatives, the system parameters, the continuously measured states, and the window definition are also given for a "baseline" configuration for each aircraft. All of the other cases considered are basically variations from the "baseline" configurations and the detailed variations from the baseline configuration are identified by case number and described individually.

4.1 DC-8

4.1.1 DC-8 "Baseline" Configuration, Case D1

The linear perturbed longitudinal equations of motion for the DC-8 were taken from Reference 1 and they are*

$$\dot{u} = X_u u + X_w w - g\theta\cos\gamma_o - X_u u_g - X_w w_g + X_{\delta_e}\delta_e + X_{\delta_{th}}\delta_{th} - X_u u_w - X_w w_w$$

$$\dot{w} = Z_u u + Z_w w + u_o q - g\theta\sin\gamma_o - Z_u u_g - Z_w w_g + Z_{\delta_e}\delta_e + Z_{\delta_{th}}\delta_{th} - Z_u u_w - Z_w w_w$$

$$\dot{q} = M_u u + M_w w + M_q q - M_u u_g - M_w w_g + M_{\delta_e}\delta_e + M_{\delta_{th}}\delta_{th} - M_u u_w - M_w w_w$$

$$\dot{\theta} = q$$

$$\dot{d} = u_o\theta - w$$

*$Z_{\dot{w}}$ and $M_{\dot{w}}$ were taken to be zero in these equations.

The system differential Equation 1 was derived in Reference 3 and is repeated here. For the system differential equation

$$\dot{x}(t) = Ax(t) + Bu(t) + \xi^*(t) + v^*(x(t),t), \tag{1}$$

$$X = \begin{bmatrix} u_{as} \\ w \\ q \\ \theta \\ u_g \\ w_g \\ y_1 \\ y_2 \\ d \\ \delta_e \\ \delta_{th} \end{bmatrix}$$

$$A = \begin{bmatrix}
X_u & X_w & 0 & -g\cos\gamma_o & \omega_{ug} & -X_w & 0 & 0 & 0 & X_{\delta e} & X_{\delta th} \\
Z_u & Z_w & U_o & -g\sin\gamma_o & 0 & -Z_w & 0 & 0 & 0 & Z_{\delta e} & Z_{\delta th} \\
M_u & M_w & M_q & 0 & 0 & -M_w & 0 & 0 & 0 & M_{\delta e} & M_{\delta th} \\
0 & 0 & 1 & 0 & 0 & 0 & 0 & 0 & 0 & 0 & 0 \\
0 & 0 & 0 & 0 & -\omega_{ug} & 0 & 0 & 0 & 0 & 0 & 0 \\
0 & 0 & 0 & 0 & 0 & -\omega_{wg} & 0 & 0 & 0 & 0 & 0 \\
0 & 0 & 0 & 0 & 0 & 0 & -\omega_{bb} & 0 & 0 & 0 & 0 \\
0 & 0 & 0 & 0 & 0 & 0 & 0 & -\omega_{fn} & 0 & 0 & 0 \\
0 & -1 & 0 & U_o & 0 & 0 & 0 & 0 & 0 & 0 & 0 \\
0 & 0 & 0 & 0 & 0 & 0 & 0 & 0 & 0 & \frac{-1}{Te} & 0 \\
0 & 0 & 0 & 0 & 0 & 0 & 0 & 0 & 0 & 0 & \frac{-1}{Tt}
\end{bmatrix}$$

$$B = \begin{bmatrix}
0 & 0 \\
0 & 0 \\
0 & 0 \\
0 & 0 \\
0 & 0 \\
0 & 0 \\
0 & 0 \\
0 & 0 \\
0 & 0 \\
\frac{1}{Te} & 0 \\
0 & \frac{1}{Tt}
\end{bmatrix}, \quad u = \begin{bmatrix} \delta_{ec} \\ \delta_{thc} \end{bmatrix}, \quad \xi^* = \begin{bmatrix}
-\xi_u \\ 0 \\ 0 \\ 0 \\ \xi_u \\ \xi_w \\ \xi_{bb} \\ \xi_{fn} \\ 0 \\ 0 \\ 0
\end{bmatrix}$$

$$v^* = \begin{bmatrix} -X_w w_d \sin\gamma_o - \dot{w}_d \cos\gamma_o + q w_d \sin\gamma_o - \theta X_w w_d \cos\gamma_o \\ -Z_w w_d \sin\gamma_o - \theta Z_w w_d \cos\gamma_o \\ -M_w w_d \sin\gamma_o - \theta M_w w_d \cos\gamma_o \\ 0 \\ 0 \\ 0 \\ 0 \\ 0 \\ 0 \\ 0 \\ 0 \end{bmatrix}$$

where

$$w_d = \begin{cases} \omega_{st} & , h > 200 \text{ ft} \\ \omega_{st} + s_n (200 - h), & 100 \text{ ft} \leq h \leq 200 \text{ ft} \end{cases}$$

In these equations, the state equation for longitudinal velocity, u, was replaced by a state equation for longitudinal airspeed, u_{as}, so that u_{as} could be considered as a sensed variable. The control vector, u, consists of commanded elevator and thrust inputs (δ_{ec} and δ_{thc}, respectively). The elevator and thrust responses were modeled by first-order lags with time lags of 0.06666 and 1.0 sec, respectively. The explicit dependence of v* on x and h and the approximate linearity of v* with respect to x as discussed in Section 3.9 may be clearly seen.

For the observation equation

$$y(n) = Hx(n) + \eta(n), \tag{16}$$

$$H = \begin{bmatrix} 0 & 0 & 0 & 0 & 0 & 0 & 1 & 1 & 1 & 0 & 0 \end{bmatrix}$$

Thus, with the state vector, x, as defined, y represents a sample data measurement of glideslope deviation from the reference glideslope track corrupted by beam bends, fluctuation noise, and white noise, i.e.,

$$y(n) = y_1(n) + y_2(n) + d(n) + \eta(n)$$

The stability derivatives and aircraft parameters used were generally taken from Reference 1 and are listed in Table IV

TABLE IV

DC-8 STABILITY DERIVATIVES AND AIRCRAFT PARAMETERS, LANDING APPROACH

X_u = -0.03730 1/sec

X_w = 0.13600 1/sec

Z_u = -0.28300 1/sec

Z_w = -0.75000 1/sec

M_u = 0.0 1/sec-ft

M_w = -0.00461 1/sec-ft

M_q = -0.59400 1/sec

$X_{\delta e}$ = 0.0 ft/rad-sec^2

$X_{\delta th}$ = 0.10600 ft/percent RPM-sec^2

$Z_{\delta e}$ = -9.25000 ft/rad-sec^2

$Z_{\delta th}$ = -0.00097 ft/percent RPM-sec^2

$M_{\delta e}$ = -0.92300 1/rad-sec^2

$M_{\delta th}$ = 0.00007 1/percent RPM-sec^2

U_o = 228 ft/sec

γ_o = -3°

T_e = 0.06666 sec

T_t = 1.0 sec

The parameters used to describe the atmospheric disturbances are given in Table V. For the "baseline" configuration the steady wind, w_{st}, and the wind shear, w_{sh}, were taken to be zero. The rms gust intensities

TABLE V

ATMOSPHERIC DISTURBANCE PARAMETERS, DC-8

w_{st}	=	0.0	ft/sec
s_h	=	0.0	ft/sec/ft
σ_{ug}	=	10.00000	ft/sec
ω_{ug}	=	0.34000	rad/sec
σ_{wg}	=	6.50000	ft/sec
ω_{wg}	=	3.95000	rad/sec

used in this case represent severe turbulence. It turns out that this is a fortuitous choice for a baseline consideration inasmuch as the results indicate that landing guidance requirements and flight control requirements for precision approach with a scanning beam guidance system may be dictated by the requirement to suppress gust effects on the aircraft motion. The gust break frequencies, ω_{ug} and ω_{wg} were taken from Reference 1.

The parameters used to define the landing guidance system are given in Table VI and are based on the values given in Table III for a state-of-the-art microwave scanning beam guidance system. A nonzero rms error due to beam bends was assumed. The theoretical errors are multiplied by 3 to account for accuracy degradations that might be encountered in operational practice. The angular errors are converted to the corresponding displacement errors at the 100-ft-decision altitude for a 3° glideslope. These errors are relatively small compared to the errors associated with a conventional ILS landing system (Reference 11).

The 3σ constraints on the control activity are generally defined by the control authority of the automatic flight control system or the physical limitations of the control surface travel and the associated actuators. The control authorities of the automatics are imposed for safety considerations; this allows sufficient manual authority to override a hard over failure of the automatic system. In most current

TABLE VI

LANDING GUIDANCE SYSTEM PARAMETERS, 3° GLIDESLOPE

	Theoretical (deg)	Operational (deg)	100-Ft Decision Altitude
σ_{bias}	0.027	0.081	2.72 ft
σ_{bb}	0.011	0.033	0.96 ft
σ_{fn}	0.018	0.054	1.83 ft
σ_{η} (or $V\frac{1}{2}$)	—	—	0.46 ft
ω_{bb}	—	—	0.0775 rad/sec
ω_{fn}	—	—	$2.8/T_o$ rad/sec

aircraft, the authorities on automatic control system are rather "stingy" and reflect a mistrust in the reliability of the automatics. The control constraints used in the baseline configuration are given in Table VII. The elevator constraint was placed on the 3σ elevator rate (or equivalently actuator rate) since it was believed that this would indirectly result in reasonable 3σ values for elevator deflection (and it indeed did!).

TABLE VII

3σ CONSTRAINTS ON CONTROL ACTIVITY, DC-8

Control Variable	3σ Constraint
Elevator Rate ($\dot{\delta}_e$)	0.44 rad/sec
Engine Thrust Activity (δ_{th})	5.00% RPM

For the baseline configuration, it was assumed that

θ - pitch attitude (perturbed)

q - pitch rate

u_{as} - longitudinal airspeed (perturbed)

were continually sensed (presumably onboard the aircraft). Sensed pitch attitude and pitch rate are fundamental to an automatic flight control system which involves controlling or regulating the short period longitudinal motion of an aircraft. Sensed longitudinal airspeed is also required if the auto-throttle control is to be effective.

For the baseline configuration, the normal deviation of ± 12 ft from the reference glideslope was used to define the 100-ft-decision-altitude window. This is based upon the current FAA longitudinal Category II window definition.

4.1.2 Case D2, Baseline Control, Low Gusts

In this case, the control system model defined by the baseline configuration was used and the inputs corresponding to gust disturbances were reduced. This possibility allows for the evaluation of landing approach performance in a low gust environment with a flight control system designed to suppress severe gust disturbances. The gust intensities used were

$$\sigma_{ug} = 2.5 \text{ ft/sec}$$
$$\sigma_{wg} = 1.0 \text{ ft/sec}$$

4.1.3 Case D3 Baseline Control, Low Gusts and Moderate Beam Bends

As in Case D2, the control system model defined by the baseline configuration was used and the inputs corresponding to gust disturbances were reduced; however, the input corresponding to beam bends was increased. This case allows for the evaluation of landing approach performance with a flight control system designed to suppress severe gust disturbances where in fact a low gust environment is encountered and the beam bends are more severe than in the flight control design consideration. The gust intensities and guidance system parameters used in this case are

$$\sigma_{ug} = 2.5 \text{ ft/sec}$$
$$\sigma_{wg} = 1.0 \text{ ft/sec}$$
$$\sigma_{bb} = 3.0 \text{ ft}$$

4.1.4 Case D4 Baseline Control, Low Gusts and Severe Beam Bends

Case D4 is the same as D3, except that extremely severe beam bends were considered. This allows for the consideration of the case where the low frequency beam bends dominate the glideslope tracking errors. The gust intensities and guidance system parameters used were

$$\sigma_{ug} = 2.5 \text{ ft/sec}$$

$$\sigma_{wg} = 1.0 \text{ ft/sec}$$

$$\sigma_{bb} = 9.6 \text{ ft}$$

4.1.5 Case D5, Low Gusts

This case is similar to Case D2 in the fact that the inputs corresponding to gust disturbances were reduced. However, in this case the control law was optimized for each data rate considered instead of using the control law for the baseline configuration. This allows consideration of the case where the flight control is not designed to regulate against glideslope errors in a severe turbulence environment. The rms gust intensities used in this case are

$$\sigma_{ug} = 2.5 \text{ ft/sec}$$

$$\sigma_{wg} = 1.0 \text{ ft/sec}$$

4.1.6 Case D6, Glideslope Deviation and Airspeed Window

In this case the additional dimension of airspeed perturbation was added to the baseline configuration window definition. This case therefore considers the addition of airspeed tolerances in the missed approach criteria and also demonstrates the generality of the analysis technique with respect to the window definition. To ensure that the control law formulation would be sensitive to airspeed errors, rms perturbed airspeed was added to the quadratic functional of Equation 9. As before, PMA was

minimized, subject to the control constraints described in Section 4.1.1 (baseline configuration), except that

$$J_2(u) = \sigma^2_{u_{as}} + k_1\sigma^2_d + k_2\,\sigma^2_{\delta_e} + k_3\,\sigma^2_{\delta_{th}} \qquad (10)$$

was used to define the feedback matrix. The window was defined as follows:

$$\Delta d = \pm 12.0 \text{ ft}$$

$$\Delta u_{as} = \pm 8.45 \text{ ft/sec}$$

4.1.7 Case D7, 3σ Elevator Deflection Constraint

In this case, the 3σ constraint on elevator rate activity was replaced by a 3σ constraint on the elevator deflection activity. This allows for the consideration of alternative control constraints, and specifically for the case where the control authority associated with the automatic flight control system is more stringent with respect to deflection position than deflection rates (or in the case where full authority was given to the automatics and the physical limitation on elevator deflection dominates the physical limitations on the actuator rates). The 3σ constraints on control activity used in this case are (corresponding to Table VII)

Elevator Position (δ_e) = 0.1266 rad

Engine Thrust Activity (δ_{th}) = 5.00%

4.1.8 Case D8, Relaxed Elevator Rate Constraint

In this case the 3σ constraint on the elevator rate was relaxed from the baseline configuration. This corresponds to the possibility of allowing more authority to the automatic flight control system or using an elevator actuator with an increased rate capability. The 3σ constraints on control activity used in this case are (corresponding to Table VII)

Elevator Actuator Rate ($\dot{\delta}_e$) = 0.88 rad/sec

Engine Thrust Activity (δ_{th}) = 5.00% RPM

4.1.9 Case D9, Direct Lift Control

It has been demonstrated (Reference 12) that glideslope tracking can be significantly improved via direct lift control. Direct lift control implies that the control surfaces are used to generate normal forces on the aircraft without significant changes in pitch attitude. This might be accomplished through the complementary use of a canard and elevator of flaperons and elevator. In the analysis of data rate requirements for future aircraft, the particular implementation is not important, thus in this case a rather idealized direct lift control was considered. This was done within the framework of the baseline configuration by introducing a new control input vector

$$u = \begin{bmatrix} \delta_{ec} \\ \delta_{dc} \end{bmatrix}$$

where δ_{dc} is the commanded direct lift. Thus, the automatic throttle control was replaced by a hypothetical direct lift control.

Additional changes from the baseline configuration involve:

(1) Replacing the thrust lag equation by an actuator lag equation for the hypothetical direct lift control surface,

$$\dot{\delta}_d = \frac{1}{T_d}(-\delta_d + \delta_{dc})$$

where δ_d is the direct lift control surface deflection. T_d was taken to be 0.06666 sec.

(2) Replacing the thrust stability derivatives ($X_{\delta th}$, $Z_{\delta th}$, $M_{\delta th}$) by a hypothetical set of direct lift stability derivatives ($X\delta_d$, $Z\delta_d$, $M\delta_d$). Thus, the A and B matrices and state vector of Equation 1 become

$$A = \begin{bmatrix}
X_u & X_w & 0 & -g\cos\gamma_o & \omega_{ug} & -X_w & 0 & 0 & 0 & X_{\delta e} & X_{\delta d} \\
Z_u & Z_w & U_o & -g\sin\gamma_o & 0 & -Z_w & 0 & 0 & 0 & Z_{\delta e} & Z_{\delta d} \\
M_u & M_w & M_q & 0 & 0 & -M_w & 0 & 0 & 0 & M_{\delta e} & M_{\delta d} \\
0 & 0 & 1 & 0 & 0 & 0 & 0 & 0 & 0 & 0 & 0 \\
0 & 0 & 0 & 0 & -\omega_{ug} & \dot{\theta} & 0 & 0 & 0 & 0 & 0 \\
0 & 0 & 0 & 0 & 0 & -\omega_{wg} & 0 & 0 & 0 & 0 & 0 \\
0 & 0 & 0 & 0 & 0 & 0 & -\omega_{bb} & 0 & 0 & 0 & 0 \\
0 & 0 & 0 & 0 & 0 & 0 & 0 & -\omega_{fn} & 0 & 0 & 0 \\
0 & -1 & 0 & U_o & 0 & 0 & 0 & 0 & 0 & 0 & 0 \\
0 & 0 & 0 & 0 & 0 & 0 & 0 & 0 & 0 & \frac{-1}{Te} & 0 \\
0 & 0 & 0 & 0 & 0 & 0 & 0 & 0 & 0 & 0 & \frac{-1}{Td}
\end{bmatrix}$$

$$B = \begin{bmatrix}
0 & 0 \\
0 & 0 \\
0 & 0 \\
0 & 0 \\
0 & 0 \\
0 & 0 \\
0 & 0 \\
0 & 0 \\
0 & 0 \\
\frac{1}{Te} & 0 \\
0 & \frac{1}{Td}
\end{bmatrix}, \qquad X = \begin{bmatrix}
u_{as} \\
w \\
q \\
\theta \\
u_g \\
w_g \\
y_1 \\
y_2 \\
d \\
\delta_e \\
\delta_d
\end{bmatrix}$$

The direct lift stability derivatives were taken as

$$X_{\delta d} = 0.0 \quad \text{ft/rad} - \text{sec}^2$$

$$Z_{\delta d} = -50.0 \quad \text{ft/rad} - \text{sec}^2$$

$$M_{\delta d} = 0.0 \quad \text{1/rad} - \text{sec}^2$$

$$(T_d = 0.06666 \text{ sec})$$

The $Z_{\delta d}$ value corresponds to a control effectivity of roughly 0.1 g normal acceleration for 4° of surface deflection. The choice of $X_{\delta d} = M_{\delta d} = 0$ causes the direct lift control to be relatively uncoupled from the θ, q, and u_{as} equations (especially since $M_{\dot{w}} = 0$).

The 3σ control constraints used in this case are (corresponding to Table VII)

Elevator Rate ($\dot{\delta}_e$) = 0.44 rad/sec

Direct Lift Control Rate ($\dot{\delta}_d$) = 0.44 rad/sec

The continuously sensed variables were taken to be the same as in the baseline configuration (u_{as}, θ, q). Thus, the full potential of the direct lift control was not realized such as it might be if sensed vertical rate or normal acceleration were considered. This case is conceptually considered in Case C7 for the CH-53A.

4.1.10 Case D10, Continuously Measured $\dot{d}$

In this case, "w" was considered as a continuously measured aircraft variable, along with pitch attitude, pitch rate, and longitudinal airspeed. Since the equation for glideslope deviation rate is

$$\dot{d} = U_o\theta - w$$

This is equivalent to sensing $\dot{d}$ (glideslope deviation rate) continuously.

Physically this might be realized by sensing altitude rate, $\dot{h}$, onboard the aircraft by an inertial system or deriving altitude rate from barometric altitude or radar altitude complemented by a normal accelerometer. In terms of the state vector used in the baseline configuration, Section 4.1.1., the following states were assumed to be continually (and perfectly) measured.

θ - pitch attitude (perturbed)

q - pitch rate

u_{as} - longitudinal airspeed (perturbed)

w - normal velocity (perturbed)

4.1.11 Case D11, Integral Feedback of Glideslope Deviation

The control law described in Section 3.5 does not directly account for disturbances due to the steady wind and wind shear. This can be indirectly accomplished by including a state in the system equations corresponding to integral of glideslope deviation. In this way a linear feedback law given by Equation 8 incorporates an integral control which suppresses steady errors due to steady winds and compensates for wind shears. This is what was done in this case. The following differential equation was included in the system differential Equation 1:

$$\dot{y}_3 = d$$

The changes to x, A, B, ξ^*, and v* in Equation 1 and H in Equation 16 are apparent. In order to force the optimal control law to include a nonzero feedback of the integral of glideslope deviation, the cost functional of Equation 9 was modified to include a weighting on the rms value of y_3 as follows

$$J_1(u) = 0.01\ \sigma^2_{y_3} + \sigma^2_d + k_1\sigma^2_{\delta_e} + k_2\ \sigma^2_{\delta th}$$

The relative weighting on σ^2_d of 100 times that on $\sigma^2_{y_3}$ was somewhat arbitrary; however, it did result in feedback gain ratios for glideslope deviation to elevator/integral of glideslope deviation to elevator in

the range of 16.4 to 14.2 (see Table XXVII of Appendix A for listing by data rate). This compares favorably with the corresponding feedback gain ratio from Reference 1 of 11.3, where a conventional flight control design was considered which included integral feedback of glideslope deviation.

All other details of the baseline configuration were maintained in this case.

4.2 CH-53A

4.2.1 CH-53A "Baseline" Configuration, Case C-1

The linearized longitudinal equations of motion for the CH-53A were taken from Reference 2 and are

$$\begin{aligned}
\dot{u} &= X_u u + X_w w + X_q q + (X_\alpha - g)\theta + X_{\dot{B}_1}\dot{B}_1 \\
&\quad + X_{B_1} B_1 + X_{\delta_c}\delta_c - X_u u_g - X_w w_g \\
&\quad - X_u u_w - X_w w_w \\
\dot{w} &= Z_u u + Z_w w + Z_q q + (Z_\alpha - g\sin\gamma_0)\theta \\
&\quad + Z_{\dot{B}_1}\dot{B}_1 + Z_{B_1} B_1 + Z_{\delta_c}\delta_c \\
&\quad - Z_u u_g - Z_w w_g - Z_q q_g \\
&\quad - Z_u u_w Z_w w_w \\
\dot{q} &= M_u u + M_w w + M_{\dot{w}}\dot{w} + (M_q + M_{\dot{\alpha}})q \\
&\quad + M_\alpha\theta + M_{\dot{B}_1}\dot{B}_1 + M_{B_1} B_1 + M_{\delta_c}\delta_c \\
&\quad - M_u u_g - M_w w_g - M_q q_g \\
&\quad - M_u u_w - M_w w_w \\
\dot{\theta} &= q \\
\dot{d} &= -w
\end{aligned}$$

The gust gradient effect, q_g, is represented by the differential equation

$$\dot{q}_g = -U_o\, a\, q_g - a\, \dot{w}_g$$

The system equations

$$\dot{x}\,(t) = Ax(t) + Bu(t) + \xi^*(t) + v^*(x(t),t) \qquad (1)$$

for the CH-53A are derived in Reference 13 and

$$X = \begin{bmatrix} u_{as} \\ w \\ \theta \\ q \\ u_g \\ w_g \\ q_g \\ B_1 \\ \delta_c \\ d \\ y_1 \\ y_2 \end{bmatrix}$$

$$
A = \begin{bmatrix}
X_u & -X_w & (X_\alpha - g) & X_q & \omega_{ug} & -X_w & 0 & (X_{\delta_1}, X_{\delta_2}, T_{\beta_1}) & X_{\delta_c} & 0 & 0 & 0 \\
-Z_u & Z_w & \left(q_{ss} U_c - Z_\alpha\right) & -Z_q & 0 & Z_w & Z_q & \left(Z_{\delta_1} T_{\beta_1} - Z_{\beta_1}\right) & -Z_{\delta_c} & 0 & 0 & 0 \\
0 & 0 & 0 & 1 & 0 & 0 & 0 & 0 & 0 & 0 & 0 & 0 \\
\left(M_u + M_{\dot{w}} Z_u\right) & \left(M_w + M_{\dot{w}} Z_w\right) & \left\{M_{\dot{w}}\left(Z_\alpha - q_{ss} U_c\right) + M_\alpha\right\} & \left\{M_{\dot{w}} Z_q + M_q + M_{\dot{\alpha}}\right\} & 0 & \left(M_{\dot{w}} Z_w + M_w\right) & \left(M_{\dot{w}} Z_q + M_q\right) & \left\{M_{\dot{w}}\left(Z_{\beta_1} T_{\beta_1} - Z_{\beta_1}\right) - T_{\beta_1}\left(M_{\dot{w}} Z_{\beta_1} + M_{\beta_1}\right)\right\} & \left(M_{\dot{w}} Z_{\delta_c} + M_{\delta_c}\right) & 0 & 0 & 0 \\
0 & 0 & 0 & 0 & -\omega_{ug} & 0 & 0 & 0 & 0 & 0 & 0 & 0 \\
0 & 0 & 0 & 0 & 0 & -\omega_{wg} & 0 & 0 & 0 & 0 & 0 & 0 \\
0 & 0 & 0 & 0 & 0 & a\omega_{wg} & -U_o a & 0 & 0 & 0 & 0 & 0 \\
0 & 0 & 0 & 0 & 0 & 0 & 0 & -T_{\beta_1} & 0 & 0 & 0 & 0 \\
0 & 0 & 0 & 0 & 0 & 0 & 0 & 0 & -T_{\delta_c} & 0 & 0 & 0 \\
0 & 1 & 0 & 0 & 0 & 0 & 0 & 0 & 0 & 0 & 0 & -\omega_{qz} \\
0 & 0 & 0 & 0 & 0 & 0 & 0 & 0 & 0 & 0 & -\omega_{qz} & 0
\end{bmatrix}
$$

$$B = \begin{bmatrix} X_{\dot{B}_1}\tau_{B_1} & 0 \\ Z_{\dot{B}_1}\tau_{B_1} & 0 \\ 0 & 0 \\ \tau_{B_1}(M_w^{\cdot}Z_{\dot{B}_1}+M_{\dot{B}_1}) & 0 \\ 0 & 0 \\ 0 & 0 \\ 0 & 0 \\ \tau_{B_1} & 0 \\ 0 & \tau_{\delta c} \\ 0 & 0 \\ 0 & 0 \\ 0 & 0 \end{bmatrix}, \quad u = \begin{vmatrix} B_{1c} \\ \delta_{cc} \end{vmatrix}, \quad \xi^* = \begin{bmatrix} -\xi_{ug} \\ 0 \\ 0 \\ 0 \\ \xi_{ug} \\ \xi_{wg} \\ -a\xi_{wg} \\ 0 \\ 0 \\ 0 \\ \xi_{y1} \\ \xi_{y2} \end{bmatrix}$$

$$v^* = \begin{bmatrix} -X_w w_d \sin\gamma_o - \theta X_w w_d \cos\gamma_o - \dot{w}_d \cos\gamma_o + q w_d \sin\gamma_o \\ -Z_w w_d \sin\gamma_o - \theta Z_w w_d \cos\gamma_o \\ -(M_w^{\cdot}Z_w + M_w)w_d \sin\gamma_o - \theta(M_w^{\cdot}Z_w + M_w)w_d \cos\gamma_o \\ 0 \\ 0 \\ 0 \\ 0 \\ 0 \\ 0 \\ 0 \\ 0 \\ 0 \\ 0 \end{bmatrix}$$

where

$$w_d = \begin{cases} \omega_{st} & , h > 200 \text{ ft} \\ \omega_{st} + s_n (200 - h), & 100 \text{ ft} \leq h \leq 200 \text{ ft} \end{cases}$$

In these equations, the state equation for longitudinal velocity, u, was replaced by a state equation for longitudinal airspeed, u_{as}, so that u_{as} could be considered as a sensed motion variable. The control vector, u, consists of commanded cyclic pitch, B_{1c}, and commanded collective pitch, δ_{cc}. The cyclic and collective pitch responses, B_1 and δ_c, respectively, were modeled by first-order lags,

$$\dot{B}_1 = -\tau_{B1} B_1 + \tau_{B1} B_{1c}$$

$$\dot{\delta}_c = -\tau_{\delta c} \delta_c + \tau_{\delta c} \delta_{cc}$$

The time constants τ_{B1} and $\tau_{\delta c}$ were taken to be 10.0 sec^{-1} in agreement with Reference 2.

Corresponding to the state vector, x, the H in the observation equation

$$y(n) = H\, x\,(n) + \eta(n) \qquad (16)$$

was taken to be

$$H = \begin{bmatrix} 0 & 0 & 0 & 0 & 0 & 0 & 0 & 0 & 0 & 1 & 1 & 1 \end{bmatrix}$$

This causes the observation to be of the desired form i.e.,

$$y(n) = d(n) + y_1(n) + y_2(n) + \eta(n)$$

The stability derivatives and other aircraft parameters for the CH-53A were taken from Reference 2 and are listed in Table VIII.

The parameters used to describe the atmospheric disturbances are given in Table IX. As for the DC-8, the baseline configuration was defined with zero steady wind and wind shear. The rms gust intensities used in this case represent severe turbulence. The gust break frequencies and the break frequency for the gust gradient were taken from Reference 2.

TABLE VIII

CH-53A STABILITY DERIVATIVES AND AIRCRAFT PARAMETERS*

X_u	= -0.0227	1/sec
X_w	= -0.00053	1/sec
X_α	= -0.05330	ft/rad-sec^2
X_q	= 1.69	ft/rad-sec
$X_{B1}^{\cdot}$	= -1.69	ft/rad-sec
X_{B1}	= 32.3	ft/rad-sec^2
$X_{\delta c}$	= -3.21	ft/rad-sec^2
Z_u	= -0.08930	1/sec
Z_w	= -0.6940	1/sec
Z_α	= -70.3	ft/rad-sec^2
Z_q	= 0.0954	ft/rad-sec
$Z_{B1}^{\cdot}$	= -0.0954	ft/rad-sec
Z_{B1}	= 67.3	ft/rad-sec^2
$Z_{\delta c}$	= -311.0	ft/rad-sec^2
M_u	= 0.0032	rad/sec-ft
$M_w^{\cdot}$	= -0.0021	rad/ft
M_w	= 0.00170	rad/sec-ft
M_α	= 0.171	1/sec^2
$M_\alpha^{\cdot}$	= -0.584	1/sec
M_q	= -0.562	1/sec
$M_{B1}^{\cdot}$	= 0.441	1/sec
M_{B1}	= -4.455	1/sec^2

*Stability derivatives are for trimmed level flight at sea level.

TABLE VIII (CONTD)

$M_{\delta c}$	= 1.95	$1/sec^2$
γ_o	= -6°	
U_o	= 101	ft/sec (60 kts)
τ_{BI}	= 10	1/sec
$\tau_{\delta c}$	= 10	1/sec

TABLE IX

ATMOSPHERIC DISTURBANCE PARAMETERS, CH-53A

w_{st}	= 0.0	ft/sec
w_{sh}	= 0.0	ft/sec
σ_{ug}	= 10.0	ft/sec
ω_{ug}	= 0.15	rad/sec
σ_{wg}	= 6.5	ft/sec
ω_{wg}	= 1.01	rad/sec
a	= 0.0173	1/ft ($a = \sqrt{3}/L_w, L_w$ = 100 ft)

The rms displacement errors at the 100-ft-decision altitude and the corresponding half power frequencies for the landing guidance system were taken to be the same as for the DC-8. These values are given in Table VI. This choice of values for the displacement errors actually assumes poorer accuracy of the landing guidance system than was assumed for the DC-8. In fact, for the angular errors listed in Table VI, the displacement errors at the 100-ft-decision altitude for a 6° glideslope would be about 1/2 those errors for a 3° glideslope (assuming the glideslope transmitter is located at the glideslope intercept point beside the runway). This is because the distance from the glideslope transmitter to the 100-ft-decision altitude for a 6° glideslope is approximately half that distance for a 3° glideslope. Using the values of the displacement errors at the 100-ft-decision altitude from Table VI would, however, correspond to angular errors listed in Table VI for a

6° glideslope if the glideslope transmitter is located approximately 1000 ft forward of the aircraft's glideslope intercept point with the runway.

The 3σ constraints on control activity used for the baseline configuration for the CH-53A was based on a set of working control authorities for the CH-53A as taken from Reference 3 and given in Table X. The limits defined by Table X serve as 3σ constraints on the control activity and if these constraints are satisfied, the limits will only be exceeded 0.26% of the time. Only the rate limits were considered in the determination of the control law based on the assumption that this would indirectly result in 3σ angular deflections less than those given in Table X. This turned out to be the case. In defining the 3σ constraint on $\dot{B}_1$, the distinction between the rate contribution due to the SAS and the rate contribution due to the AFCS was not made. In fact, the rate limit for the $B_{1\ AFCS}$ was used to define the rate limit for B_1. This results in a particular stringent authority limit for the automatics. The resulting control constraints used in the baseline configuration are given in Table XI. In Case C-5 described in Section 4.2.5, these limits were relaxed.

TABLE X

WORKING CONTROL AUTHORITIES AND RATE LIMITS FOR THE CH-53A

Control	Control Authority	Rate Limits
B_{1SAS}	± 2.7 deg (± 0.047 rad)	None
B_{1AFCS}	± 12.4 deg (± 0.216 rad)	5.4 deg/sec (0.094 rad/sec)
δ_c	± 5.9 deg (± 0.103 rad)	2.6 deg/sec (0.0454 rad/sec)

SAS - Stability Augmentation System
AFCS - Automatic Flight Control System

TABLE XI

3σ CONSTRAINTS ON CONTROL ACTIVITY, CH-53A

Control Variable	3σ Constraint
Cyclic Pitch Rate (B_1)	0.0942 rad/sec
Collective Pitch Rate (δ_c)	0.0453 rad/sec

The continually sensed states for the CH-53A baseline configuration were taken to be the same as for the DC-8 baseline configuration, i.e.,

θ - pitch attitude (perturbed)

q - pitch rate

u_{as} - longitudinal airspeed (perturbed)

Also as in the case of the DC-8 baseline configuration, the normal deviation of $\pm$ 12 ft from the reference glideslope was used to define the 100-ft-decision-altitude window for the CH-53A baseline configuration.

4.2.2 Case C2, Baseline Control, Low Gusts

In this case, as in Case D2, the control system model defined by the baseline configuration was used and the inputs corresponding to gust disturbances were reduced. This possibility allows for evaluation of landing approach performance in a low gust environment where with a flight control system designed to suppress severe gust disturbances. The gust intensities used were

$\sigma_{ug} = 2.5$ ft/sec

$\sigma_{wg} = 1.0$ ft/sec

4.2.3 Case C3, Baseline Control, Moderate Beam Bends

As in Case C2, the control system model defined by the baseline configuration was used; however, the input corresponding to beam bends

was increased. This allows for consideration of the case where turbulence is encountered and the beam bends are greater than might be expected in normal operations. The rms-beam-bends error was taken to be

$$\sigma_{bb} = 3.1 \text{ ft}$$

4.2.4 Case C4, Baseline Control, Severe Beam Bends

Case C4 is the same as C3, except that extremely severe beam bends were considered. The rms-beam-bends error was

$$\sigma_{bb} = 9.6 \text{ ft}$$

4.2.5 Case C5, Severe Beam Bends

This case is similar to C5 in the fact that the input corresponding to the beam-bends error was increased. However, in this case the control law was optimized for each data rate considered. This allows consideration of the case where the flight control system design accounts for severe beam bends (and as it turns out, the glideslope tracking errors are dominated by the low frequency beam bends). The rms-beam-bends error was taken to be

$$\sigma_{bb} = 9.6 \text{ ft}$$

4.2.6 Case C6, Relaxed Control Rate Constraints

In this case the 3σ constraints on the control rates were relaxed from the baseline configuration. This corresponds to the possibility of allowing more authority to the automatic flight control system with respect to the rate constraints. The 3σ constraints on control activity used in this case are (corresponding to Table XI)

Cyclic Pitch Rate (B_1) = 0.141 rad/sec

Collective Pitch Rate (δ_c) = 0.119 rad/sec

4.2.7 Case C7, Continually Measured $\dot{d}$

In this case, "w" was considered as a continuously measured aircraft variable, along with pitch attitude, pitch rate, and longitudinal airspeed. Since equation for glideslope deviation rate is

$$\dot{d} = -w$$

this is equivalent to sensing d (glideslope deviation rate). Physically, this might be realized by sensing altitude rate, h, on board the aircraft by an inertial system or deriving altitude rate from barometric altitude or radar altitude complimented by a normal accelerometer. In terms of the state vector used in the baseline configuration, Section 4.1.1., the following states were assumed to be continually (and perfectly) measured.

θ - pitch attitude (perturbed)

q - pitch rate

u_{as} - longitudinal airspeed (perturbed)

w - normal velocity (perturbed)

4.3 W Cases, NonZero Steady Wind and Wind Shear

For each of the cases described in Section 4.1 and 4.2, the effects of steady wind and wind shear on approach performance were considered. As discussed in Section 3.9, the state covariance matrix was determined for the process from the case where the steady wind and wind shear are zero and the "deterministic" steady-wind and wind-shear inputs were used to compute the mean value of the process at the 100-ft-decision altitude (the control law being that one used for the case where the steady wind and wind shear are zero). These cases are designated D1W through D11W and C1W through C7W corresponding to each of the cases described in Sections 4.1 and 4.2.

The steady-wind and wind-shear values used in each of these cases are

$$w_{st} = 42.2 \text{ ft/sec (headwind)}$$

$$s_h = 0.06750 \text{ ft/sec/ft (increasing headwind)}$$

The corresponding deterministic wind profile is shown in Figure 6.

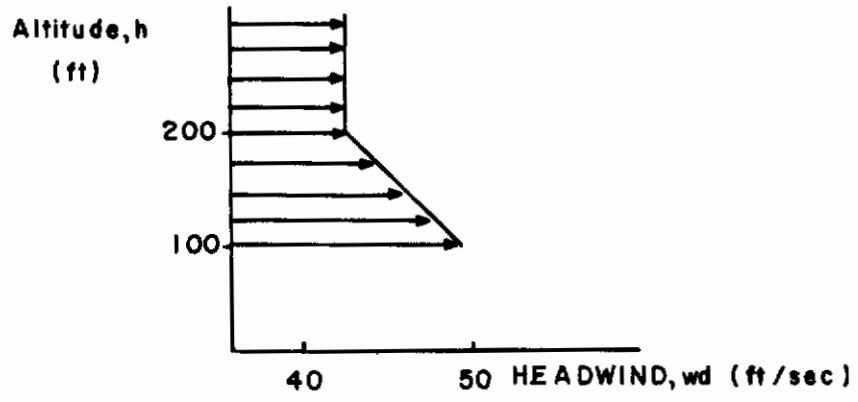

Figure 6. Deterministic Wind Profile for W Cases

SECTION V

RESULTS

A digital computer program was developed to implement the landing approach model and to automatically compute the probability of a missed approach as a function of the data rate of the glideslope deviation measurements. The computer program takes as inputs the data rate of the measured glideslope deviation, the aircraft stability derivatives, nominal longitudinal airspeed, glide-path angle, gust parameters, steady-wind velocity, wind-shear gradient, guidance-noise parameters, 3σ constraints on control activity, and the tolerances on the aircraft variables that define the 100-ft-decision-altitude window. The program is structured so that changes in the system Equations 1 and 16 can be easily implemented in the program. Changes in the system equation result from

(1) Changes in the aircraft equations of motion (for example, going from the DC-8 to the CH-53A, and adding a state for integral of glideslope deviation as in Case D11).

(2) Addition or deletion of control points (i.e., Case D9 where the auto-throttle was replaced by direct lift control).

(3) Changes in the measurement model or sensor complement (i.e., Case D10 and C7, where glideslope deviation rate was considered as a continuously sensed variable).

For each of the cases described in Section IV, the landing approach performance was computed as a function of the sample data rate for the glideslope deviation measurement. The detailed computational results are given in Appendix A.

In Section 5.1 the results obtained using the model described herein are compared with similar results for landing approach where a detailed flight control system was considered and continuously measured glideslope deviation was assumed.

In Section 5.2 an analysis is presented of the effects of sample data rate for the glideslope deviation measurement on the landing approach performance.

5.1 VALIDATION OF THE OPTIMAL MODEL FOR THE FLIGHT CONTROL SYSTEM

A particularly attractive feature of the analysis technique is the optimal model for the flight control system. This aspect of the system model allows for the completely automated computation of landing performance as a function of data rate since detailed designs of the flight control system do not have to be developed. The optimal approach also provides a convenient method for considering mixed continuous and sampled data measurements, as is the case with landing approach with a scanning beam guidance system. In addition, the optimal design fully exploits the aircraft's responses in a glideslope tracking situation within the limits of the onboard sensors, guidance measurements, control authorities, and control points. In this way, peculiarities that might be associated with a specific flight control system do not distort the results. Furthermore, the results are applicable to innovations and sophistications inevitable in future aircraft flight control systems.

It is desirable, however, that the optimal approach provide realistic results with respect to actual flight control system designs. Thus, in this section the results obtained using the "optimal" model are compared with a more conventional approach where a detailed flight control system design is used in the analysis.

In Reference 1 a landing approach analysis was performed for the DC-8 aircraft where the system model was essentially the same as in this report, with the exception of two items:

(1) A detailed flight control system design was considered in Reference 1.

(2) The results of Reference 1 were based on continuously measured glideslope deviation. Cases D8 and D8W (where 3σ constraints on the

elevator rate were relaxed) were used to compare with the results from Reference 1 since the rms control activities, (σ_{δ_e}), in D8 and D8W are comparable to those computed in Reference 1. Continuously measured glideslope deviation was approximated by using a sample data rate in Cases D8 and D8W of 100 samples/sec. Table XII gives a detailed comparison of the system model used in Cases D8 and D8W and the model used in Reference 1.

Table XIII gives a detailed comparison of the results obtained for cases D8 and D8W and those given in Reference 1. The comparison is extremely good! Although the comparison of PMA for case D8 shows about a 15% variation, this is extremely close, considering the ranges of PMA that were encountered in the results and the sensitivity of PMA to σ_d. Also no auto-throttle was considered in Reference 1 for the DC-8.

Similar comparisons are shown in Table XIV for cases D6 and D7; however, these configurations do not match the configuration used in Reference 1 as well as case D8. In the case of D6 and D6W (longitudinal airspeed error was included in the "window" definition), the PMA is dominated by airspeed errors; and the use of an auto-throttle in cases D6 and D6W and the use of integral control in Reference 1 causes larger differences in the comparison of these configurations. Also in Cases D7 and D7W (3σ constraints on elevator rate were replaced by a 3σ constraint on elevator deflection), the elevator rate of 0.6367 rad/sec is excessive and probably not consistent with the more conservative results of Reference 1. However, even in these cases, the comparisons are still good.

A similar comparison of results can be made for the CH-53A by using the results of Reference 2. Again, the system model used in Reference 2 essentially differs from the one used herein by the following details:

(1) A detailed flight control system design was considered in Reference 2.

(2) The results of Reference 2 were based on continuously measured glideslope deviation. Cases C6 and C6W (where the 3σ constraints on

TABLE XII

COMPARISON OF DC-8 MODELS FOR APPROACH ANALYSIS

Parameters	Cases D8 and D8W	Reference 1	Comments
Stability Derivatives	Table IV	Table IV except for $M_{\dot{w}}$	In Reference 1, $M_{\dot{w}} = -.00085$ Case D8, D8W, $M_{\dot{w}} = 0.0$
U_o	228 ft/sec	228 ft/sec	
γ_o	-3°	-2.8°	
$1/T_e$	15 sec^{-1}	15 sec^{-1}	
$1/T_{th}$	1. sec	-	No throttle control was assumed in Ref. 1
w_{st} (D7 and D7W)	0. and 42.2 ft/sec	0. and 42.2 ft/sec	Both zero and non zero head winds and shear gradients were considered in Ref. 1 as in Cases D8 and D8W
S_h (D7 and D7W)	0. and .0675 ft/sec per ft	0. and .0675 ft/sec per ft	
σ_{u_g}	10. ft/sec	10. ft/sec	
ω_{u_g}	.34 rad/sec	.34 rad/sec	
σ_{wg}	6.5 ft/sec	6.5 ft/sec	A second order power spectral density for w_g was assumed in Ref. 1.
ω_{wg}	3.95 rad/sec	3.95 rad/sec	
T_o	.01 sec	0. sec	Continuous glideslope deviation measurements were assumed in Ref. 1
σ_{bias}	2.72 ft	0.	Bias errors were not considered in Ref. 1
σ_{bb}	.96 ft	0.	Beam bend errors were assumed zero in Ref. 1
σ_{fn}	1.83 ft	1.32 ft	(In Ref. 1 a factor of 2 was used to relate the theoretical errors to the errors that might be encountered in operational use (vs. a factor of 3 in this report).
ω_{f_n}	$2.8/T_o$ = 288 rad/sec	14.0 rad/sec	T_o = 0.2 sec was used to define ω_{f_n} in Ref. 1
$\sigma_{\dot{\delta}_e}$	.293 rad/sec	-	This value was not given in Ref. 1
σ_{δ_e}	.031 rad	.0422 rad	
"window"	$\Delta d = \pm 12$ ft	$\Delta d = \pm 12$ ft	

TABLE XIII

COMPARISON OF RESULTS FOR DC-8 APPROACH ANALYSIS

	Cases D8 and D8W	Reference 1
$\sigma_{u_{as}}$	9.41 ft/sec	11.7 ft/sec[1]
σ_d	5.15 ft	5.75 ft
σ_θ	0.0236 rad	0.0287 rad
σ_{δ_e}	0.0310 rad	0.0422 rad
$\sigma_{\dot{\delta}_e}$	0.293 rad/sec	(not given)
$\overline{d}$ (D8W)	-2.92 ft	1.49 ft[2]
PMA[3] (D8)	0.0295	0.0366
PMA[3] (D8W)	0.0412	0.0430

Notes:

(1) There was no throttle control considered in Reference 1 for the DC-8.

(2) Integral feedback of glideslope deviation was used in Reference 1 to suppress errors due to steady wind and wind shear.

(3) Probability of a Missed Approach (PMA).

TABLE XIV

COMPARISON OF RESULTS FOR DC-8 APPROACH ANALYSIS

	Cases D6 and D6W	Cases D7 and D7W	Reference 1
$\sigma_{u_{as}}$	9.32	9.45	11.7 ft/sec
σ_d	5.67	4.72	5.75 sec
σ_θ	0.0210	0.0258	0.0287 rad
σ_{δ_e}	0.0253	0.0416	0.0422 rad
$\sigma_{\dot{\delta}_e}$	0.180	0.6367	(not given)
$\bar{u}_{as}$	0.89	0.886	-7.94 ft/sec
$\bar{d}$	-3.46	-2.47	1.49 ft
PMA (D6)	0.384	-	0.492[1]
PMA (D6W)	0.411	-	0.580[1]
PMA (D7)	-	0.0113	0.0366
PMA (D7W)	-	0.0230	0.0430

Note:

(1) Different PMAs are computed for Reference 1 to compare with D6 and D6W than for the D7, D7W, D8, and D8W cases, since the window definition is changed.

control rates were relaxed) were used to compare with the results from Reference 1, since the rms control rates are comparable. Continuously measured glideslope deviation was approximated by using a sample data rate in Cases C6 and C6W of 100 samples/sec. Table XV gives a detailed comparison of the system model used in Reference 2.

Table XVI gives a detailed comparison of the results obtained for cases C6 and C6W and those given in Reference 2. The results are comparable, but do not compare as favorably as in the case of the DC-8!

TABLE XV

COMPARISON OF CH-53A MODELS FOR APPROACH ANALYSIS

Parameters	Cases C6 and C6W	Reference 2	Comments
Stability Derivatives	Table VIII	Table VIII	
U_o	101 ft/sec	101 ft/sec	
γ_o	-6°	-6°	
$\tau_{B1}, \tau_{\delta_c}$	10 sec^{-1}	10 sec^{-1}	
w_{st} (C6 and C6W)	0 and 42.2 ft/sec	0 and 42.2 ft/sec	Both zero and non-zero head winds and shear gradients were considered in Ref. 2 as in cases C6 and C6W.
S_h (C6 and C6W)	0 and .0675 ft/sec per ft	0 and .0675 ft/sec per ft	
σ_{ug}	10 ft/sec	10 ft/sec	
ω_{ug}	.15 rad/sec	.15 rad/sec	
σ_{wg}	6.5 ft/sec	6.5 ft/sec	A second order power spectral density was assumed for w_g in Ref. 2 .
ω_{wg}	1.01 rad/sec	-	More than one value given for each of these in Ref. 2 . Not clear which one was used.
a	.0173 rad/sec	-	
T_o	.01 sec	0.	Continuous glideslope deviation measurements were assumed in Ref. 2 .
σ_{bias}	2.72 ft	0.	Bias errors weren't considered in Ref. 2 beam bends were assumed zero in Ref. 2 . In Ref. 2 the GSIP was assumed to be 2000 in front of the transmitter and a factor of 2 was assumed for operational degradation.
σ_{bb}	.96 ft	0.	
σ_{fn}	1.83 ft	1.95 ft	
ω_{fn}	$2.8/T_o$ = 228 rad/sec	14.14 rad/sec	
σ'_{B1}	.0469 rad/sec	.0469 rad/sec	3σ constraint on control rates in Case 7 were picked to match the control rates obtained in Ref. 2 .
σ_{B1}	.0115 rad	.0176 rad	
σ'_{δ_c}	.0398 rad/sec	.0398 rad/sec	
σ_{δ_c}	.0089 rad	.0164 rad	
"window"	$\Delta d \pm 12$ ft	$\Delta d = \pm 12$ ft	

TABLE XVI

COMPARISON OF RESULTS FOR CH-53A APPROACH ANALYSIS

	Cases C6 and C6W	Reference 2
$\sigma_{u_{as}}$	10.38 ft/sec	7.86 ft/sec
σ_d	6.27 ft	4.00 ft
σ_w	3.26 ft/sec	3.22 ft/sec
σ_θ	0.0425 rad	0.0297 rad
$\sigma_{\dot{B}1}$	0.0469 rad/sec	0.0469 rad/sec
σ_{B1}	0.0115 rad	0.0176 rad
$\sigma_{\dot{\delta}_c}$	0.0398 rad/sec	0.0398 rad/sec
σ_{δ_c}	0.0088 rad	0.0164 rad
$\overline{d}$	-5.55	-3.74 ft(1)
PMA (C6)	0.0556	0.0026
PMA (C6W)	0.1545	0.0198

(1) Integral feedback of glideslope deviation was used in Reference 2 to suppress errors due to steady wind and wind shear.

The values of probability of a missed approach (PMA) for the CH-53A were generally higher than might be expected in all cases except for C6, where the constraints on control activity were relaxed. Part of the problem results from the particularly stringent constraints on control activity. In fact, in Case C6, where the control constraints were relaxed, the values of PMA are reasonable. One case was run for the relaxed control constraints with T_o = 0.01 sec where it was assumed that $\dot{h}$ was continuously and perfectly measured, and σ_d was reduced to 4.05 ft with a corresponding PMA of 0.003. (This case is not documented in this report because a full set of data rates were not considered.)

The "W" cases for the CH-53 (nonzero steady wind and wind shear) resulted in exceedingly high values of PMA. This was primarily due to the large steady glideslope deviation error due to the steady head wind considered in those cases. This problem can be conceptually corrected by using integral feedback of glideslope deviation or by trimming the helicopter to the known steady wind during the approach. At any rate, the trends in PMA still provide insight into the effects of data rate on landing approach performance even though the values of PMA were unduly large.

In general, the results given in this section tend to verify the validity of the model and demonstrate that the optimal model of the flight control system does provide realistic results.

5.2 ANALYSIS OF THE EFFECTS OF DATA RATE ON APPROACH PERFORMANCE

For each case described in Section IV, the landing approach performance was computed as a function of sample data rate for the glideslope deviation measurements (hereafter called data rate). Data rates from 2 samples/sec to 100 samples/sec were considered. The detailed results are tabulated in Appendix A.

Measures of landing approach performance were definitized in Section II and included the probability of a missed approach (PMA), proabable missed approaches per arrival (PMA/ARR), and maximum acceptable limits on pitch perturbations and normal acceleration for pilot acceptance.

It turns out that neither the rms perturbed pitch attitude nor the rms acceleration is very sensitive to data rate. For each case considered, the rms perturbed pitch attitude, σ_θ, never varies by more than 20% over the range of data rates considered. For the DC-8, σ_θ actually tends to decrease with decreasing data rates. For each case considered, the rms normal acceleration, σ_{nz}, never varies by more than 30% over the range

of data rates considered. Furthermore, in those cases where σ_{nz} varies by more than 15%, the 4 σ_{nz} values are well below the 0.5 g maximum deviation for pilot acceptance.

Thus, it can be concluded that the data rate requirements are not influenced by limitations in perturbed pitch attitude or normal acceleration for pilot acceptance.

The sensitivity of rms glideslope deviation, σ_d, and consequently PMA and PMA/ARR, to data rate is more profound; and it is these measures of landing approach performance that are considered in this analysis. In particular, PMA/ARR is the performance measure used because it is intuitively meaningful and directly relates to the number of go arounds that will be executed over a period of time and to the terminal area congestion.

The raw values of PMA/ARR vary widely over the different cases considered. So, to allow for a reasonable comparison of data rate effects from case to case, the values of PMA/ARR are normalized. This is done by normalizing the PMA/ARR for each data rate considered by the PMA/ARR for continuously sensed glideslope deviation error for that corresponding case. The continuous case was approximated by a data rate of 100 samples/sec. Notationally, this is represented by

$$\overline{\text{PMA/ARR}}(1/T_o) = \frac{\text{PMA/ARR}(1/T_o)}{\text{PMA/ARR}(100)}$$

and the value of $\overline{\text{PMA/ARR}}(1/T_o)$ represents the approach performance degradation at a given sample rate, $(1/T_o)$, relative to the approach performance for continuously sensed glideslope deviation. In this way it is possible to compare the effects of data rate on performance for cases where the actual performance is greatly different.

5.2.1 Effect of Deterministic Winds on Performance Sensitivity to Data Rate

Figures 7 and 8 illustrate the effect of considering nonzero steady wind and wind shear on the performance sensitivity to data rate for baseline configuration cases, D1 and C1. In these cases the consideration of nonzero steady wind and wind shear does not have a profound effect on the performance sensitivity to data rate for data rates above 4 samples/sec. This result holds in all the cases considered except those for D5, D9, D10, C2, and C7. Cases D5 and C2 are "low gust" cases and the effects of deterministic winds in these cases are discussed further in Section 5.2.3. The peculiar effect of the deterministic wind on case D10 and C7 is discussed in Section 5.2.7 (effects of continuously sensed glideslope deviation rate).

From Figures 7 and 8, it can also be seen that the performance degradation with decreasing sample rates becomes slightly more severe when the deterministic winds are considered for the baseline cases. This is not always the case, and in seven of the cases considered, the performance sensitivity to data rate decreased when the deterministic winds were introduced. In case D11, where integral feedback of the glideslope deviation was used to suppress the glideslope error due to steady winds, there was virtually no change in the sensitivity to data rate when the deterministic winds were considered.

It appears that a data rate of at least 10 samples/sec would be desirable to suppress the detrimental effects of the severe gusts. Below this value, performance degradation becomes significant and deteriorates rapidly with decreasing sample rate.

5.2.2 Effect of Beam-Bend Errors on Performance Sensitivity to Data Rate

To evaluate the effects of beam-bend errors on the performance-data rate tradeoff, the control laws defined for the baseline cases were used for the flight control system model and the rms-beam-bend

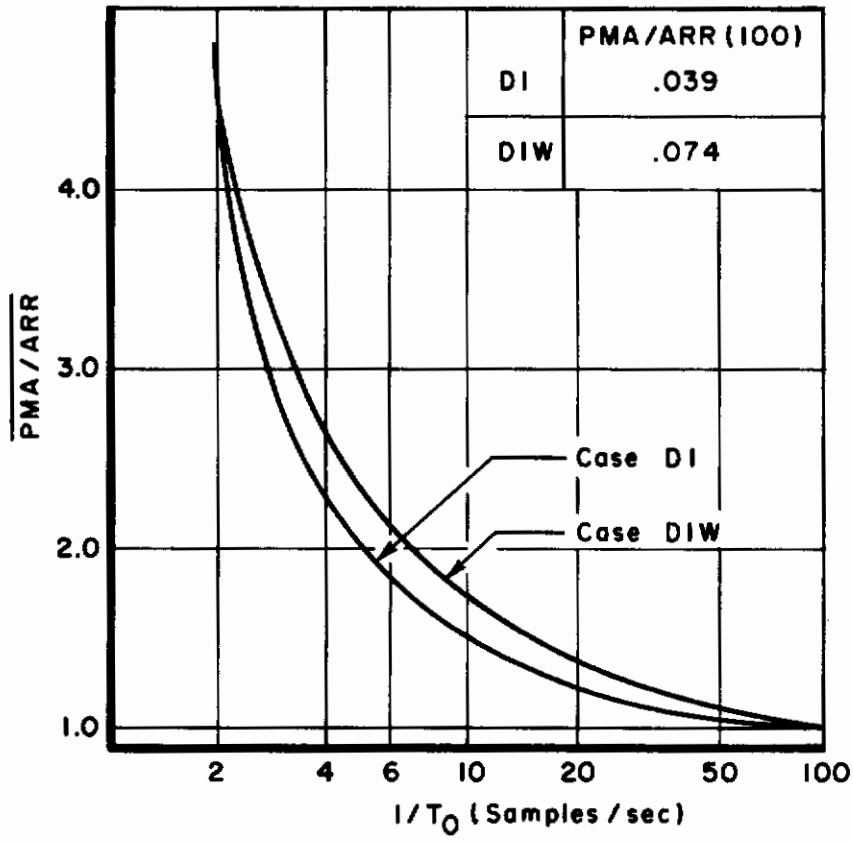

Figure 7. Comparison of $\overline{PMA/ARR}$ for Cases DI and DIW (Effects of "Deterministic" Winds)

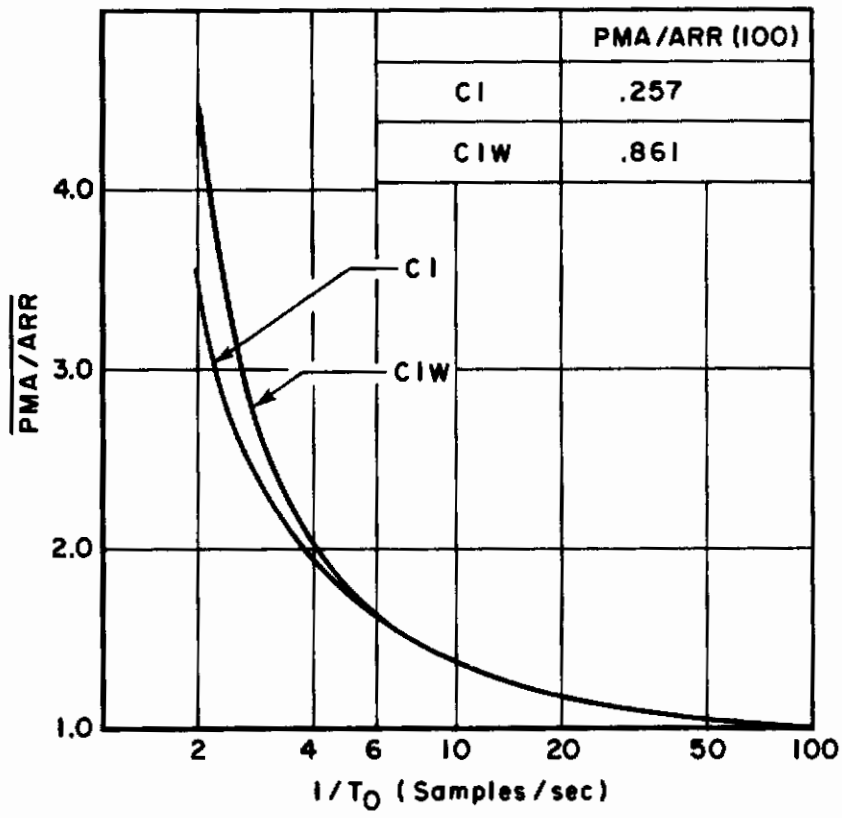

Figure 8. Comparison of $\overline{PMA/ARR}$ for Cases C1 and C1W (Effects of "Deterministic" Winds)

errors were varied. For the DC-8 a low gust environment was considered and for the CH-53A a severe gust environment was considered. The results are illustrated in Figures 9, 10, 11, and 12.

For a low gust environment (Cases D2, D3, and D4) as the beam-bend errors become more severe, the performance becomes less sensitive to data rate. For rms-beam-bend errors of 9.6 ft, the performance is essentially unaffected by data rate for rates above 2 samples/sec. As would be expected, the PMA/ARR increases with increasing beam-bend errors.

In the presence of severe turbulence (Cases C1, C3, and C4) the effects of increasing beam-bend errors are less profound although the same trend is observed, i.e., decreasing performance sensitivity to data rate with increasing beam-bend errors. In the case where the deterministic winds are also considered (Figure 12), the effect is very slight. This is because of the dominance of the glideslope tracking error by the steady head wind. These results do not significantly change when the control law is optimized so as to account for severe beam bends. This fact is substantiated by Figure 13, where the results using the baseline control are compared with those obtained by optimizing the control law so as to account for the severe beam bends.

It can be concluded that if the glideslope tracking errors are dominated by those errors induced by beam bends, the approach performance is comparatively insensitive to data rate for data rates of 2 samples/sec or more. This result is consistent with the fact that the bandwidth of of the beam-bend errors is so small compared to the bandwidth of the aircraft dynamics, it is virtually impossible for the Kalman filter to estimate the beam-bend error from the reference glideslope. Thus in the absence of gust upsets, essentially the same tracking performance can be achieved by low data rates as can be achieved by continuously sensing the glideslope deviation.

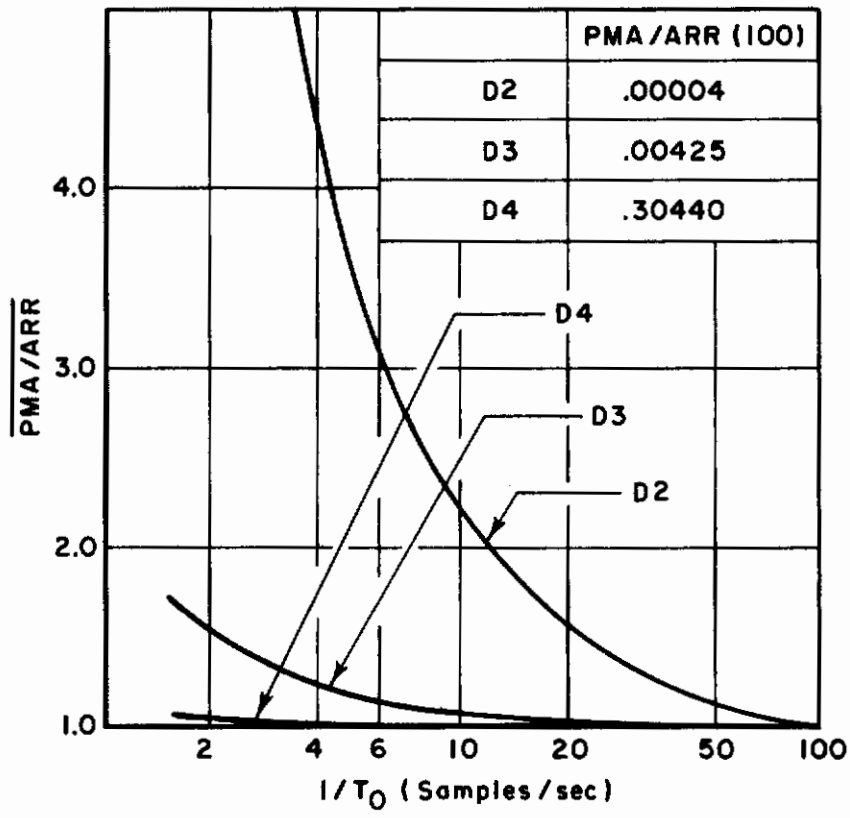

Figure 9. Comparison of $\overline{PMA/ARR}$ for Cases D2, D3, and D4 (Effects of Beam Bend Errors, Low Gusts Environment)

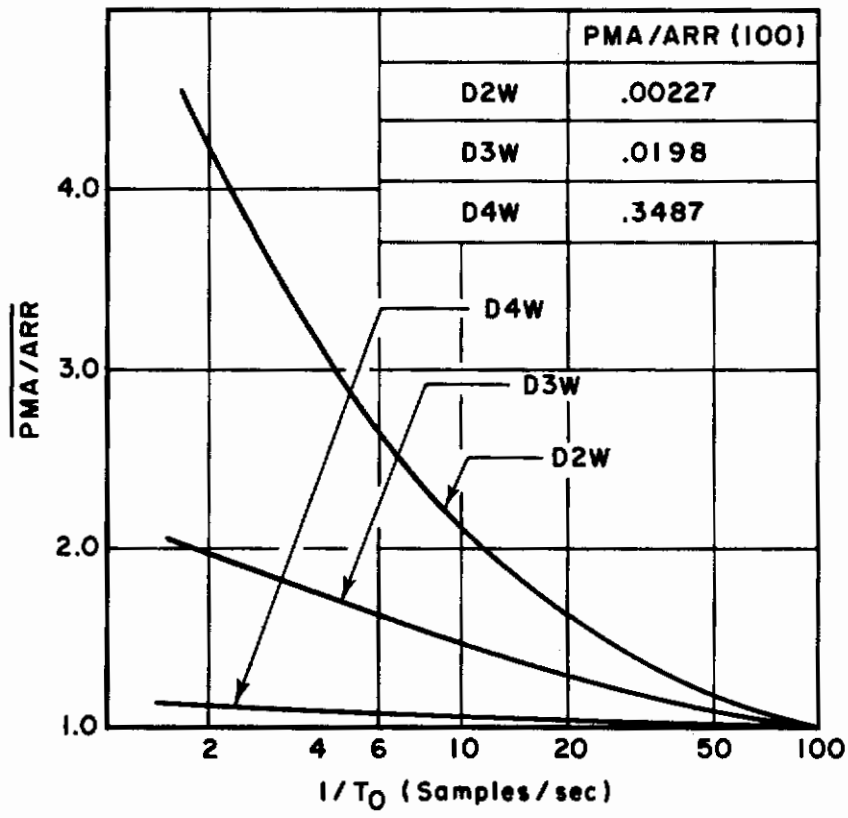

Figure 10. Comparison of $\overline{PMA/ARR}$ for Cases D2W, D3W, and D4W (Effects of Beam Bend Errors, Low Gust Environment)

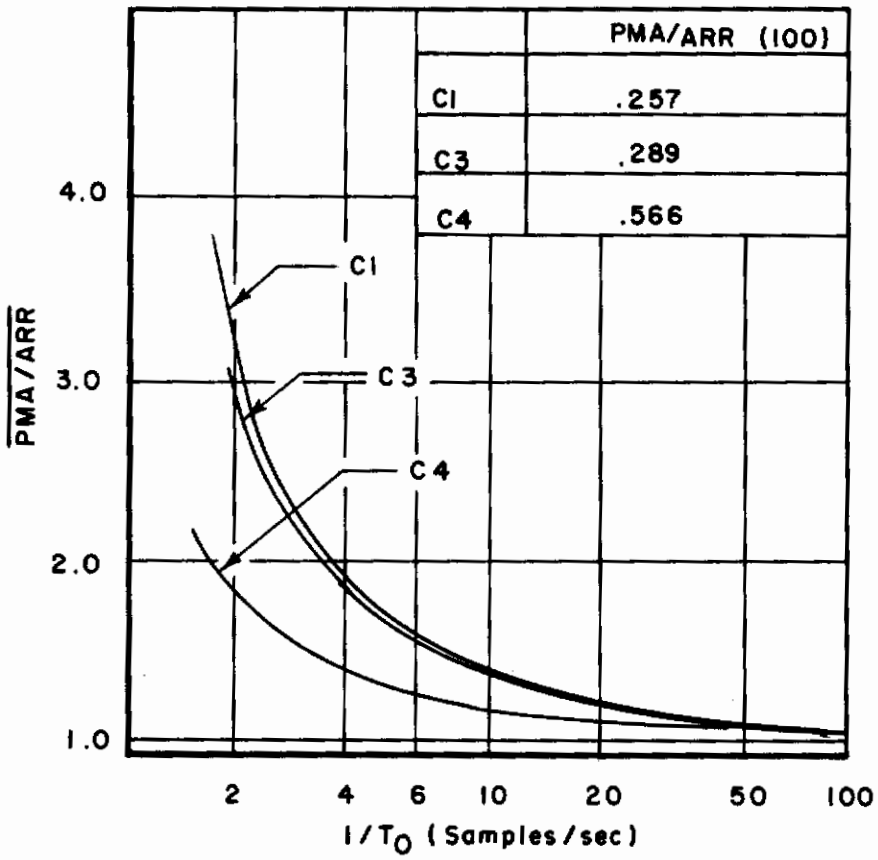

Figure 11. Comparison of $\overline{PMA/ARR}$ for Cases C1, C3, and C4 (Effects of Beam Bends, High Gust Environment)

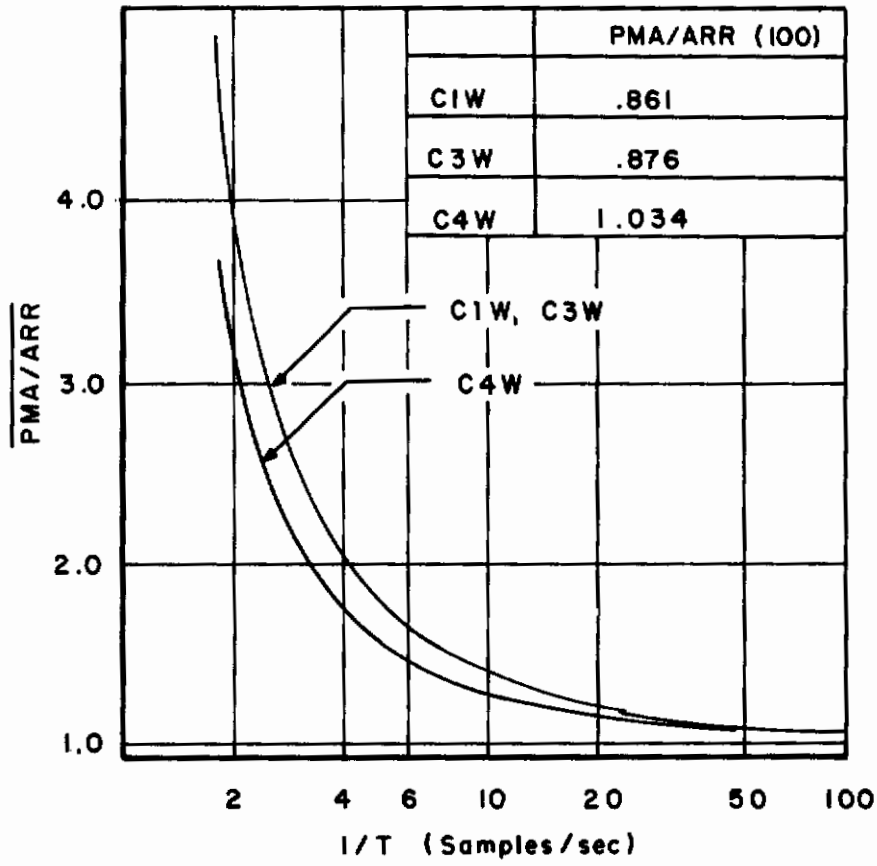

Figure 12. Comparison of $\overline{PMA/ARR}$ for Cases C1W, C3W, and C4W (Effects of Beam Bends, High Gust Environment)

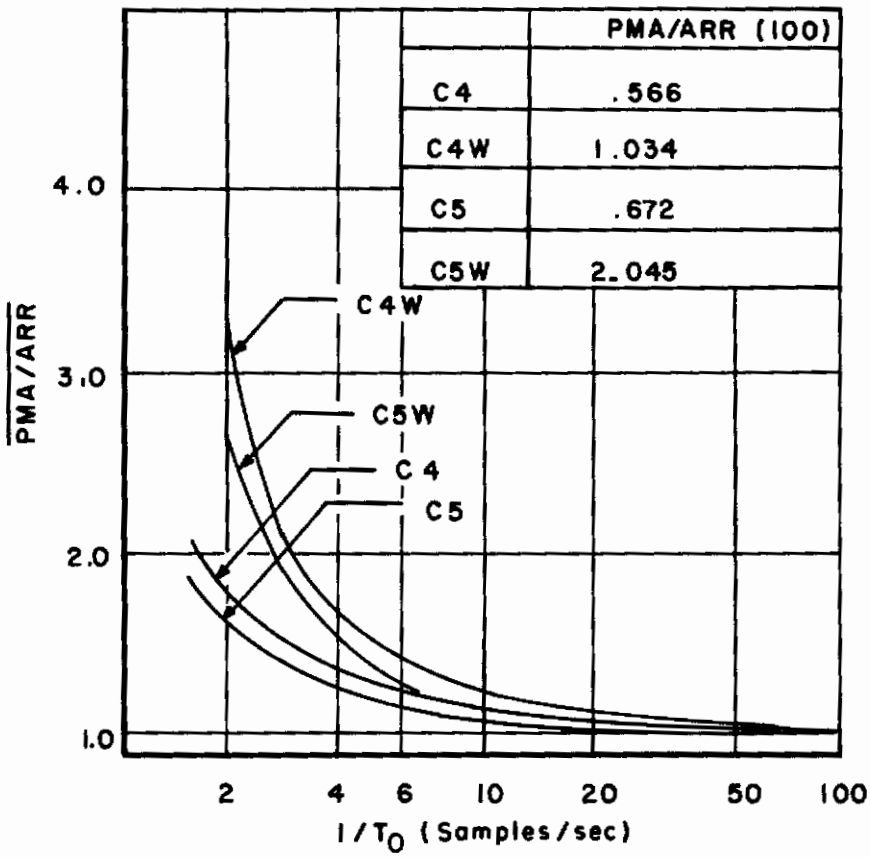

Figure 13. Comparison of $\overline{PMA/ARR}$ for C4, C4W, C5, and C5W (Effects of Beam Bends, High Gust Environment)

5.2.3 Effects of Gust Intensities on Performance Sensitivity to Data Rate

Most of the cases considered in this report were based upon operating in a severe turbulence environment--and rightfully so, since this provides worst-case conditions and presumably identifies the most stringent requirements on the landing guidance system and the aircraft flight control system. However, in the majority of the low visibility landing situations, the turbulence will be low to moderate. This is especially true when the visibility is obscured by fog. So it is of interest to look at the effects of gust intensities on the performance sensitivity to data rates.

These effects are evaluated by comparing the baseline case (D1 and C1) to those cases where the baseline control laws were used and the inputs corresponding to gust intensities were reduced (Cases D2 and C2). These results are illustrated in Figures 14, 15, 16, and 17.

The outcome was that the performance sensitivity to data rate increased in every case except D5W when a low gust environment was considered. And, notably, the effects were very significant.

It can be seen from Figures 14 and 16 that although the PMA/ARR is decreased by at least 2 orders of magnitude in a low gust environment, the effect of data rate on $\overline{\text{PMA/ARR}}$ is more pronounced for a low gust environment (especially for the DC-8, Figure 14). This effect is still present even in the case where the control system is optimized for a low gust environment (Case D5 in Figure 14).

When the deterministic winds were considered for a low gust environment, some peculiar results occurred (Figures 15 and 17)!

Notice that in Figure 15 for Case D5W, the degradation in performance, $\overline{\text{PMA/ARR}}$, is not monotone with respect to data rate! Also PMA/ARR increases by at least 4 orders of magnitude when the deterministic winds are considered! This results from the fact that when low gusts are used

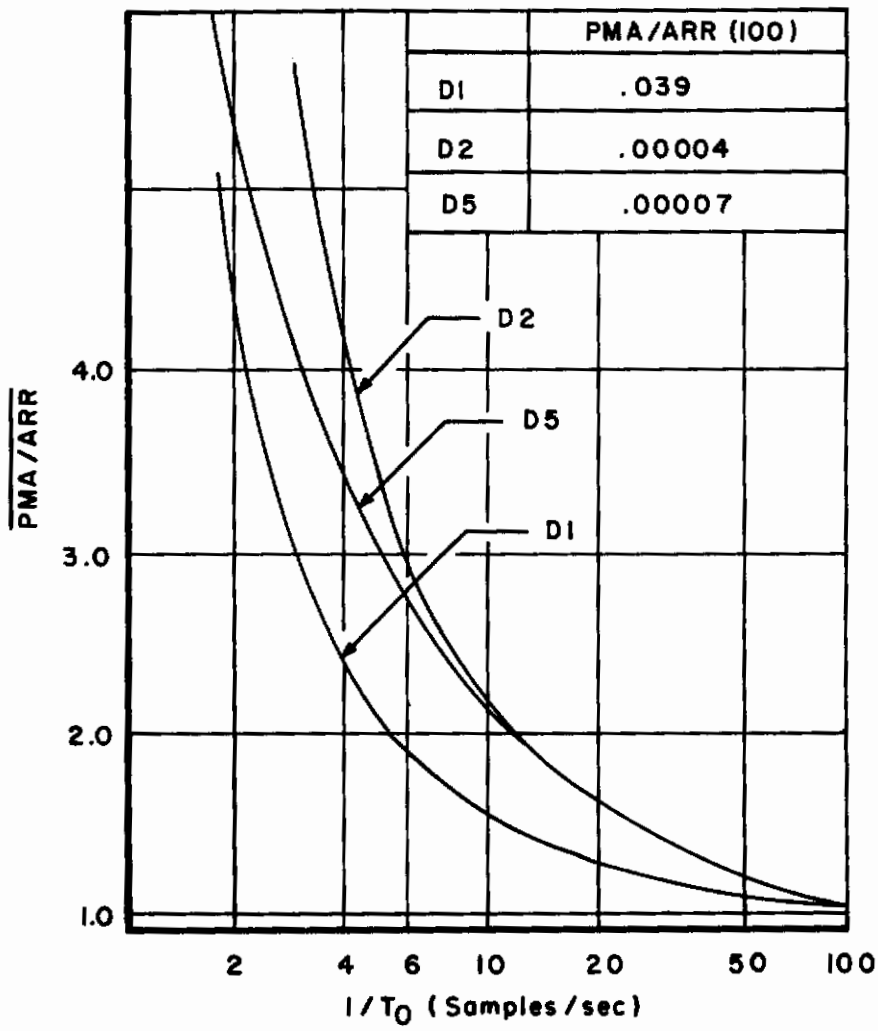

Figure 14. Comparison of $\overline{PMA/ARR}$ for Cases D1, D2, and D5 (Effects of Low Gust Environment)

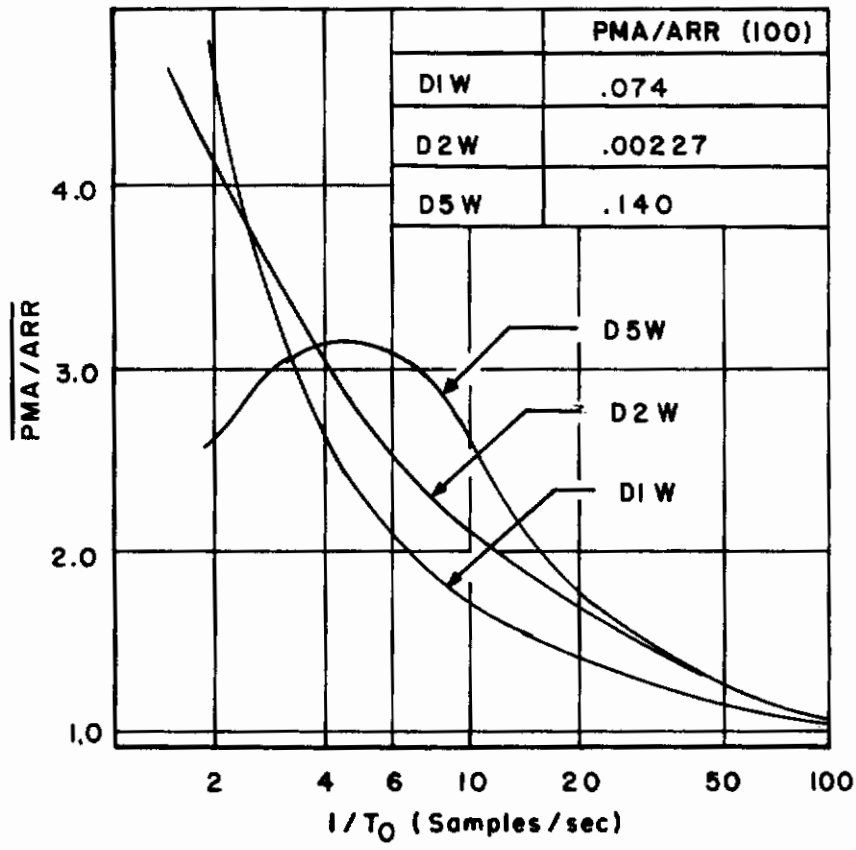

Figure 15. Comparison of $\overline{PMA/ARR}$ for Cases D1W, D2W, and D5W (Effects of Low Gust Environment)

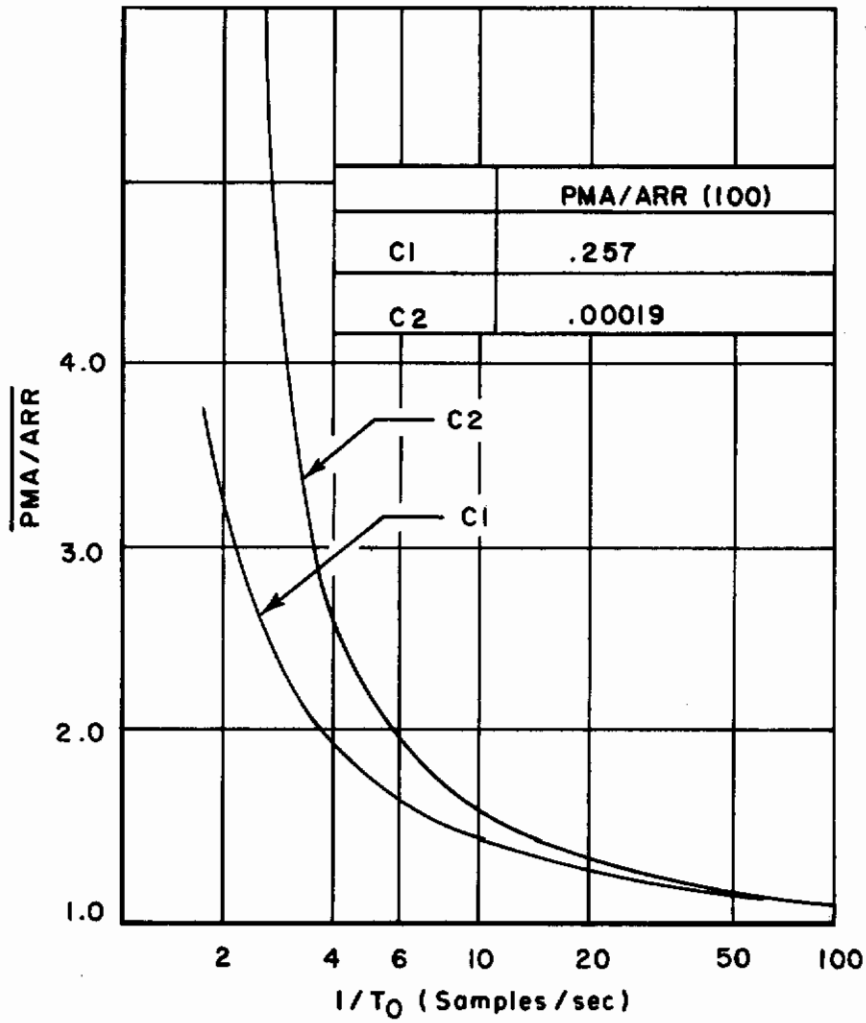

Figure 16. Comparison of $\overline{PMA/ARR}$ for Cases C1 and C2 (Effects of Low Gust Environment)

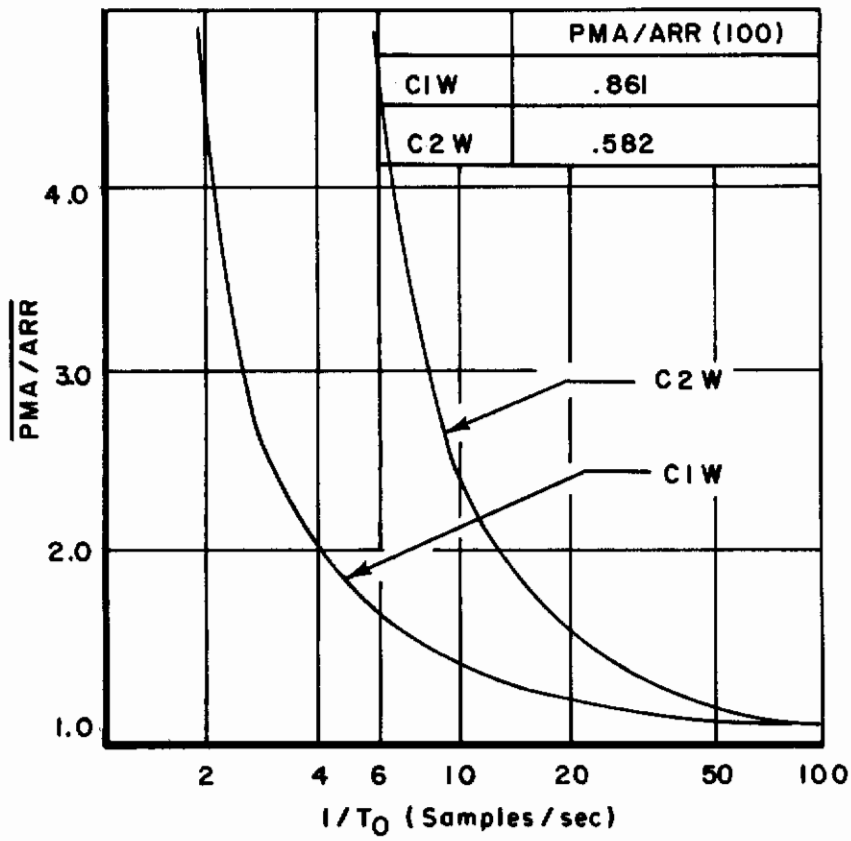

Figure 17. Comparison of $\overline{PMA/ARR}$ for Cases C1W and C2W (Effects of Low Gust Environment)

to determine the optimal control law, a rather "loose" throttle control is developed, and the effects of a steady input (corresponding to the steady wind) become very pronounced. Consequently, when the steady headwind is considered, the mean glideslope offset error is large and the performance is extremely poor. Furthermore, in this case, data rate is not a dominate factor in the approach performance between data rates of 2 and 10 samples/sec. This case (D5) represents a poorly designed flight control system and therefore the effect of data rate on performance is not considered to be particularly meaningful in establishing data rate requirements for a scanning beam landing guidance system.

An anomoly was also encountered with case C2 when the deterministic wind was considered (C2W). The PMA/ARR increased by 3 orders of magnitude and the performance sensitivity to data rate became extremely severe. For example, given a data rate of 4 samples/sec, the probable number of missed approaches per arrival was 7! (hopefully the pilot is very patient and the stewardesses are allowed to serve more than 2 drinks if this situation were to exist). This result was caused by the fact that for data rates less than 16 samples/sec, the magnitude of the mean deviation due to deterministic winds was greater than 12 ft (the window dimension for glideslope deviation at the decision altitude). Combined with the fact that the standard deviation of the glideslope error was small (for low gust disturbances) this resulted in a large value of PMA (most of the probability density function lies outside the window). The problem is then compounded by the sensitivity of PMA/ARR to values of PMA near 1:

$$\text{PMA/ARR} = \frac{\text{PMA}}{1 - \text{PMA}}$$

Thus, for this case, the results are extremely sensitive to the window definition and depend explicitly on the assumption that missing the window constitutes a missed approach. Furthermore, it is most likely that additional compensation (integral feedback) would be added to the automatic flight control system design to prevent the severe stand off

errors encountered in this case. These considerations, therefore, make data from case C2W inappropriate for evaluating the effects of data rate on landing performance.

This leaves as a basis for sound comparison cases C1 and C2 and cases C1W and C2W. Without any other considerations, cases C2 and C2W dictate significantly higher data rates in order to achieve the same values of $\overline{PMA/ARR}$ compared to cases C1 and C1W (the baseline configuration). However, in view of the extremely low values of PMA/ARR for cases C2 and C2W, it is doubtful that increased data rates would be considered based only on the performance degradation in these cases if there were any significant impact on the scanning beam guidance system.

5.2.4 Effects of the 100-ft-Decision-Altitude Window Definition on Performance Sensitivity to Data Rate

In Case D6 an additional dimension of perturbed airspeed was added to the 100-ft-decision-altitude-window definition. This consideration is based on the fact that airspeed errors at the initiation of flare can result in a stall for the case where the airspeed is too low, or there is a long landing or runway overrun in the case where the airspeed is too high. The effect of adding the perturbed airspeed dimension to the window is shown in Figure 18 by comparing case D1 with cases D6 and D6W. The approach performance becomes significantly worse and is comparatively insensitive to data rate. This results from the fact that the airspeed errors dominate the value of PMA/ARR and the effective use of the auto-throttle to reduce airspeed errors is relatively independent of the information rate for glideslope deviation measurements.

The perturbed airspeed dimension of $\pm$ 5 kts used in this case was based on a "guesstimate" by several airline pilots of an acceptable tolerance for Category II operations (Reference 5). It is likely, however, that a pilot would ignore the high frequency fluctuations in perturbed airspeed and base his decision about the adequacy of his airspeed on the low frequency variations in airspeed which are more

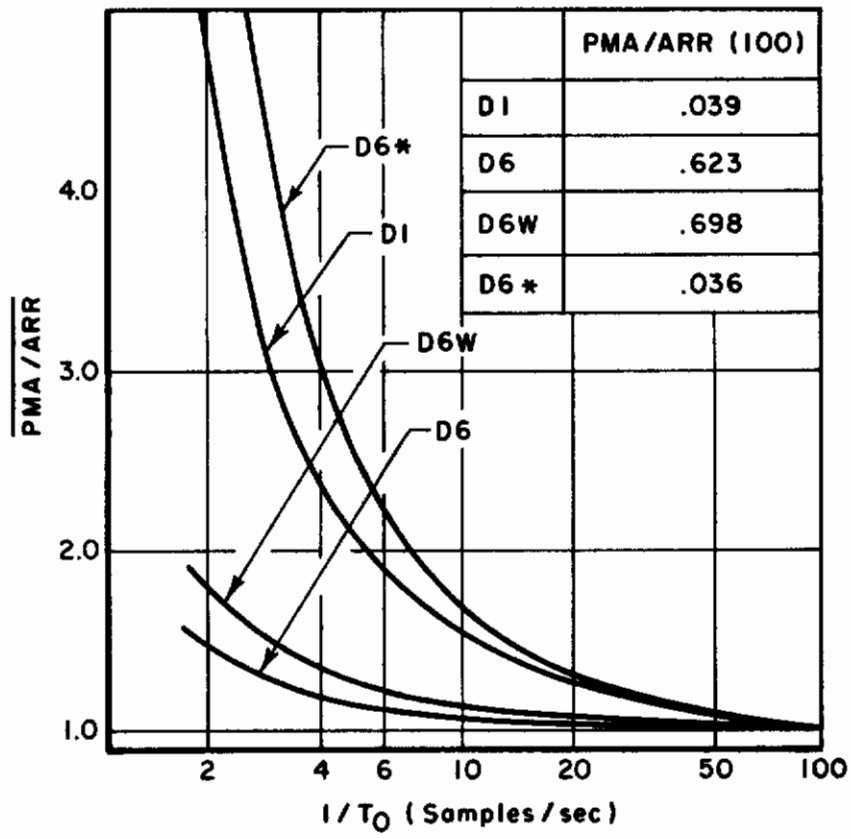

Figure 18. Comparison of $\overline{PMA/ARR}$ for Cases D1, D6, and D6W (Effect of Airspeed Window Dimension)

crucial to a successful landing. It was suggested in Reference 1 that a more appropriate measure for the window dimension is a short-term average of the perturbed airspeed. This can be approximated by filtering the perturbed airspeed, u_{as}, through a first-order low-pass filter and using that output as the low-frequency airspeed error to be compared with the $\pm$ 5 kts tolerance. A filter time constant of 5 seconds was suggested in Reference 1. This type of approach would be more representative of whether the aircraft was at an airspeed so significantly different from the trim speed as to execute a missed approach. This approach to defining the airspeed window was not tried in this study but it is clear that the resulting values of $\overline{PMA/ARR}$ would be somewhere in between the values obtained for Cases D6 and D1, depending on the value of the filter time constant used.

One interesting feature of Case D6 is that the resulting optimal model for the flight control system uses the full throttle control authority as specified by the 3σ constraint of $\pm$ 5% engine RPM. This is also true in cases D7, D8, and D11; however, in all other DC-8 cases considered (and especially in the baseline case, D1) the resulting control activity for the auto-throttle was negligible. This is an encouraging demonstration of the effectiveness of the optimal approach taken in this analysis to define the flight control system. That is, the design automatically resulted in active throttle control when it was needed, as in the case where airspeed errors significantly affect the probability of a missed approach. Conversely, in those cases where the auto-throttle did not effectively improve the approach performance, the throttle control was relatively inactive. In order to consider the conceptual possibility of a design where an active auto-throttle is used and yet the approach performance is basically independent of airspeed errors, the results of case D6 were used to compute the values of PMA/ARR using only the glideslope deviation dimension to define the 100-ft-decision-altitude window. The resulting values of PMA/ARR are shown in Figure 18 and are identified as case 6D*. It can be seen from Figure 18 that the resulting values of PMA/ARR are not significantly different from case D1, although the approach performance is slightly more sensitive to data rate than in case D1.

The effect of the glideslope deviation window dimension was also considered in the analysis of the results. It was demonstrated in Section 5.2.3 that in those cases (D5 and C2) where the flight control system does not effectively regulate against steady inputs (corresponding to the steady wind), the results are extremely sensitive to the tolerances in glideslope deviation that define the window at the 100-ft-decision altitude. In fact, the validity of the results for those cases (C5 and C2) depends explicitly on the validity of the window definition and on the assumption that a missed approach is equivalent to missing the window. The use of a 100-ft-decision altitude window as an absolute basis for defining a successful landing approach is not totally defensible. It is, however, reasonable to accept the use of a 100-ft-decision-altitude window to define a relative landing approach performance, provided that an effective flight control system is considered which will reasonably suppress the detrimental effects of the deterministic winds. Unfortunately the tolerances of $\pm$ 12 ft used to define the allowable deviation in glideslope deviation at the 100-ft-decision altitude have not been fully verified as accurate allowable glideslope deviation for the safe continuation of the landing approach through flare.

To evaluate the sensitivity of $\overline{PMA/ARR}$ to the window dimension for glideslope deviation, a $\pm$ 20% change to the $\pm$ 12-ft-glideslope-deviation-window dimension was considered, using the results of the baseline configuration for the DC-8, case D1. The resulting values of $\overline{PMA/ARR}$ are plotted in Figure 19. In Figure 19, D1+ denotes the results using a glideslope deviation window of $\pm$ 14.4 ft, and D1- denotes the results using a glideslope deviation window of $\pm$ 9.6 ft. It can be seen from Figure 19 that the results do depend upon the choice of the glideslope-deviation window. With the "smaller" landing window, the approach performance becomes significantly poorer and less sensitive to data rate. With the "wider" window, the approach performance improves and is more sensitive to data rate.

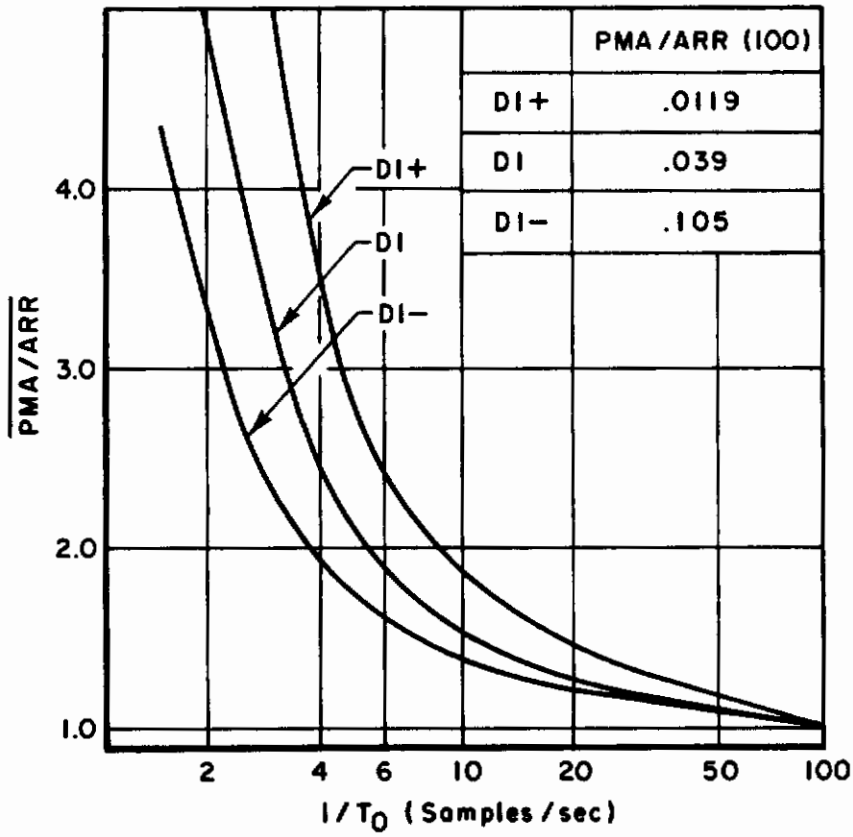

Figure 19. Comparison of $\overline{PMA/ARR}$ for Case DI with Varying Δd (Effect of the Glideslope Deviation Window Dimension)

Things would be much simpler if the performance sensitivity were independent of the window definition or if the window definition could be precisely determined for the safe continuation of the landing. Unfortunately this is not the case with either the airspeed or glideslope deviation dimension of the window! Therefore certain assumptions and judgments must be made in order to arrive at definitive conclusions about actual data rate requirements. First of all, it is assumed that the glideslope-deviation errors dominate the probability of a missed approach compared to the effect of airspeed errors. Thus the airspeed dimension of the window is not considered in the analysis. This approach results in an upper bound on the values of $\overline{PMA/ARR}$ (and consequently on data rate requirements) in the case where some sort of short-term-average airspeed error is used to determine whether or not the landing should be continued into flare.

The values of PMA for case D1 with the $\pm$ 12-ft-glideslope-deviation window seem intuitively to be fairly realistic considering the magnitude of the measurement errors and atmospheric disturbances used--much more than with the $\pm$ 9.6-ft-window dimension. Additionally, future improvements in flare laws and manuever control would tend to increase the allowable glideslope deviation at the 100-ft-decision altitude for continuation of the landing. Thus the $\pm$ 12-ft-glideslope-deviation window is considered as a reasonable basis for the analysis and if anything, this value may be slightly conservative if future improvements in flare control are hypothesized.

5.2.5 Effects of Flight Control Authority on Performance Sensitivity to Data Rate

The effect of the control authorities associated with an automatic flight control system on the sensitivity of performance to data rate is examined in this section.

In case D7, the optimal flight control system was designed with an rms constraint on elevator deflection instead of an rms constraint on elevator rate used in all the other DC-8 cases. This case conceptually

corresponds to the case where high elevator actuator rates can be achieved and are not limited by the automatic flight control system; but the elevator position is limited for physical or safety reasons. In Figure 20 the results for this case are compared with the corresponding results for case D1 where an rms constraint on the elevator rate was used in the optimization procedure. It can be seen that the performance becomes much more sensitive to data rate in case D7 where the elevator deflection constraint is used in the optimal design. It should be pointed out that σ_{δ} for case D7 was approximately 1.5 times larger than for case D1, and $\sigma_{\dot{\delta}}$ for case D7 was from 3 to 4 times larger than the values obtained in case D1. In fact, the resulting increase in the performance sensitivity to data rate results directly from the increased control activity (or equivalently, the increased control authority). It is interesting to note that in case D7 where the elevator rates were unconstrained, the resulting optimal flight control included a fully active throttle control.

The possibility of increased control authorities is also considered in cases D8 and C6. In case D8 the constraint on rms elevator rate was doubled from that used in case D1. In case C6 the rms constraints on cyclic pitch and collective pitch rates were increased from the values used in case C1. The resulting effect on performance sensitivity to data rate is shown in Figures 21 and 22. It can be seen from these figures that the performance is more sensitive to data rate with increased control authority. This effect is more profound in the case of the CH-53A, probably because rate constraints specified in the baseline configuration, C1, are particularly restrictive.

It is reasonable to expect that with an increased reliance on the automatic flight control system in low visibility landing approach, and a corresponding increase in system reliabilities, that fuller authority will be given to the automatic flight control system. Under these circumstances, data rates of as high as 20 samples/sec would be desirable in order to effectively suppress glideslope errors due to gust upset.

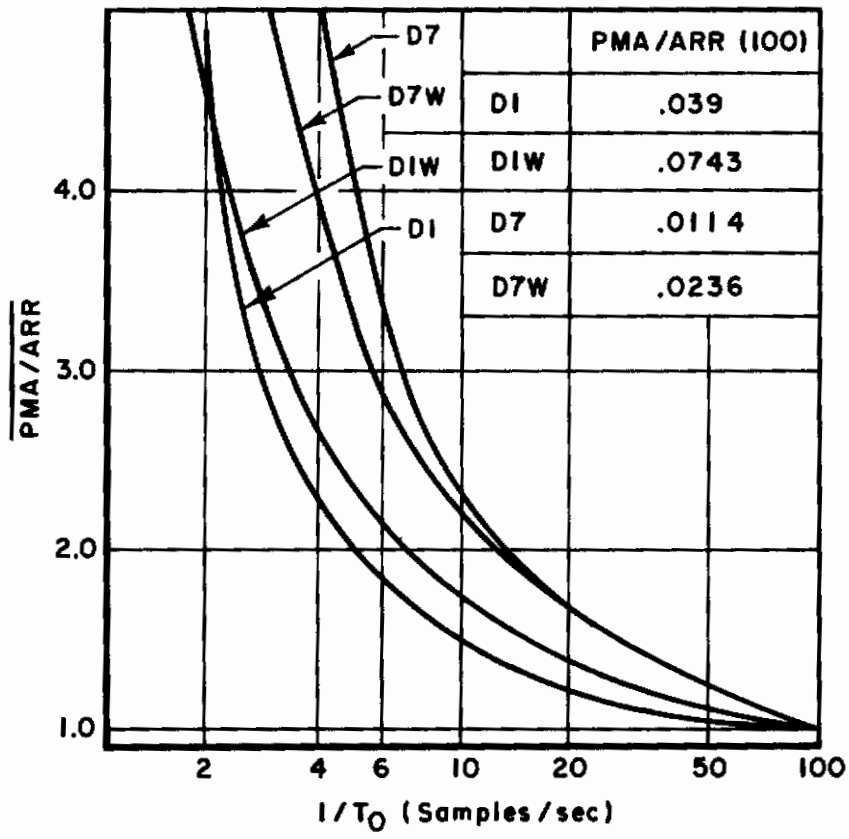

Figure 20. Comparison of $\overline{PMA/ARR}$ for Cases DI, DIW, D7, and D7W (Effect of Control Authority Limits)

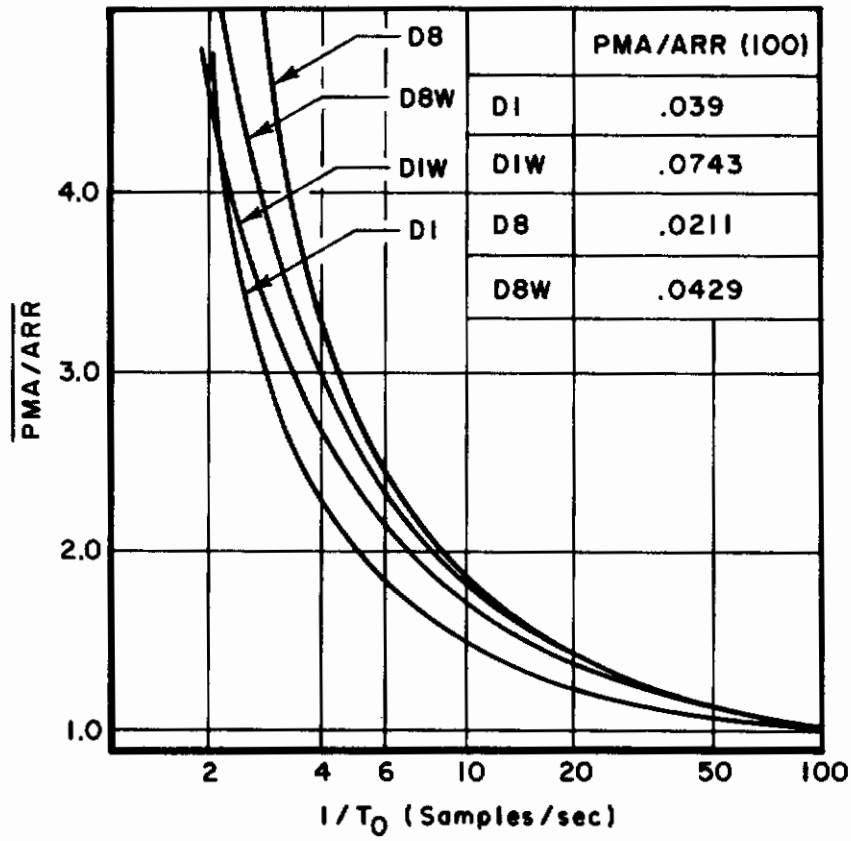

Figure 21. Comparison of $\overline{PMA/ARR}$ for Cases DI, DIW, D8, and D8W (Effect of Control Authority Limits)

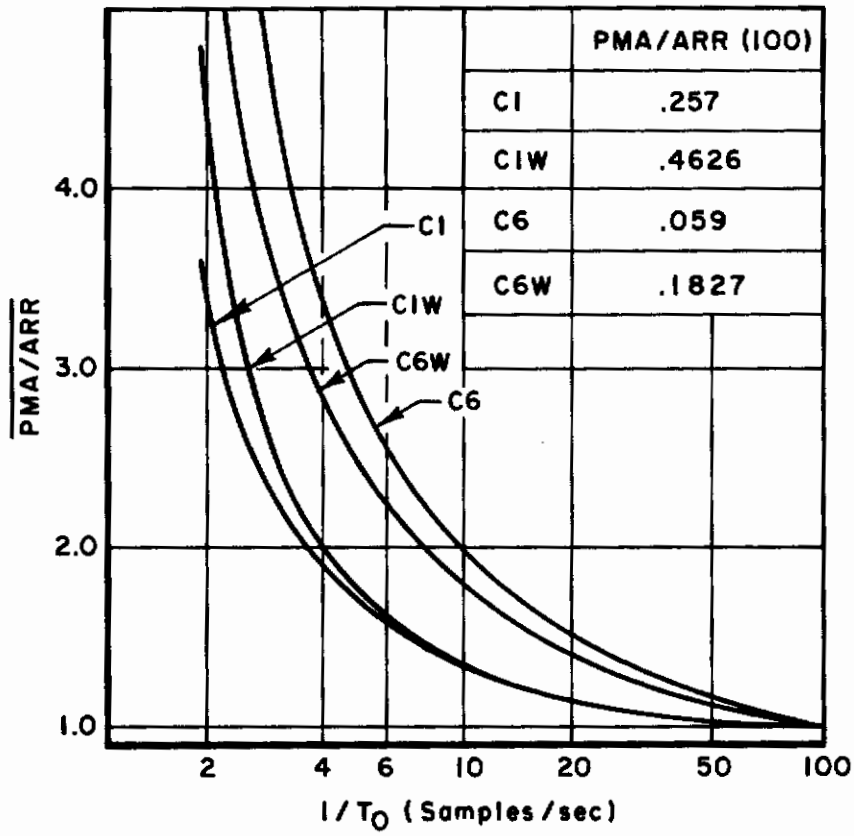

Figure 22. Comparison of $\overline{PMA/ARR}$ for Cases C1, C1W, C6, and C6W (Effects of Control Authority Limits)

5.2.6 Effects of Direct Lift Control on Performance Sensitivity to Data Rate

The effect of a direct lift controller on the sensitivity of approach performance to data rate can be conceptually determined by comparing the results for the DC-8 and the CH-53A. This is because the CH-53A can effectively control lift directly through collective pitch. To provide a valid comparison, it is desirable to select a DC-8 configuration and a CH-53A configuration which consider the same measurement errors, gust intensities, and onboard sensors. Also, since the results are sensitive to the control authority used (Section 5.2.5), a commonality may be established by considering cases with comparable performances. This is done by comparing cases D1 and C6 (Figure 23).

The effect of a direct lift controller on the sensitivity of approach performance to data rate can also be evaluated by comparing the results of cases D1 and D9. This is done in Figure 24. Recall that in case D9, a hypothetical direct lift controller was considered for the DC-8.

It can be seen in these cases that the use of direct lift control results in a case where the performance is considerably more sensitive to data rate than the case where conventional control surfaces are used. This is not a surprising result. With direct lift control, glideslope tracking errors due to gust upset can be directly suppressed through lift control without aircraft rotation. Thus comparatively slow dynamics associated with the phugoid mode are avoided and the glideslope tracking bandwidth is increased. Consequently, higher data rates can be effectively used to control against the relatively high frequency gust disturbances. Based on the results shown in Figure 23, data rates as high as 20 samples/sec would be desirable to effectively suppress glideslope errors when direct lift control is available. And, it is quite likely that many advanced aircraft of the future will be designed with a direct lift control capability.

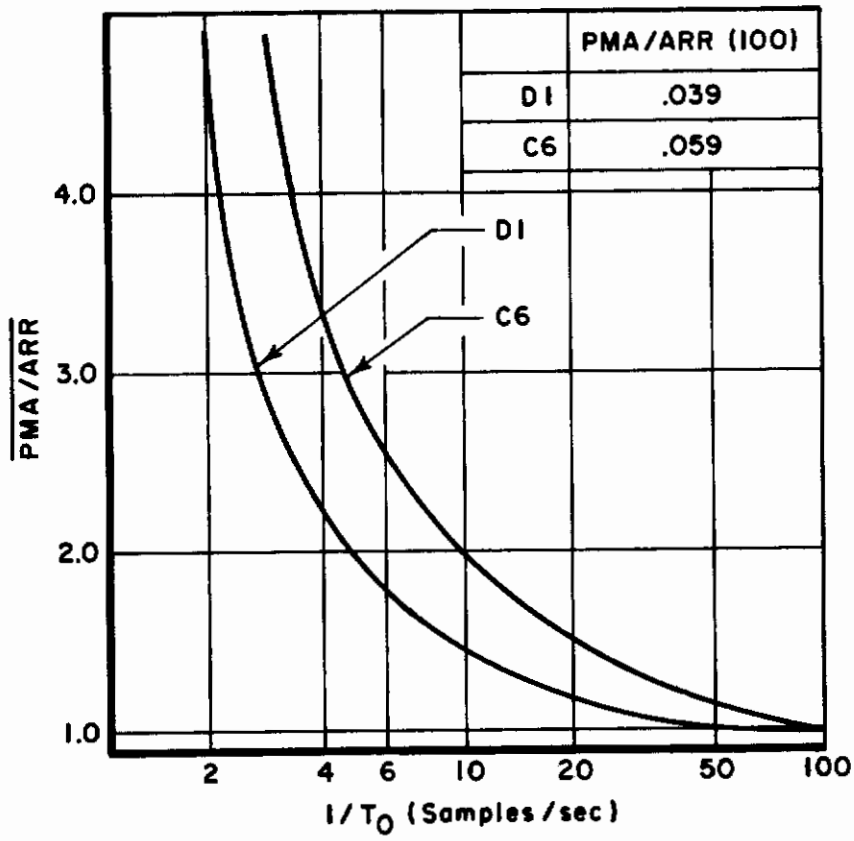

Figure 23. Comparison of $\overline{PMA/ARR}$ for Cases D1 and C6 (Effect of Direct Lift Control)

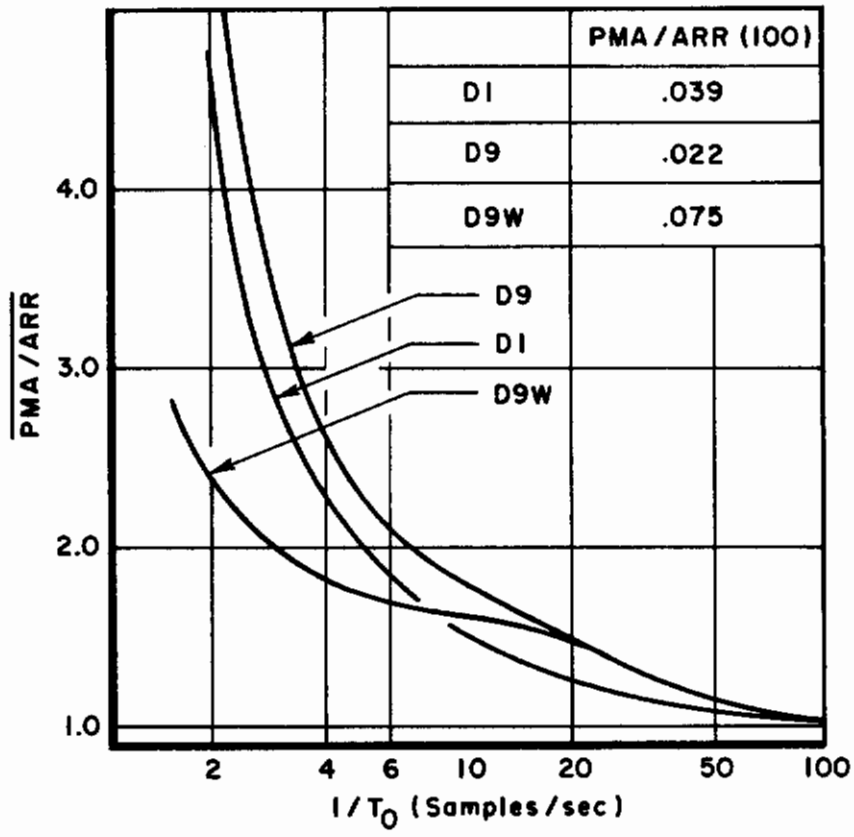

Figure 24. Comparison of $\overline{PMA/ARR}$ for Cases D1, D9, and D9W (Effects of Direct Lift Control)

5.2.7 Effects of Continuously Measured Glideslope Deviation Rate on Performance Sensitivity to Data Rate

It is reasonable to expect that the use of continuously sensed glideslope deviation rate could be effectively used to reduce glideslope tracking errors as well as data rate requirements. Such a measurement might be realized via an onboard inertial measurement unit or from a derived rate using a normal accelerometer. However obtained, such information could be used to improve glideslope error measurement accuracy, and hence to obtain an improved quality rate feedback signal.

In cases D10 and C7, the model was structured so that glideslope deviation rate was considered as a continually sensed motion variable. The only difference between cases D10 and D1 is that continuously sensed glideslope deviation rate is considered in case D10. In the same manner, cases C1 and C7 are identical except that case C7 includes continuously sensed glideslope deviation rate. The results of case D10 are compared to case D1 in Figure 25 and the results of case C7 are compared to case C1 in Figure 26. As anticipated, the landing performance improved in cases D10 and C7 and there is a significant decrease in the performance sensitivity to data rate.

The W-cases (where the deterministic winds are included) are also illustrated in Figures 25 and 26. In these cases the results are quite surprising inasmuch as relative minimums in the approach performance are obtained for finite data rates! An examination of the data in Appendix A shows that these minimums are induced by the effect of the data rate on the mean glideslope deviation error defined by the deterministic winds. A rational explanation of these results is not immediately available. One possible explanation is that continuously sensed glideslope deviation rate, together with the deterministic winds, causes the performance to be sensitive to the increasing bandwidth of the fluctuation noise with increasing data rate in the range of 4 to 15 samples/sec. This is pure speculation, however, and no concrete explanation of this result is offered.

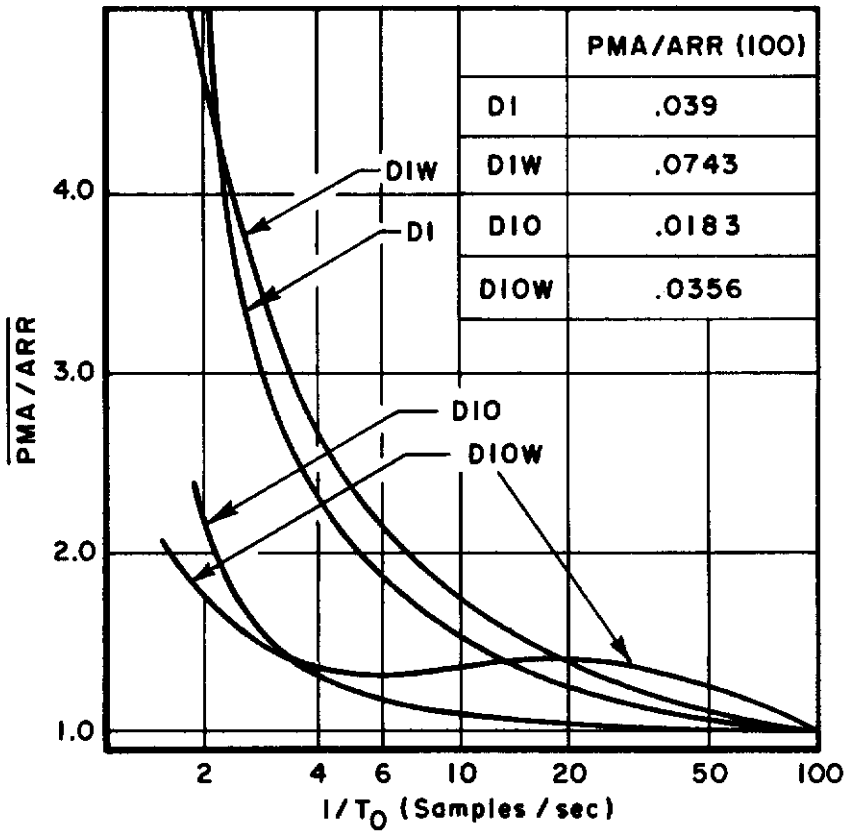

Figure 25. Comparison of $\overline{PMA/ARR}$ for Cases D1, D1W, D10, D10W (Effect of Continuously Sensed Glideslope Deviation Rate)

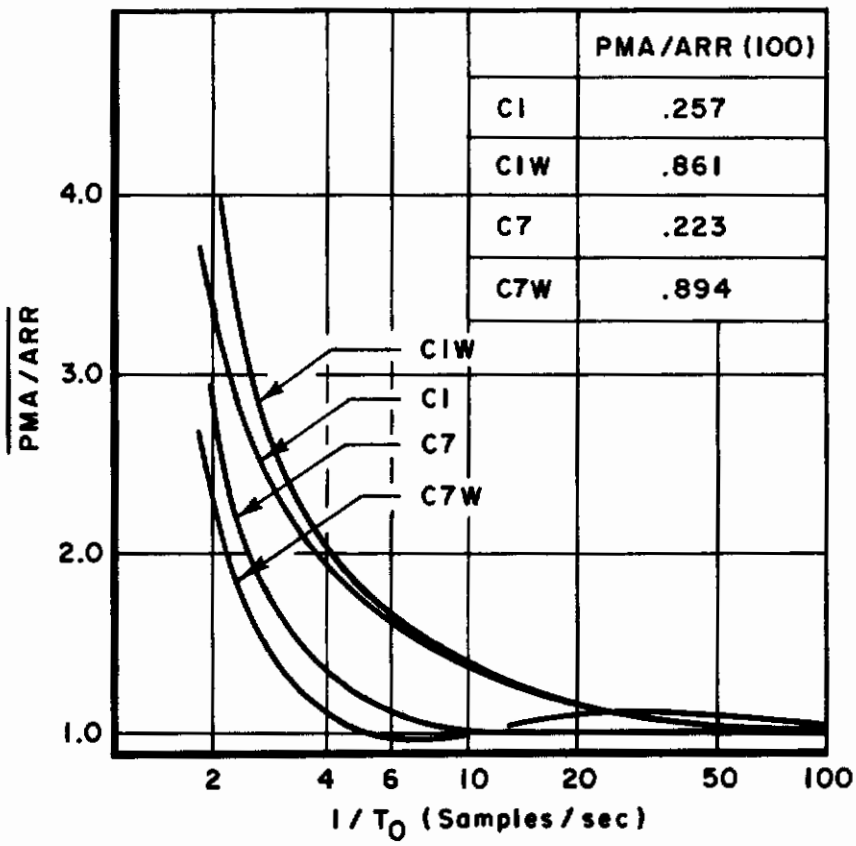

Figure 26. Comparison of $\overline{PMA/ARR}$ for Cases C1, C1W, C7, and C7W (Effect of Continuously Sensed Glideslope Deviation Rate)

At any rate, it is clear from the results shown in Figures 25 and 26 that a data rate of 5 samples/sec is quite adequate if glideslope deviation rate is continually sensed onboard the aircraft.

5.2.8 Effects of Integral Feedback of Glideslope Deviation on Performance Sensitivity to Data Rate

In all likelihood, a modern automatic approach flight control system would include integral feedback compensation in order to suppress glideslope offset due to steady winds and wind shear. The optimal control law developed for the baseline configuration (D1) does not include this type of compensation; however, integral feedback of glideslope deviation is induced in the control law for case D11. The results for these two cases are compared in Figure 27.

In the case where steady winds and wind shear are not considered, the approach performance is slightly degraded by the integral feedback. However, the integral feedback does significantly improve the approach performance in the presence of the steady winds and wind shear.

The approach performance is also more sensitive to data rate in the case where integral feedback is included. This is a reasonable result inasmuch as the addition of the integral feedback reduces the control system's stability margin and would consequently cause performance to be more sensitive to the quality of the glideslope deviation measurement.

This result indicates that with the practical consideration of integral feedback of glideslope deviation, a data rate of 10 to 20 samples/sec would still be desirable to effectively suppress glideslope

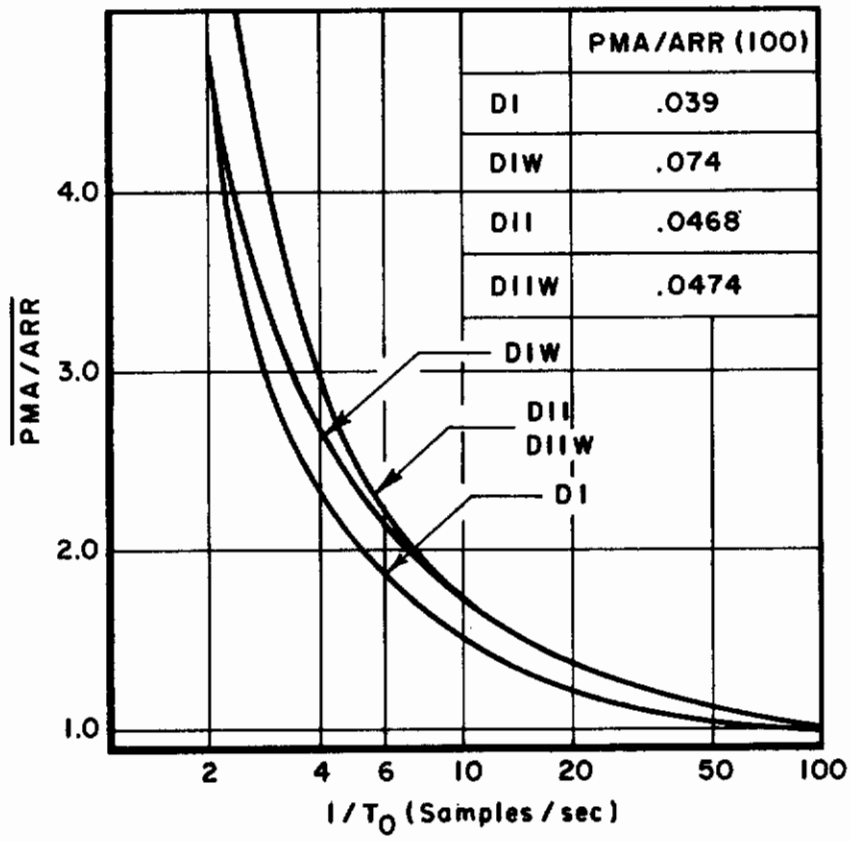

Figure 27. Comparison of $\overline{PMA/ARR}$ for Cases D1, D11, and D11W (Effects of Integral Feedback Control)

errors due to gust upset (provided that the flight control system does not include the appropriate sensors for deriving continuous glideslope deviation rate*).

*Results developed subsequent to the submittal of this report for review and publication indicate that with integral feedback of glideslope deviation (as in case D11) and continuously sensed glideslope deviation rate, a data rate of 5 samples/sec is quite adequate. This result is consistent with the results discussed in Section 5.2.7 and is reported in proceedings for the 1972 Joint Automatic Control Conference in a paper entitled "Investigation of Data Rate Requirements for Low Visibility Approach with a Scanning Beam Landing Guidance System" by the authors of this report.

SECTION VI

SUMMARY AND CONCLUSIONS

The degree to which concrete conclusions can be made based upon the results of this report depend somewhat on the audacity of the "concluder." Since there are not any other results of this type available, certain liberties can be taken. This may seem to be the case in discussing definitive data rate requirements. It is, however, recognized that the final decision of what is the "right" data rate will involve a complicated tradeoff of performance, economics, feasibility, and signal format.

This section is divided into three parts. Section 6.1 presents conclusions that are related to the low visibility landing approach model used in this analysis. The conclusion relating to the landing system requirements and particularly to data rate requirements are given in Section 6.2. Finally, in Section 6.3 some areas of further study and other possible uses of the results are suggested.

6.1 THE LOW VISIBILITY LANDING APPROACH MODEL

The mathematical model used in this analysis was restricted so as to consider only the longitudinal aircraft motion and the resulting longitudinal tracking errors associated with a low visibility landing approach. This restriction was based upon the assumption that the lateral tracking errors do not significantly affect landing approach performance (as discussed in Section II). If, in fact, the lateral tracking errors do significantly affect landing approach performance, the results obtained for the longitudinal glideslope tracking performance are still valid, since the equations of motion and the possible approach outcomes are relatively independent for the longitudinal and lateral cases. Furthermore, the analysis technique discussed in this report could be easily applied to the analysis of data rate requirements for the runway centerline tracking with a scanning beam guidance system.

It was mentioned in the introduction that the analysis technique used in this investigation is only claimed to apply to the consideration

of an automatic landing approach. This is because a pilot model was not explicitly used in the flight control system model. It is expected that piloted approach performance would be less sensitive to data rate than in the case where an automatic flight control system is considered, provided sufficient control authority is given to the automatic system. This is because higher glideslope tracking bandwidths can be obtained with the automatic system than would result with the pilot in the loop. Thus, increased data rates can be more effectively used by the automatic system to suppress glideslope deviations due to gust upset.

It is feasible (though perhaps not easy) to extend the optimal flight control model used in this analysis to an optimal model for the pilot and perform a similar analysis for piloted landing approach. In Reference 14, an optimal pilot model using an optimal estimator and an optimal feedback matrix was used quite successfully to predict piloted landing approach performance. It is therefore reasonable to expect that the same trends in data rate requirements would be observed from the results of a piloted approach analysis as were observed in this investigation.

It was shown in Section 5.1 that the model (and in particular, the optimal model for the flight control system) yields reasonable results for the case where the glideslope deviation is continuously sensed. This is based on the comparison of the results with those in References 1 and 2, where actual flight control system designs were considered in the analysis. No similar comparisons are available in the case where the glideslope deviation is sampled. It is expected, however, that the approach performance degradation due to the sample data rate would be more severe in the case where a "practical" filter is used to estimate or reconstruct a continuous estimate of the glideslope deviation. This is because a near optimal estimator was used in this analysis to derive the estimate of the glideslope deviation and the optimality would tend to "pay off" more with decreasing data rate.

The computed values of the probable missed approaches per arrival (PMA/ARR) and the approach performance sensitivity to data rate ($\overline{PMA/ARR}$) depend on the 100-ft-decision-altitude-window definition used to define a successful approach. This effect was discussed in Section 5.2.4 and it was shown that the effect on the results can be significant. The definitive values for data rate requirements are based on the use of $\pm$ 12-ft-glideslope deviation (and no airspeed dimension) to define the window (Figure 3). However, the general trends that were discussed in the results are valid for all of the window definitions discussed in this study.

6.2 LOW VISIBILITY LANDING SYSTEM REQUIREMENTS

It is clear from the results, that under certain (realistic) circumstances, data rate has a profound effect on the approach performance that can be achieved. This effect is accentuated by examining the relative degradation of the performance from the case where the glideslope measurements are continuous. Compared to the effects of the anticipated guidance measurement errors discussed in Section 3.3, the data rate is the dominate factor in whether or not a scanning beam landing guidance system is going to be completely effective in low visibility landing approach.

The results also indicate that the gust intensity has a most profound effect on approach performance (much more than even the effects of data rate for data rates of 5 samples/sec or more). Also, the effective suppression of glideslope tracking errors in a severe turbulence environment is going to depend primarily on the flight control system (assuming that the data rate is adequate). Thus, for a microwave scanning beam guidance system with an adequate data rate (5 samples/sec or greater), the limiting factor in achieving an all-weather category II low visibility landing capability may well be the flight control system.

The results also demonstrate the interaction that exists between the flight control system and the landing guidance system (the "avionics"). For example, three ways of modifying the flight control

system to suppress the glideslope errors due to gust upset were considered in this investigation: (1) increased control authority, (2) direct lift control, and (3) the complementary use of sensed glideslope deviation rate. In the first two cases, the data rate requirements increase (in the sense that the approach performance becomes more sensitive to data rate). In the third case, the data rate requirements decreased (in the sense that the approach performance becomes less sensitive to data rates).

The following trends were also observed in the results:

(1) In general, the consideration of deterministic winds did not have a profound effect on the approach performance sensitivity to data rate.

(2) In the case where beam-bend errors dominate the glideslope tracking errors, the performance is relatively insensitive to data rate for data rates greater than 2 samples/sec. (This is probably a moot point since the "beam bends" associated with a microwave scanning beam guidance system will be relatively small.)

(3) In a low gust environment, the approach performance is very sensitive to data rate. However, the probabilities of a missed approach are extremely small.

One possible way of specifying the data rate requirements is to require that the performance degradation due to data rate from the case where glideslope deviation is continuously measured be less than a certain factor. This is equivalent to requiring that the value of $\overline{\text{PMA/ARR}}$ be less than a specific value for the data rate selected. Under these circumstances, however, the value of PMA/ARR for the continuous case must also be considered, since it would be impractical to set the data rate requirement based on a case where the probabilities of missing the approach are relatively insignificant. The use of this method to specify data rate requirements is demonstrated in Table XVII, where values of $\overline{\text{PMA/ARR}}$ of 1.5, 1.75, 2.0, and 3.0 were used in the table to define the data rate requirements for the various cases considered.

The data rate requirements are listed according to the various effects considered and the corresponding section of the results where these effects were analyzed.

Based on the results given in Table XVII it appears that a data rate of between 10 and 20 samples/sec is extremely desirable to fully realize the full flight control system potential for suppressing errors due to gust upset. If glideslope deviation rate is sensed continuously onboard the aircraft, then a data rate of 5 samples/sec is adequate. However, defining the data rate based on this type of capability would certainly place a penalty on flight control system requirements (i.e., addition of inertial sensors) in order to achieve a Category II low visibility landing capability.

6.3 POSSIBLE EXTENSIONS TO THE INVESTIGATION

There are a number of possible complementary investigations or extensions to this study that would help to further solve the problem of defining data rate requirements for a scanning beam low visibility landing system. Some of them are

(1) An investigation of the 100-ft-decision-altitude-window requirements in order to determine a window definition which is consistent with a successful approach. A study along these lines is reported in Reference 15.

(2) Development of a queuing theory model for the landing process which could use the probabilities of a missed approach to evaluate the traffic conjestion in the terminal area. If such a model could be developed, the relation between data rate and the "ultimate" performance measure, operating costs in dollars, might be obtained.

(3) A study into whether or not the optimal control solutions developed for the analysis can be used to design practical automatic flight control systems for landing approach with a scanning beam guidance system.

TABLE XVII

DATA RATE REQUIREMENTS DEFINED BY AN UPPER BOUND ON $\overline{PMA/ARR}$

Consideration	Case	PMA/ARR(100)	Data Rate Requirement** for $\overline{PMA/ARR} \leq$				Section Discussed
			1.5	1.75	2.0	3.0	
Baseline Configuration - Severe gusts	D1	.039	10	6	5	3	5.2.1
	D1W	.074	15	9	7	4	
	C1	.257	7	5	4	3	
	C1W	.861	7	5	4	3	
Severe Beam Bends	D4	.304	2*	2*	2*	2*	5.2.2
	C4	.566	3	3	2*	2*	
Low Gust Environment	D2	.00004	25	16	12	6	5.2.3
	D2W	.00227	26	16	11	4	
	C2	.00019	10	7	5	3	
Increased Control Authority	D7	.0114	28	18	14	7	5.2.5
	D7W	.0236	28	18	13	6	
	D8	.0211	18	11	8	5	
	D8W	.0429	18	11	8	4	
	C6	.059	21	14	10	5	
	C6W	.1827	16	11	8	4	
Direct Lift Control	D9	.0220	20	11	7	4	5.2.6
	D9W	.0749	18	5	3	2*	
	C6	.059	21	14	10	5	
Continually Sensed Glideslope Deviation Rate	D10	.0183	3	3	2*	2*	5.2.7
	D10W	.0356	3	2*	2*	2*	
	C7	.223	4	3	3	2*	
	C7W	.894	3	3	2*	2*	
Integral Feedback	D11	.0468	15	10	8	4	5.2.8
	D11W	.0474	15	10	8	4	

* Data rates less than 2 samples/sec were not considered

**Samples/sec

(4) An experimental validation of the approach performance sensitivity to data rate via computer simulation or fixed base simulation.

(5) Development of an analysis procedure that could be used to evaluate the effects of data rate on landing performance under category III low visibility conditions (i.e., automatic landing goes to touch down). The performance measure would be landing safety and would be based on the possible outcomes that result in an accident (such as excessive sink rate, landing short, etc.) An optimal model of the flight control system and the flare guidance system could be used to simplify the analysis and allow for a digital computer solution for the probability of an accident as a function of data rate.

(6) An investigation into the effects on the data rate requirement for the case where direct lift control is combined with the use of continuously sensed glideslope deviation rate.

(7) Investigate the stability margins associated with the optimal designs to ensure that the results do not depend upon flight control system models which are unrealistic with respect to aircraft parameter uncertainties.

REFERENCES

1. D. Graham, W. F. Clement, L. G. Hofmann, Investigation of Measuring System Requirements for Instrument Low Approach, Systems Technology, Inc., AFFDL-TR-70-102, February 1971.

2. L. G. Hofmann, W. F. Clement, D. Graham, R. E. Blodgett, K. V. Shah, Investigation of Measuring System Requirements for Low Visibility Landing, Systems Technology, Inc., AFFDL-TR-71-151, January 1972.

3. M. D. Zuckerman, Investigation of Glide-Slope Information Rate Requirements for a Low Visibility Aircraft Landing, Masters Thesis, Air Force Institute of Technology, GE/EE/71-30, March 1971.

4. J. A. Gorham, et al., Where Are We Now With All-Weather Landing? AIAA Report 67-572, American Institute of Aeronautics and Astronautics Guidance, Control and Flight Dynamics Conference, August 1967.

5. W. A. Johnson and D. T. McRuer, Development of a Category II Approach System Model, Systems Technology, Inc., STI TR-182-1, December 1969.

6. Anonymous, Standard Performance Criteria for Autopilot/Coupler Equipments, Paper 31-63/DO-118, Radio Technical Commission for Aeronautics SC-79, Washington D. C., 14 March 1963.

7. Anonymous, Supplemental Data on Scanning Beam Guidance System for Approach and Landing, Prepared for RTCA SC-117, by AIL Division of Cutler-Hammer, Inc., August 1969.

8. A. E. Bryson and Y. Ho, Applied Optimal Control, Blaisdell Publishing Co., Waltham, Mass., 1969.

9. R. E. Kalman, "A New Approach to Linear Filtering and Prediction Problems", ASME Journal of Basic Engineering, 82, March 1969.

10. A. P. Sage, Optimum Systems Control, Prentice Hall, Inc., Englewood Cliffs, New Jersey, 1968.

11. W. A. Johnson, D. T. McRuer, Development of a Category II Approach System Model, Systems Technology, Inc., STI-TR-182-1, December 1969.

12. G. L. Nelson and R. C. Lorenzetti, Direction Lift Control for LAMS B-52, Masters Thesis, Air Force Institute of Technology, GGC/EE/68-8, June 1968.

13. P. R. Stolz, Microwave ILS Scanning Beam Data Rate Analysis for the CH-53/A, Masters Thesis, Air Force Institute of Technology, GSA/MA/72-18, to be published.

REFERENCES (CONTD)

14. D. L. Kleinman and S. Baron, Analytic Evaluation of Display Requirements for Approach to Landing, BBN Report No. 2075, March 1971.

15. W. A. Johnson and R. H. Hoh, Determination of ILS Category II Decision Height Window Requirements, Systems Technology, Inc., STI-TR-182-4, January 1971.

APPENDIX A

DETAILED COMPUTATIONAL RESULTS

In this appendix the detailed computational results are tabulated by case number and data rate. In each table the results peculiar to the W case are also given.

TABLE XVIII

DETAIL COMPUTATIONAL RESULTS FOR CASE D1

	Control Activity									W-Case				
$1/T_\theta$ (sec^{-1})	PMA	PMA/ARR	$3\sigma_{\delta_e}$ (rad/sec)	$3\sigma_{\delta_{th}}$ (% RPM)	σ_d (ft)	$\sigma_{u_{as}}$ (ft/sec)	σ_{n_z} (ft/sec^2)	σ_θ (rad)	σ_{δ_e} (rad)	PMA	PMA/ARR	$\bar{d}$ (ft)	$\bar{u}_{as}$ (ft/sec)
2	.1511	.178	.440	.1038	8.35	9.56	4.50	.0198	.0245	.253	.3381	-6.01	-.576
4	.0864	.0945	.433	.0354	6.99	9.57	4.87	.0205	.0258	.166	.1989	-4.99	-.665
6	.0684	.0734	.440	.0241	6.58	9.78	4.95	.0209	.0263	.163	.1579	-4.57	-.671
8	.0604	.0643	.440	.0205	6.39	9.58	4.98	.0211	.0265	.121	.1379	-4.36	-.638
10	.0566	.0600	.428	.0199	6.29	9.58	5.00	.0211	.0264	.114	.1288	-4.24	-.661
12	.0527	.0557	.437	.0176	6.19	9.59	5.01	.0212	.0266	.106	.1185	-4.10	-.673
14	.0505	.0531	.436	.0169	6.13	9.59	5.02	.0213	.0266	.101	.1124	-4.01	-.684
16	.0489	.0514	.432	.0171	6.09	9.59	5.02	.0213	.0265	.098	.1089	-3.96	-.668
18	.0476	.0500	.429	.0166	6.06	9.59	5.03	.0214	.0265	.096	.1057	-3.91	-.678
20	.0467	.0488	.427	.0176	6.03	9.59	5.03	.0214	.0264	.093	.1029	-3.86	-.685
50													
100	.0375	.0390	.409	.0166	5.73	9.59	5.03	.0217	.0258	.069	.0743	-3.33	-.700

TABLE XIX

DETAIL COMPUTATIONAL RESULTS FOR CASE D2

		Control Activity								W-Case			
$1/T_o$ (sec^{-1})	PMA	PMA/ARR	$3\sigma_{\dot{\delta}_e}$ (rad/sec)	$3\sigma_{\delta_{th}}$ (% RPM)	σ_d (ft)	$\sigma_{u_{as}}$ (ft/sec)	σ_{n_z} (ft/sec^2)	σ_θ (rad)	σ_{δ_e} (rad)	PMA	PMA/ARR	$\bar{d}$ (ft)	$\bar{u}_{as}$ (ft/sec)
2	.00031	.00031	.441	.0254	3.318	2.35	.843	.00529	.00880	.00934	.00943	-4.14	-.532
4	.00017	.00017	.408	.00868	3.169	2.35	.900	.00533	.00898	.00688	.00693	-4.17	-.628
6	.00012	.00012	.400	.00589	3.122	2.35	.910	.00532	.00905	.00571	.00574	-4.08	-.663
8	.00010	.00010	.397	.00502	3.099	2.35	.911	.00529	.00899	.00524	.00524	-4.02	-.635
10	.00009	.00009	.376	.00487	3.087	2.35	.907	.00523	.00879	.00495	.00497	-3.98	-.660
12	.00008	.00008	.382	.00429	3.077	2.35	.908	.00524	.00884	.00449	.00451	-3.90	-.672
14	.00007	.00007	.379	.00412	3.070	2.35	.907	.00522	.00878	.00442	.00423	-3.85	-.684
16	.00007	.00007	.374	.00418	3.066	2.35	.905	.00520	.00869	.00405	.00407	-3.82	-.669
18	.00007	.00007	.370	.00406	3.062	2.35	.903	.00518	.00862	.00387	.00389	-3.79	-.679
20	.00006	.00006	.367	.00431	3.059	2.35	.902	.00517	.00856	.00371	.00393	-3.76	-.686
50													
100	.00004	.000004	.346	.00406	3.035	2.35	.893	.00509	.00788	.00227	.00227	-3.33	-.700

TABLE XX

DETAIL COMPUTATIONAL RESULTS FOR CASE D3

			Control Activity							W-Case			
$1/T_o$ (sec^{-1})	PMA	PMA/ARR	$3\sigma_{\dot{\delta}_e}$ (rad/sec)	$3\sigma_{\delta_{th}}$ (% RPM)	σ_q (ft)	$\sigma_{u_{as}}$ (ft/sec)	σ_{n_z} (ft/sec^2)	σ_α (rad)	σ_{δ_e} (rad)	PMA	PMA/ARR	$\bar{d}$ (ft)	$\bar{u}_{as}$ (ft/sec)
2	.00658	.00662	.462	.0256	4.40	2.37	.885	.00603	.00930	.0312	.0386	-4.14	-.532
4	.00517	.00519	.420	.0088	4.27	2.38	.960	.00621	.00969	.0335	.0346	-4.17	-.628
6	.00481	.00484	.408	.0060	4.23	2.38	.983	.00630	.00996	.0307	.0316	-4.08	-.663
8	.00464	.00466	.400	.0051	4.21	2.38	.991	.00632	.01007	.0291	.0300	-4.02	-.635
10	.00453	.00455	.381	.0049	4.20	2.38	.990	.00627	.00996	.0282	.0290	-3.98	-.660
12	.00448	.00450	.387	.0043	4.19	2.38	.998	.00633	.01016	.0268	.0275	-3.90	-.672
14	.00443	.00445	.384	.0042	4.19	2.38	1.000	.00634	.01020	.0260	.0267	-3.85	-.684
16	.00440	.00442	.379	.0042	4.18	2.38	1.000	.00633	.01019	.0255	.0262	-3.82	-.669
18	.00437	.00439	.375	.0041	4.18	2.38	1.000	.00632	.01018	.0250	.0256	-3.79	-.679
20	.00435	.00437	.372	.0044	4.18	2.38	1.000	.00631	.01019	.0245	.0251	-3.76	-.686
50													
100	.00423	.00425	.355	.0041	4.17	2.38	1.005	.00633	.01061	.0198	.0198	-3.33	-.700

TABLE XXI

DETAIL COMPUTATIONAL RESULTS FOR CASE D4

			Control Activity							W-Case			
$1/T_o$ (sec^{-1})	PMA	PMA/ARR	$3\sigma_{\dot{\delta}_e}$ (rad/sec)	$3\sigma_{\delta_{th}}$ (% RPM)	σ_d (ft)	$\sigma_{u_{as}}$ (ft/sec)	σ_{n_z} (ft/sec^2)	σ_θ (rad)	σ_{δ_e} (rad)	PMA	PMA/ARR	$\bar{d}$ (ft)	$\bar{u}_{as}$ (ft/sec)
2	.245	.320	.638	.0280	10.26	2.60	1.24	.0111	.0134	.280	.389	-4.14	-.532
4	.236	.309	.523	.0096	10.12	2.61	1.44	.0120	.0152	.275	.379	-4.17	-.628
6	.234	.306	.482	.0065	10.08	2.61	1.55	.0125	.0167	.272	.373	-4.08	-.663
8	.234	.305	.459	.0056	10.07	2.61	1.60	.0128	.0177	.270	.370	-4.02	-.635
10	.233	.303	.434	.0054	10.05	2.61	1.61	.0128	.0181	.269	.367	-3.98	-.660
12	.233	.304	.438	.0048	10.05	2.61	1.66	.0130	.0190	.267	.364	-3.90	-.672
14	.233	.303	.433	.0046	10.05	2.61	1.68	.0132	.0195	.266	.363	-3.85	-.684
16	.233	.303	.426	.0047	10.05	2.61	1.69	.0132	.0199	.266	.362	-3.82	-.669
18	.233	.303	.422	.0046	10.05	2.61	1.69	.0132	.0202	.265	.361	-3.79	-.679
20	.232	.303	.419	.0048	10.05	2.61	1.70	.0132	.0204	.265	.360	-3.76	-.686
50													
100	.233	.304	.436	.0046	10.06	2.61	1.79	.0136	.0231	.259	.349	-3.33	-.700

TABLE XXII

DETAIL COMPUTATIONAL RESULTS FOR CASE D5

$1/T_o$ (sec^{-1})	PMA	PMA/ARR	Control Activity $^3\sigma_{\delta_e}$ (rad/sec)	Control Activity $^3\sigma_{\delta_{th}}$ (% RPM)	σ_d (ft)	$\sigma_{u_{as}}$ (ft/sec)	σ_{n_z} (ft/sec^2)	σ_θ (rad)	σ_{δ_e} (rad)	W-Case PMA	W-Case PMA/ARR	W-Case $\bar{d}$ (ft)	W-Case $\bar{u}_{as}$ (ft/sec)
2	.00042	.00042	.439	.00401	3.43	2.36	.837	.00579	.00800	.183	.224	-8.89	-8.89
4	.00023	.00023	.436	.00268	3.23	2.36	.869	.00537	.00695	.196	.244	-9.24	-9.24
6	.00019	.00019	.432	.00260	3.18	2.36	.872	.00523	.00674	.183	.224	-9.12	-9.12
8	.00016	.00016	.433	.00255	3.16	2.36	.874	.00517	.00671	.168	.202	-8.96	-8.96
10	.00015	.00015	.437	.00250	3.14	2.36	.875	.00515	.00672	.156	.184	-8.82	-8.82
12	.00014	.00014	.436	.00250	3.13	2.36	.875	.00513	.00671	.146	.172	-8.70	-8.70
14	.00013	.00013	.436	.00250	3.13	2.36	.875	.00512	.00672	.138	.160	-8.60	-8.60
16	.00012	.00012	.434	.00270	3.12	2.36	.875	.00511	.00671	.132	.152	-8.52	-8.52
18	.00012	.00012	.438	.00264	3.11	2.36	.876	.00511	.00673	.127	.145	-8.44	-8.44
20	.00011	.00012	.438	.00264	3.11	2.36	.876	.00510	.00673	.122	.139	-8.37	-8.37
50													
100	.00007	.00007	.438	.00250	3.07	2.36	.876	.00507	.00670	.072	.078	-7.51	-7.51

TABLE XXIII

DETAIL COMPUTATIONAL RESULTS FOR CASE D6

			Control Activity								W-Case			
$1/T_\sigma$ (sec^{-1})	PMA	PMA/ARR	$3\sigma_{\delta_e}$ (rad/sec)	$3\sigma_{\delta_{th}}$ (% RPM)	σ_d (ft)	$\sigma_{u_{as}}$ (ft/sec)	σ_{n_z} (ft/sec^2)	σ_θ (rad)	σ_{δ_e} (rad)		PMA	PMA/ARR	$\bar{d}$ (ft)	$\bar{u}_{as}$ (ft/sec)
2	.475	.905	.440	4.98	8.95	8.95	4.46	.0170	.0276		.547	1.209	-6.55	.869
4	.421	.729	.440	5.00	7.15	9.26	4.84	.0187	.0244		.481	.925	-5.32	.898
6	.408	.689	.440	4.98	6.62	9.29	4.93	.0253	.0197		.458	.846	-4.85	.899
8	.403	.675	.440	4.98	6.41	9.30	4.96	.0199	.0256		.448	.813	-4.61	.899
10	.400	.666	.440	4.99	6.29	9.31	4.98	.0201	.0257		.442	.793	-4.45	.898
12	.398	.661	.440	4.99	6.20	9.31	4.99	.0202	.0257		.438	.779	-4.33	.897
14	.397	.657	.438	4.99	6.14	9.31	5.00	.0203	.0257		.435	.770	-4.25	.896
16	.395	.654	.439	4.99	6.08	9.31	5.01	.0204	.0257		.432	.761	-4.17	.895
18	.394	.651	.438	4.99	6.05	9.31	5.01	.0204	.0257		.430	.754	-4.11	.893
20	.394	.649	.438	4.99	6.01	9.32	5.02	.0204	.0257		.428	.750	-4.06	.892
50														
100	.384	.623	.440	5.00	5.67	9.32	5.02	.0210	.0253		.411	.698	-3.46	.890

TABLE XXIV

DETAIL COMPUTATIONAL RESULTS FOR CASE D7

$1/T_o$ (sec^{-1})	Control Activity									W-Case			
	PMA	PMA/ARR	$3\sigma_{\delta_e}$ (rad)	$3\sigma_{\delta_{th}}$ (% RPM)	σ_d (ft)	$\sigma_{u_{as}}$ (ft/sec)	σ_{n_z} (ft/sec^2)	σ_θ (rad)	$\sigma_{\dot{\delta}_e}$ (rad/sec)	PMA	PMA/ARR	$\bar{d}$ (ft)	$\bar{u}_{as}$ (ft/sec)
2	.1248	.1426	.108	5.00	7.81	9.41	4.66	.0243	.434	.1678	.2016	-3.75	.798
4	.0558	.0591	.127	3.36	6.27	9.54	5.27	.0273	.600	.0862	.0943	-3.08	.478
6	.0381	.0396	.126	3.08	5.75	9.55	5.36	.0269	.581	.0638	.0681	-3.00	.471
8	.0303	.0312	.127	4.98	5.51	9.45	5.38	.0264	.577	.0546	.0578	-3.00	.847
10	.0257	.0264	.127	4.97	5.37	9.45	5.38	.0262	.574	.0493	.0519	-2.97	.855
12	.0234	.0239	.126	4.94	5.28	9.45	5.38	.0259	.573	.0459	.0459	-2.94	.855
14	.0221	.0226	.126	4.94	5.22	9.45	5.38	.0258	.573	.0434	.0454	-2.92	.861
16	.0210	.0214	.126	4.99	5.17	9.45	5.38	.0257	.577	.0413	.0431	-2.89	.872
18													
20	.0193	.0196	.126	4.98	5.09	9.45	5.38	.0256	.583	.0379	.0394	-2.84	.875
50	.0137	.0139	.126	4.96	4.85	9.45	5.42	.0256	.615	.0280	.0288	-2.62	.886
100	.0113	.0114	.126	4.96	4.72	9.45	5.45	.0258	.637	.0230	.0236	-2.47	.886

TABLE XXV

DETAIL COMPUTATIONAL RESULTS FOR CASE D8

			Control Activity							W-Case			
$1/T_o$ (sec^{-1})	PMA	PMA/ARR	$3\sigma_{\dot{\delta}_e}$ (rad/sec)	$3\sigma_{\delta_{th}}$ (% RPM)	σ_d (ft)	$\sigma_{u_{as}}$ (ft/sec)	σ_{n_z} (ft/sec^2)	σ_θ (rad)	σ_{δ_e} (rad)	PMA	PMA/ARR	$\bar{d}$ (ft)	$\bar{u}_{as}$ (ft/sec)
2	.1302	.1500	.878	4.74	7.92	9.37	4.56	.0218	.0304	.1831	.2240	-4.19	.871
4	.0665	.0712	.879	4.74	6.53	9.40	4.98	.0232	.0319	.1140	.1290	-3.83	.777
6	.0488	.0512	.880	4.28	6.08	9.43	5.08	.0234	.0325	.0902	.0991	-3.64	.700
8	.0418	.0436	.880	3.56	5.87	9.47	5.12	.0235	.0375	.0792	.0861	-3.53	.585
10	.0380	.0395	.880	4.88	5.75	9.41	5.13	.0233	.0324	.0734	.0792	-3.50	.878
12	.0354	.0367	.880	4.83	5.66	9.41	5.14	.0233	.0323	.0690	.0741	-3.46	.848
14	.03343	.0346	.879	4.89	5.60	9.41	5.15	.0233	.0322	.0659	.0706	-3.47	.859
16	.0319	.0329	.879	4.90	5.55	9.41	5.15	.0233	.0322	.0634	.0677	3.38	.860
18	.0306	.0316	.880	4.94	5.51	9.41	5.16	.0233	.0321	.0613	.0655	-3.35	.866
20	.0295	.0304	.879	4.90	5.48	9.41	5.16	.0233	.0321	.0595	.0633	-3.32	.866
50													
100	.0206	.0211	.879	[illegible]	5.45	9.41	5.22	.0236	.0310	.0412	.0429	-2.92	.841

TABLE XXVI

DETAIL COMPUTATIONAL RESULTS FOR CASE D9

$1/T_o$ (sec^{-1})	PMA	PMA/ARR	Control Activity $3\sigma_{\delta_e}$ (rad/sec)	Control Activity $3\sigma_{\dot{\delta}_d}$ (rad/sec)	σ_d (ft)	$\sigma_{u_{as}}$ (ft/sec)	σ_{n_z} (ft/sec^2)	σ_θ (rad)	σ_{δ_e} (rad)	σ_{δ_d}	W-Case PMA	W-Case PMA/ARR	$\bar{d}$ (ft)	$\bar{u}_{as}$ (ft/sec)
2	.1027	.1144	.438	.440	7.34	9.64	4.54	.0166	.0200	.0185	.168	.198	-4.45	-.80
4	.0546	.0578	.243	.440	6.24	9.62	4.84	.0146	.0157	.0243	.121	.137	-4.56	-.99
6	.0440	.0460	.166	.440	5.95	9.62	4.89	.0132	.0128	.0287	.112	.126	-4.68	-1.06
8	.0403	.0420	.125	.440	5.82	9.62	4.91	.0122	.0107	.0322	.111	.125	-4.81	-1.18
10	.0380	.0395	.105	.439	5.75	9.62	4.92	.0117	.0096	.0342	.109	.122	-4.87	-1.21
12	.0364	.0377	.092	.440	5.69	9.62	4.92	.0113	.0087	.0357	.108	.121	4.91	-1.27
14	.0352	.0365	.091	.432	5.66	9.62	4.92	.0114	.0087	.0356	.105	.118	-4.87	-1.26
16	.0343	.0355	.091	.426	5.63	9.62	4.92	.0114	.0086	.0355	.103	.115	-4.83	-1.27
18	.0323	.0334	.082	.440	5.57	9.63	4.93	.0111	.0080	.0370	.099	.110	-4.81	-1.29
20	.0317	.0327	.081	.435	5.55	9.63	4.93	.0112	.0080	.0369	.098	.108	-4.78	-1.30
50														
100	.0216	.0220	.071	.439	5.20	9.64	4.94	.0112	.0071	.0381	.070	.075	-4.28	-1.34

TABLE XXVII

DETAIL COMPUTATIONAL RESULTS FOR CASE D10

			Control Activity							W-Case			
$1/\tau_o$ (sec^{-1})	PMA	PMA/ARR	$3\sigma_{\dot{\delta}_e}$ (rad/sec)	$3\sigma_{\delta_{th}}$ (% RPM)	σ_d (ft)	$\sigma_{u_{as}}$ (ft/sec)	σ_{n_z} (ft/sec^2)	σ_θ (rad)	σ_{δ_e} (rad)	PMA	PMA/ARR	$\bar{d}$ (ft)	$\bar{u}_{as}$ (ft/sec)
2	.0364	.0377	.440	.0098	5.69	9.69	4.80	.0237	.0250	.0577	.0613	-2.77	-.568
4	.0228	.0233	.440	.0073	5.25	9.63	5.12	.0233	.0250	.0453	.0474	-2.97	-.666
6	.0210	.0214	.440	.0074	5.17	9.62	5.18	.0232	.0250	.0448	.0469	-3.11	-.703
8	.0202	.0207	.440	.0751	5.14	9.61	5.20	.0231	.0250	.0454	.0475	-3.22	-.642
10	.0198	.0202	.440	.0763	5.12	9.61	5.21	.0231	.0250	.0460	.0482	-3.30	-.663
12	.0195	.0199	.440	.0771	5.10	9.61	5.21	.0231	.0250	.0466	.0489	-3.36	-.677
14	.0193	.0197	.440	.0777	5.09	9.61	5.22	.0231	.0250	.0471	.0494	-3.40	-.660
16	.0192	.0195	.440	.0781	5.09	9.61	5.22	.0231	.0250	.0474	.0498	-3.44	-.670
18	.0190	.0194	.440	.0784	5.08	9.61	5.22	.0231	.0250	.0478	.0502	-3.46	-.679
20	.0191	.0193	.440	.0786	5.08	9.61	5.22	.0231	.0251	.0480	.0504	-3.49	-.667
50													
100	.0180	.0183	.440	.0849	5.04	9.61	5.23	.0231	.0251	.0344	.0356	-2.71	-.689

TABLE XXVIII

DETAIL COMPUTATIONAL RESULTS FOR CASE D11

$1/T_o$ (sec^{-1})	PMA	PMA/ARR	Control Activity: $3\sigma_{\dot{\delta}_e}$ (rad/sec)	Control Activity: $3\sigma_{\delta_{th}}$ (% RPM)	σ_d (ft)	$\sigma_{u_{as}}$ (ft/sec)	σ_{n_z} (ft/sec^2)	σ_θ (rad)	σ_{δ_e} (rad)	K_d/K_{δ_d} *	W-Case: PMA	W-Case: PMA/ARR	W-Case: $\bar{d}$ (ft)	W-Case: $\bar{u}_{as}$ (ft/sec)
2	.2200	.2821	.439	4.45	9.77	9.36	4.51	.0201	.0241	16.4	.2208	.2833	.578	.599
4	.1212	.1380	.440	4.88	7.73	9.36	4.89	.0213	.0258	15.0	.1212	.1380	-.247	.745
6	.0946	.1045	.440	3.29	7.17	9.45	4.97	.0218	.0264	14.6	.0950	.1050	-.360	.437
8	.0815	.0887	.443	4.80	6.88	9.38	5.01	.0218	.0264	14.5	.0816	.0889	-.359	.741
10	.0742	.0802	.440	5.00	6.72	9.37	5.02	.0218	.0265	14.3	.0748	.0809	-.351	.776
12														
14	.0602	.0717	.440	5.00	6.53	9.38	5.04	.0219	.0265	14.3	.0667	.0715	-.335	.775
16														
18														
20	.0602	.0641	.440	5.00	6.38	9.38	5.06	.0220	.0264	14.2	.0606	.0645	-.315	.774
50	.0500	.0525	.440	5.00	6.11	9.38	5.09	.0222	.0262	14.2	.0500	.0526	-.268	.787
100	.0447	.0468	.440	5.00	5.97	9.38	5.11	.0224	.0260	14.2	.0453	.0474	-.248	.888

* Feedback gain ratio, glideslope deviation to elevator/integral of glideslope deviation to elevator. Value used in Reference 1 was 11.3.

TABLE XXIX

DETAIL COMPUTATIONAL RESULTS FOR CASE C1

			Control Activity								W-Case			
$1/T_o$ (sec^{-1})	PMA	PMA/ARR	$3\sigma_{\dot{\delta}_{Bl}}$ (rad/sec)	$3\sigma_{\dot{\delta}_{cc}}$ (rad/sec)	σ_d (ft)	$\sigma_{u_{as}}$ (ft/sec)	σ_{n_z} (ft/sec^2)	σ_θ (rad)	$\sigma_{\delta_{Bl}}$ (rad)	$\sigma_{\delta_{cc}}$ (rad)	PMA	PMA/ARR	$\bar{d}$ (ft)	$\bar{u}_{as}$ (ft/sec)
2	.447	.809	.0942	.0453	15.8	11.19	2.65	.0535	.0072	.0056	.787	3.70	-24.0	-18.4
4	.330	.492	.0942	.0453	12.3	11.56	2.89	.0511	.0089	.0058	.638	1.77	-16.0	-20.5
6	.290	.409	.0942	.0453	11.3	11.59	2.96	.0500	.0096	.0059	.582	1.39	-14.0	-20.8
8	.271	.371	.0941	.0453	10.9	11.57	2.98	.0494	.0099	.0059	.555	1.25	-13.2	-20.7
10	.260	.351	.0940	.0451	10.6	11.55	2.99	.0490	.0100	.0060	.539	1.17	-12.8	-20.6
12	.252	.337	.0940	.0452	10.5	11.53	3.00	.0487	.0101	.0060	.527	1.11	-12.4	-20.4
14														
16	.241	.318	.0939	.0453	10.2	11.49	3.01	.0482	.0102	.0061	.512	1.05	-12.1	-20.2
18														
20	.234	.306	.0940	.0453	10.1	11.47	3.01	.0480	.0103	.0061	.503	1.01	-11.8	-20.1
50	.215	.274	.0939	.0453	9.7	11.41	3.02	.0470	.0104	.0062	.476	.91	-11.2	-19.7
100	.205	.257	.0940	.0452	9.4	11.38	3.02	.0464	.0104	.0062	.463	.86	-10.9	-19.5

TABLE XXX

DETAIL COMPUTATIONAL RESULTS FOR CASE C2

			Control Activity								W-Case			
$1/T_\sigma$ (sec^{-1})	PMA	PMA/ARR	$3\sigma_{\dot{\delta}_{BI}}$ (rad/sec)	$3\sigma_{\dot{\delta}_{cc}}$ (rad/sec)	σ_d (ft)	$\sigma_{u_{as}}$ (ft/sec)	σ_{n_z} (ft/sec^2)	σ_θ (rad)	$\sigma_{\delta_{BI}}$ (rad)	$\sigma_{\delta_{cc}}$ (rad)	PMA	PMA/ARR	$\bar{d}$ (ft)	$\bar{u}_{as}$ (ft/sec)
2	.00195	.00195	.0469	.0357	3.85	2.42	.462	.0095	.0017	.0014	.999	993.025	-24.0	-18.4
4	.00050	.00050	.0776	.0404	3.46	2.49	.582	.0090	.0024	.0015	.875	6.996	-16.0	-20.5
6	.00035	.00035	.0854	.0414	3.36	2.51	.624	.0087	.0025	.0016	.727	2.669	-14.0	-20.8
8	.00031	.00031	.0877	.0418	3.32	2.51	.637	.0086	.0026	.0016	.642	1.793	-13.2	-20.7
10	.00029	.00029	.0884	.0418	3.30	2.50	.640	.0085	.0026	.0016	.593	1.455	-12.8	-20.6
12	.00027	.00027	.0889	.0420	3.28	2.50	.641	.0084	.0026	.0016	.555	1.245	-12.4	-20.4
14														
16	.00025	.00025	.0890	.0422	3.26	2.50	.639	.0082	.0025	.0016	.509	1.035	-12.1	-20.2
18														
20	.00024	.00024	.0890	.0422	3.25	2.50	.637	.0082	.0025	.0016	.408	.925	-11.8	-20.1
50	.00021	.00021	.0885	.0422	3.21	2.49	.621	.0079	.0024	.0016	.404	.677	-11.2	-19.7
100	.00019	.00019	.0882	.0421	3.19	2.49	.608	.0078	.0024	.0016	.368	.582	-10.9	-19.5

TABLE XXXI

DETAIL COMPUTATIONAL RESULTS FOR CASE C3

			Control Activity								W-Case			
$1/T_o$ (sec^{-1})	PMA	PMA/ARR	$3\sigma_{\dot{\delta}_{Bl}}$ (rad/sec)	$3\sigma_{\dot{\delta}_{cc}}$ (rad/sec)	σ_d (ft)	$\sigma_{u_{as}}$ (ft/sec)	σ_{n_z} (ft/sec^2)	σ_θ (rad)	$\sigma_{\delta_{Bl}}$ (rad)	$\sigma_{\delta_{cc}}$ (rad)	PMA	PMA/ARR	$\bar{d}$ (ft)	$\bar{u}_{as}$ (ft/sec)
2	.454	.831	.0952	.0464	16.0	11.2	2.95	.0507	.0072	.0056	.785	3.64	-24.0	-18.4
4	.342	.519	.0955	.0462	12.6	11.6	2.90	.0513	.0090	.0058	.637	1.76	-16.0	-20.5
6	.305	.438	.0954	.0461	11.7	11.6	2.97	.0503	.0097	.0059	.582	1.39	-14.0	-20.8
8	.287	.407	.0952	.0461	11.2	11.6	2.99	.0497	.0100	.0060	.555	1.25	-13.2	-20.7
10	.276	.381	.0951	.0459	11.0	11.6	3.01	.0493	.0101	.0060	.540	1.18	-12.8	-20.6
12	.268	.367	.0952	.0460	10.8	11.5	3.01	.0490	.0102	.0061	.529	1.12	-12.4	-20.4
14														
16	.259	.349	.0951	.0461	10.6	11.5	3.02	.0486	.0103	.0061	.514	1.06	-12.1	-20.2
18														
20	.253	.338	.0952	.0462	10.5	11.5	3.03	.0483	.0104	.0062	.506	1.02	-11.8	-20.1
50	.234	.305	.0955	.0466	10.1	11.4	3.05	.0473	.0106	.0063	.480	.92	-11.2	-19.7
100	.224	.289	.0957	.0471	9.9	11.4	3.06	.0468	.0106	.0063	.470	.88	-10.9	-19.5

TABLE XXXII

DETAIL COMPUTATIONAL RESULTS FOR CASE C4

			Control Activity								W-Case			
$1/T_o$ (sec^{-1})	PMA	PMA/ARR	$3\sigma_{\dot{\delta}_{Bl}}$ (rad/sec)	$3\sigma_{\dot{\delta}_{cc}}$ (rad/sec)	σ_d (ft)	$\sigma_{u_{as}}$ (ft/sec)	σ_{n_z} (ft/sec^2)	σ_θ (rad)	$\sigma_{\delta_{Bl}}$ (rad)	$\sigma_{\delta_{cc}}$ (rad)	PMA	PMA/ARR	$\bar{d}$ (ft)	$\bar{u}_{as}$ (ft/sec)
2	.507	1.027	.104	.0560	18.1	11.3	2.67	.0554	.0074	.0058	.769	3.33	-24.0	-18.4
4	.433	.764	.107	.0543	15.3	11.7	2.95	.0538	.0094	.0061	.636	1.75	-16.0	-20.5
6	.410	.696	.106	.0533	14.6	11.7	3.05	.0531	.0103	.0063	.593	1.45	-14.0	-20.8
8	.399	.665	.106	.0529	14.2	11.7	3.10	.0526	.0107	.0064	.572	1.34	-13.2	-20.7
10	.393	.648	.105	.0527	14.0	11.7	3.12	.0522	.0110	.0065	.561	1.28	-12.8	-20.6
12	.389	.636	.105	.0529	13.9	11.7	3.15	.0520	.0111	.0066	.552	1.24	-12.4	-20.4
14														
16	.383	.620	.106	.0533	13.8	11.6	3.18	.0516	.0113	.0067	.542	1.18	-12.1	-20.2
18														
20	.379	.611	.106	.0538	13.6	11.6	3.20	.0513	.0115	.0068	.536	1.15	-11.8	-20.1
50	.368	.587	.112	.0575	13.3	11.5	3.31	.0504	.0120	.0072	.518	1.07	-11.2	-19.7
100	.362	.566	.121	.0624	13.2	11.5	3.40	.0498	.0125	.0074	.508	1.03	-10.9	-19.5

TABLE XXXIII

DETAIL COMPUTATIONAL RESULTS FOR CASE C5

			Control Activity								W-Case			
$1/T_o$ (sec^{-1})	PMA	PMA/ARR	$3\sigma_{\dot{\delta}_{BI}}$ (rad/sec)	$3\sigma_{\dot{\delta}_{cc}}$ (rad/sec)	σ_d (ft)	$\sigma_{u_{as}}$ (ft/sec)	σ_{n_z} (ft/sec^2)	σ_θ (rad)	$\sigma_{\delta_{BI}}$ (rad)	$\sigma_{\delta_{cc}}$ (rad)	PMA	PMA/ARR	$\bar{d}$ (ft)	$\bar{u}_{as}$ (ft/sec)
2	.524	1.102	.0936	.0453	18.8	11.2	2.64	.0531	.0072	.0056	.844	5.39	-30.0	-18.4
4	.456	.839	.0941	.0452	16.1	11.6	2.87	.0508	.0088	.0058	.754	3.06	-22.2	-20.5
6	.442	.791	.0928	.0451	15.4	11.5	2.92	.0497	.0092	.0059	.724	2.62	-20.3	-20.1
8	.427	.744	.0934	.0452	15.1	11.6	2.96	.0495	.0096	.0059	.709	2.44	-19.5	-20.8
10	.421	.727	.0939	.0453	14.9	11.6	2.97	.0492	.0098	.0059	.697	2.33	-19.0	-20.6
12	.418	.718	.0938	.0452	14.8	11.6	2.98	.0491	.0098	.0059	.695	2.28	-18.8	-20.6
14														
16	.413	.704	.0941	.0453	14.7	11.6	2.99	.0489	.0099	.0060	.688	2.21	-18.4	-20.5
18														
20	.411	.698	.0934	.0453	14.6	11.5	2.99	.0487	.0100	.0060	.685	2.17	-18.2	-20.3
50	.405	.681	.0932	.0452	14.4	11.5	3.00	.0484	.0101	.0061	.676	2.08	-17.8	-20.1
100	.402	.672	.0937	.0452	14.3	11.5	3.01	.0483	.0101	.0061	.672	2.04	-17.6	-20.1

TABLE XXXIV

DETAIL COMPUTATIONAL RESULTS FOR CASE C6

$1/T_o$ (sec^{-1})	PMA	PMA/ARR	Control Activity $3\sigma_{\dot{\delta}_{B1}}$ (rad/sec)	Control Activity $3\sigma_{\dot{\delta}_{cc}}$ (rad/sec)	σ_d (ft)	$\sigma_{u_{as}}$ (ft/sec)	σ_{n_z} (ft/sec^2)	σ_θ (rad)	$\sigma_{\delta_{B1}}$ (rad)	$\sigma_{\delta_{cc}}$ (rad)	W-Case PMA	W-Case PMA/ARR	$\bar{d}$ (ft)	$\bar{u}_{as}$ (ft/sec)
2	.3040	.4369	.140	.103	11.18	10.3	2.63	.0521	.0069	.0079	.449	.997	-11.46	-9.9
4	.1702	.2051	.140	.118	8.71	10.5	2.89	.0488	.0096	.0081	.350	.538	-8.40	-12.2
6	.1326	.1529	.141	.119	7.98	10.5	2.96	.0474	.0105	.0083	.295	.418	-7.52	-12.6
8	.1147	.1296	.141	.119	7.59	10.5	2.98	.0464	.0108	.0085	.263	.357	-7.05	-12.4
10	.1048	.1170	.141	.118	7.37	10.4	2.99	.0458	.0110	.0086	.245	.325	-6.79	-12.4
12	.0990	.1098	.140	.118	7.26	10.5	3.00	.0456	.0111	.0085	.238	.312	-6.69	-12.5
14														
16	.0881	.0966	.140	.118	6.98	10.4	2.99	.0446	.0111	.0088	.214	.272	-6.34	-11.9
18														
20	.0819	.0892	.141	.119	6.89	10.4	3.01	.0445	.0113	.0087	.206	.260	-6.25	-12.3
50	.0663	.0710	.140	.117	6.53	10.4	3.02	.0433	.0114	.0088	.176	.214	-5.85	-12.2
100	.0556	.0589	.141	.118	6.27	10.4	3.03	.0425	.0115	.0088	.154	.183	-5.55	-12.2

TABLE XXXV

DETAIL COMPUTATIONAL RESULTS FOR CASE C7

$1/T_o$ (sec^{-1})	Control Activity PMA	PMA/ARR	$3\sigma^{\dot{}}_{\delta_{Bl}}$ (rad/sec)	$3\sigma^{\dot{}}_{\delta_{cc}}$ (rad/sec)	σ_d (ft)	$\sigma_{u_{as}}$ (ft/sec)	σ_{n_z} (ft/sec^2)	σ_θ (rad)	$\sigma_{\delta_{Bl}}$ (rad)	$\sigma_{\delta_{cc}}$ (rad)	W-Case PMA	PMA/ARR	$\bar{d}$ (ft)	$\bar{u}_{as}$ (ft/sec)
2	.365	.576	.0940	.0452	13.25	10.9	2.62	.0510	.0069	.0062	.649	1.852	-16.5	-14.9
4	.226	.292	.0941	.0453	9.90	11.4	2.90	.0482	.0093	.0061	.484	.939	-11.4	-18.6
6	.198	.247	.0941	.0453	9.32	11.5	2.96	.0473	.0100	.0060	.459	.849	-10.9	-19.7
8	.192	.237	.0938	.0451	9.17	11.5	2.97	.0468	.0102	.0060	.459	.848	-10.9	-19.8
10	.189	.232	.0940	.0452	9.11	11.5	2.97	.0466	.0103	.0060	.464	.864	-11.0	-19.9
12	.187	.230	.0941	.0453	9.08	11.5	2.98	.0465	.0104	.0060	.469	.882	-11.2	-20.0
14														
16	.186	.228	.0941	.0453	9.06	11.5	2.98	.0463	.0104	.0060	.476	.910	-11.3	-20.0
18														
20	.185	.227	.0941	.0453	9.04	11.5	2.98	.0463	.0105	.0060	.482	.929	-11.5	-20.0
50	.182	.223	.0941	.0453	8.99	11.5	2.99	.0463	.0105	.0061	.472	.894	-11.2	-20.0
100	.181	.221	.0942	.0453	8.96	11.5	2.99	.0464	.0105	.0060	.461	.856	-11.0	-20.0

UNCLASSIFIED
Security Classification

DOCUMENT CONTROL DATA - R & D
(Security classification of title, body of abstract and indexing annotation must be entered when the overall report is classified)

1. ORIGINATING ACTIVITY (Corporate author)	2a. REPORT SECURITY CLASSIFICATION
Air Force Flight Dynamics Laboratory Wright-Patterson Air Force Base, Ohio	Unclassified 2b. GROUP

3. REPORT TITLE

ANALYSIS OF DATA RATE REQUIREMENTS FOR LOW VISIBILITY APPROACH WITH A SCANNING BEAM LANDING GUIDANCE SYSTEM

4. DESCRIPTIVE NOTES (Type of report and inclusive dates)

5. AUTHOR(S) (First name, middle initial, last name)

James D. Dillow, Major, USAF
Paul R. Stolz, Captain, USAF
Meyer D. Zuckerman, 1st Lt, USAF

6. REPORT DATE	7a. TOTAL NO. OF PAGES	7b. NO. OF REFS
February 1973	175	15

8a. CONTRACT OR GRANT NO.	9a. ORIGINATOR'S REPORT NUMBER(S)
b. PROJECT NO. 8219 c. Task 821911 d. Work Unit 003	AFFDL-TR-71-177 9b. OTHER REPORT NO(S) (Any other numbers that may be assigned this report)

10. DISTRIBUTION STATEMENT

Approved for public release; distribution unlimited.

11. SUPPLEMENTARY NOTES	12. SPONSORING MILITARY ACTIVITY
	Air Force Flight Dynamics Laboratory Wright-Patterson Air Force Base, Ohio

13. ABSTRACT

Data rate requirements for low visibility approach with a sample data measurement of glideslope deviation is investigated analytically.

A "window" is defined by specifying certain allowable deviations in the aircraft motion variables which are acceptable for continuation of the landing at a 100-ft-decision altitude. The approach performance is defined as the probability of missing the window, which corresponds to the probability of a missed approach.

The landing approach process is modeled by a system of stochastic differential equations, which account for the aircraft dynamics, atmospheric disturbances, guidance errors, and data rate. The flight control system is modeled by a state estimator and a state feedback matrix which is optimized so as to minimize the probability of a missed approach subject to rms constraints on control activity.

Performance as a function data rate was computed using DC-8 and CH-53A dynamics. Variations considered in the model include gust environment, guidance errors, window definition, control authority, control points, and onboard sensors. For each case considered, the performance degradation due to data rate was computed and plotted. Based on the allowable degradation in performance from that obtainable with continuously measured glideslope deviation, the data rate requirements can be determined.

Continued

DD FORM 1 NOV 65 1473

UNCLASSIFIED
Security Classification

UNCLASSIFIED
Security Classification

13. ABSTRACT

Continued

The study reveals that the flight control system is the limiting factor in achieving an all-weather Category II low visibility landing capability with a state-of-the-art scanning beam guidance system and data rates above 5 samples/sec. This is due to the requirements to suppress gust upset. The tradeoffs between the flight control system and scanning beam guidance system data rate requirements are illustrated by comparing the results for various flight control schemes. For example, data rate requirements are significantly reduced via onboard inertial measurements. However, the results indicate that a data rate between 10 and 20 samples/sec is extremely desirable in order to fully realize the flight control system's potential for suppressing glideslope tracking errors due to gust upset if onboard inertial sensors are not used.

14. KEY WORDS	LINK A		LINK B		LINK C	
	ROLE	WT	ROLE	WT	ROLE	WT
Low visibility landing						
Optimal flight control						
Optimal estimation of discrete systems						
Scanning beam landing guidance						
Data rate requirements						
Probability of missed approach						

☆U.S.Government Printing Office: 1973 — 759-491/407

Security Classification